



Durham E-Theses

Soliton dynamics in nonlinear planar systems

Sutcliffe, Paul Michael

How to cite:

Sutcliffe, Paul Michael (1992) *Soliton dynamics in nonlinear planar systems*, Durham theses, Durham University. Available at Durham E-Theses Online: <http://etheses.dur.ac.uk/10492/>

Use policy

The full-text may be used and/or reproduced, and given to third parties in any format or medium, without prior permission or charge, for personal research or study, educational, or not-for-profit purposes provided that:

- a full bibliographic reference is made to the original source
- a [link](#) is made to the metadata record in Durham E-Theses
- the full-text is not changed in any way

The full-text must not be sold in any format or medium without the formal permission of the copyright holders.

Please consult the [full Durham E-Theses policy](#) for further details.

Soliton Dynamics In Nonlinear Planar Systems

by

Paul Michael Sutcliffe

A thesis presented for the degree
of Doctor of Philosophy
at the University of Durham

The copyright of this thesis rests with the author.
No quotation from it should be published without
his prior written consent and information derived
from it should be acknowledged.

Department of Mathematical Sciences
University of Durham
Durham DH1 3LE
England

June 1992



2 DEC 1992

TO
ZOË AND STEVEN
WITH LOVE

× × ×

PREFACE

This thesis is based on work done by the author between October 1989 and June 1992 at the University of Durham, supported by a U.K. Science and Engineering Research Council studentship. No part of it has been previously submitted for any degree, either in this or any other university.

With the exception of the reviews in chapters *I*, *II* and section 4.2 it is believed that the material in this thesis is original work. Chapter *III* is based on a paper^[1] published in *Nonlinearity*. Chapter *IV* is based on a paper^[2] published in *Physics Letters B* and a paper^[3] to appear in *Physics Letters B*. The work in chapter *V* is a Durham preprint.^[4] Chapter *VI* is based on a paper^[5] to appear in *Physical Review D*. Finally, the work in chapter *VII* has been published^[6] in the *Journal of Mathematical Physics*. All the above are sole-author papers.

I would like to warmly thank my supervisor Prof. R.S. Ward and Dr. W.J. Zakrzewski for their guidance and encouragement. I would also like to thank R.A. Leese, N.J. Mackay and I.A.B. Strachan for many stimulating conversations.

I thank Zoë for her love and support and our son Steven for sleeping (at least a little) during the night.

Soliton Dynamics In Nonlinear Planar Systems

by

Paul Michael Sutcliffe

Ph.D Thesis, 1992

Abstract

The work in this thesis is concerned with the study of stability and scattering of solitons in planar models ie where spacetime is (2+1)-dimensional. We consider both integrable models, where exact solutions can be written in closed form, and non-integrable models, where approximations and numerical methods must be employed.

In chapter *III* we use a 'collective coordinate' approximation to study the scattering of solitons in a model motivated by elementary particle physics. In chapter *IV* we discuss a method to obtain approximate soliton configurations which can then be used to investigate soliton dynamics. In chapter *V* we perform a test of the 'collective coordinate' approximation by applying it to the study of classical and quantum soliton scattering in an integrable model, where exact results are known. Chapters *VI* and *VII* are concerned with an integrable chiral model. First we construct exact solutions using twistor methods and then we go on to study soliton stability using numerical techniques. Through computer simulations we find that there exist solitons which scatter in a way unlike any previously found in integrable models. Furthermore, this soliton scattering resembles very closely that found in certain non-integrable models, thereby providing a link between the two classes. Finally, chapter *VIII* is an outlook on current and future research.

CONTENTS

<i>I</i>	Introduction	1
<i>II</i>	Soliton theory	4
2.1.	Solitons in integrable systems	4
2.2.	The self-duality equations and the unity of integrable systems	9
2.3.	Skyrmions	13
2.4.	Sigma models and lumps	16
<i>III</i>	The dynamics of planar Skyrmions	20
3.1.	Introduction	20
3.2.	Planar Skyrmions	21
3.3.	A collective coordinate approach	23
3.4.	Skyrmion scattering	25
3.5.	Derivation of critical velocity	33
3.6.	Comparison with other methods	35
3.7.	Conclusion	36
<i>IV</i>	Solitons from instantons	37
4.1.	Introduction	37
4.2.	Skyrmions from instantons	38
4.3.	Kinks from instantons	39
4.4.	Skyrmions from kinks	47
4.5.	Conclusion	49
<i>V</i>	Classical and quantum kink scattering	51
5.1.	Introduction	51
5.2.	Sine-Gordon kinks	52

5.3. The collective coordinate approximation	53
5.4. Classical kink scattering	56
5.5. Quantum kink scattering	57
5.6. Conclusion	63
VI Yang-Mills-Higgs solitons	64
6.1. Introduction	64
6.2. The Yang-Mills-Higgs-Bogomolny equation	64
6.3. Twistor construction of solitons	65
6.4. Sigma model formulations	69
6.5. Soliton stability	71
6.6. Modified equations	78
6.7. Integrability	79
6.8. Remarks on soliton scattering	80
6.9. Conclusion	81
VII Soliton scattering in an integrable chiral model	82
7.1. Introduction	82
7.2. The integrable chiral model	82
7.3. Connection with the $O(3)$ σ -model	84
7.4. Soliton - Soliton scattering	89
7.5. Soliton - Anti-Soliton scattering	93
7.6. An interpolating chiral model	99
7.7. Remarks on other methods	101
7.8. Conclusion	101
VIII Outlook	102
References	106

CHAPTER I.

Introduction

The simplest mathematical equations are those which are linear, since their solutions possess simple addition properties which allow more complicated solutions, or even the most general, to be constructed by combining simple ones. Although linear equations are often easy to solve they are usually far too simple to describe systems which occur in the real world, and only nonlinear equations can provide the complicated behaviour we observe in all fields of scientific study.

To obtain solutions of nonlinear systems is in general very difficult, if not impossible, with some nonlinear systems being chaotic, so that infinitely small changes in the initial state of the system results in wildly different evolutions. A particularly interesting class of nonlinear equations is those which possess so called soliton solutions. Roughly speaking, solitons are lump-like or wave-like solutions to nonlinear equations which are localised in space and move at constant speed with little change of shape. Their existence is unexpected, since in the vast majority of equations dispersion effects would lead to the breakup or collapse of a lump. It is only in very special equations that dispersion effects are exactly balanced by nonlinearities thereby allowing soliton solutions to exist.

Not only are solitons interesting mathematical structures but their application in the natural sciences is immense. Solitons occur in many fields including nonlinear optics, hydrodynamics, superconductivity, cosmology, plasma and particle physics, and even in biophysics, where they are relevant in protein dynamics. Their use in the modern technologies of telecommunications and the design of computer hardware mean they will soon affect our everyday lives.

The majority of equations possessing soliton solutions occur in one space dimension, so that soliton dynamics is confined to motion along a line. Early pioneering investigations of solitons used computers and numerical simulations to study soliton dynamics, and discovered the characteristic property of solitons, which is that they retain their shape as they emerge from collisions with other solitons. Such numerical studies inspired a vast amount of later analytical work and today many techniques exist for analysing equations



possessing soliton solutions. Areas of mathematics such as group theory, complex analysis and algebraic geometry are all important in the study of solitons and have led to techniques which may be used, among other applications, for constructing exact solutions which describe multi-soliton configurations where each soliton moves with an independent speed, undergoes multiple collisions and emerges intact with an unchanged speed. Although solitons occur in nonlinear equations there are remarkable methods by which two independent soliton solutions can be combined to produce a third. This linear-like aspect of soliton theories is one of the important properties that distinguish them from general nonlinear systems.

In more than one space dimension the situation is far less well understood. There are examples of equations possessing soliton solutions but most are simple extensions of familiar examples from one space dimension. Some higher dimensional systems which possess soliton solutions have originated in physical theories, particularly in the area of elementary particle physics. The localised structure of solitons together with their collision properties make them ideally suited to describe elementary particles. Ideas from physics have also led to work which unifies those equations with soliton solutions and gives a deeper understanding of the origin of solitons. Although the physicist and mathematician have not studied solitons in total isolation, many methods and perspectives are quite different in the two approaches. A combination of techniques from both fields appears to be required in order to gain a better understanding of higher dimensional soliton systems.

In this thesis we shall be concerned with investigating the dynamics of solitons in planar systems *ie* where space is two dimensional. Some of the systems have a close relationship with well known soliton systems in one space dimension, while others are new systems which arise from physical theories. In order to investigate the dynamics of solitons one must study how they interact (what happens if two lumps collide) and how they behave if they are slightly perturbed or deformed.

Planar systems are particularly interesting models to study for the following main reasons;

- A two dimensional space allows a much greater freedom of motion than the much studied, but more restrictive, one dimensional space systems, where the solitons are confined to motion on a line.
- Computers which are currently available have now reached the point at which studies of dynamical solitons in planar systems are just feasible.

- Many physical processes occur in which space can effectively be regarded as two dimensional. For example, in condensed matter physics many important phenomena take place in layers of a material, which are therefore effectively planar systems. As an application, planar models which possess soliton solutions are currently popular models for high temperature superconductivity.

This thesis is laid out as follows. In chapter *II* we shall review some of the main equations of soliton theory, and use one of the most well known, the Korteweg de Vries equation, to discuss some of the many techniques that are used to study soliton systems. We shall then review recent work, which has origins in the physical theory of gauge fields, that attempts to unify the known soliton equations as special cases of one master system. To close the chapter we shall discuss an application of solitons in the field of elementary particle physics, and describe how soliton-like objects occur in a large class of interesting systems known as σ -models. In chapter *III* we shall study a planar model, motivated by physics, in which the solitons are interpreted as elementary particles. Using a combination of analytical techniques and numerical computation the interaction and scattering of solitons in this model is investigated. In chapter *IV* it is described how approximations to solitons may be obtained through calculating instanton holonomies. The example studied in detail is that of the sine-Gordon model and through a curious observation we are in turn able to use the generated approximations to obtain Skyrme fields. Chapter *V* is concerned with testing the main approximation method used in studying soliton scattering. The method is tested in both the classical and quantum regime by applying it to the study of kink scattering in the sine-Gordon model, where exact results are known. Chapters *VI* and *VII* are concerned with a planar model in which exact analytic solutions can be found in closed form. In chapter *VI* we use twistor methods to construct the soliton solutions, give several useful formulations of the model, and investigate the stability of the soliton under radially symmetric perturbations. In chapter *VII* we use a numerical scheme to study the initial value problem for this model. Although exact multi-soliton solutions can be found analytically, in which soliton scattering is trivial, we find that soliton scattering can also be highly non-trivial in the same model. Finally, chapter *VIII* is an outlook of current and future research.

CHAPTER II.

Soliton Theory

2.1 SOLITONS IN INTEGRABLE SYSTEMS

One of the key equations of soliton theory is the KdV equation^[7]

$$u_t + 6uu_x + u_{xxx} = 0 \quad (2.1)$$

which was introduced in 1895 by Korteweg and de Vries to describe the propagation of waves on the surface of a shallow channel. It is easily verified that it has the travelling wave solution

$$u = 2k^2 \operatorname{sech}^2 k(x - 4k^2 t - x_0) \quad (2.2)$$

where x_0 gives the phase of the wave and $2k^2$ is the amplitude, which is equal to half the speed. In 1965 Zabusky and Kruskal^[8] performed numerical simulations of the KdV equation in connection with the study of phonon interactions in a one-dimensional anharmonic lattice, from which the KdV equation arises in the continuum limit. They found that from certain initial data a series of pulses emerged, each resembling the solitary wave solution (2.2). Since the speed of a solitary wave is proportional to its amplitude then the pulses eventually separated until they lined up in order of increasing size. Zabusky and Kruskal were using periodic boundary conditions in their simulations, so that the faster pulses eventually caught up to the slower ones and produced the following remarkable result. The larger pulse would overtake the smaller one and, despite the highly nonlinear interaction, would reappear intact with an unchanged speed and size. The only effect of the interaction was a phase shift of the pulses. This elastic collision behaviour is responsible for the pulse being named a soliton, which is meant to convey a particle-like nature (*cf* phonon, proton *etc*).

The numerical discovery of the soliton led to analytical work which centered first on the study of the conservation laws of the KdV equation and culminated in the much celebrated inverse scattering transformation (IST)^[9].

A conservation law is an equation of the form

$$\partial_t T = \partial_x F \quad (2.3)$$

where F is known as the current and T is the associated charge density. Provided the integrals of T and F are well defined, each conservation law leads to a conserved quantity since

$$\partial_t \int_{-\infty}^{+\infty} T dx = 0 \quad (2.4)$$

where suitable boundary conditions are imposed. (In the case of periodic boundary conditions the range of integration is over one period.) For example, the KdV equation may be written in the form (2.3) with

$$\begin{aligned} T &= u \\ F &= -(3u^2 + u_{xx}) \end{aligned} \quad (2.5)$$

and the associated conserved quantity is mass. It was shown^[10] by Miura that the KdV equation has an infinite number of conservation laws, and hence an infinite number of conserved quantities. These were found through the use of a nonlinear transformation, which is now known as the Miura map, and is an interesting mathematical object in its own right.

The IST is a nonlinear analogue of the Fourier transform, and relies upon the fact that the KdV equation can be written as the compatibility condition of an overdetermined linear system. Consider the following linear system

$$\mathcal{L}\Psi = \lambda\Psi \quad (2.6)$$

$$\Psi_t = \mathcal{P}\Psi \quad (2.7)$$

where \mathcal{L} and \mathcal{P} are operators, and λ is a complex constant known as the spectral parameter.

The compatibility condition for (2.6) and (2.7) is the equation

$$\mathcal{L}_t = [\mathcal{P}, \mathcal{L}] \quad (2.8)$$

Equations (2.6) and (2.7) are known as a Lax pair.^[11] The first equation may be considered as a scattering problem, in which case (2.8) is the condition that the spectrum remains constant. (2.8) is therefore known as an equation of isospectral flow. The connection with the KdV equation is made by choosing the following form for \mathcal{L} and \mathcal{P}

$$\begin{aligned} \mathcal{L} &= \partial^2 + u \\ \mathcal{P} &= 4\partial^3 + 6u\partial + 3u_x \end{aligned} \quad (2.9)$$

where ∂ denotes partial differentiation with respect to x . With this choice (2.8) becomes the KdV equation (2.1). The scattering equation (2.6) is the time-independent Schrödinger equation of quantum mechanics, with the potential given by the initial value of u . The determination of the scattering data from a given potential had already been studied^[12] by Gelfand and Levitan. The important observation, which lies at the heart of the IST, is that (2.7) results in the time evolution of the scattering data being particularly simple. This suggests the following method for solving the initial value problem of the KdV equation.

- (i). Determine the initial scattering data $S(0)$ given the potential u at $t = 0$.
- (ii). Solve the linear time evolution problem to give the scattering data $S(t)$.
- (iii). Invert the scattering transformation to obtain the solution $u(t)$ to the KdV equation.

For some special cases (when the spectrum of the scattering problem is discrete) the scattering transformation and its inversion can be solved exactly in closed form. In such cases the IST produces the multi-soliton solutions of the KdV equation.

The IST is a very powerful method for solving certain nonlinear evolution equations. Although initially applied to the KdV equation it was later used to solve other systems which also possess soliton solutions. The sine-Gordon equation,

$$\phi_{tt} - \phi_{xx} = \sin \phi \quad (2.10)$$

which arose first in the context of hyperbolic geometry,^[13] is another important equation of soliton theory. It too has a Lax pair formulation, and the IST can be applied to construct exact multi-soliton solutions. As with the KdV equation it has an infinite number

of conserved quantities. It would therefore seem that equations such as the KdV and sine-Gordon equation are in some sense special, and indeed they are examples of so called integrable systems. For systems with a finite number of degrees of freedom the notion of integrability is well defined, and relates the number of conserved quantities to the number of degrees of freedom of the system. For more general systems, such as the KdV equation, a definition of integrability is much more difficult to give. For our purposes we shall consider a system to be integrable if it can be written as the compatibility condition for an overdetermined linear system, and possesses an infinite number of conserved quantities. Many other definitions are possible,^[14] such as requiring the system to have the Painlevé property, or involving the applicability of some technique such as the IST. It should be stressed that integrable systems are very much the exception rather than the rule, and it is only in very special equations that dispersion effects are exactly balanced by nonlinearities thereby allowing soliton solutions to exist. It is characteristic of integrable systems that exact multi-soliton solutions may be constructed in closed form. In addition to the IST a variety of other methods have also been used to construct multi-soliton solutions, including Bäcklund transformations,^[15] where multi-soliton solutions are generated through a recursive procedure, and the direct bilinear method of Hirota.^[16] The direct method is a particularly convenient way of constructing soliton solutions, and does not make use of an associated linear problem, but instead relies upon finding a change of variables which then reduces the given equation to a certain bilinear form. As an example we shall use the Hirota method to construct the N-soliton solution of the KdV equation. The change of variable required for the KdV equation is

$$u = 2(\log \tau)_{xx} \quad (2.11)$$

upon which the KdV equation becomes

$$(D_x D_t + D_x^4)\tau \cdot \tau = 0 \quad (2.12)$$

where the Hirota derivatives are defined by

$$D_t^n D_x^m f \cdot g = (\partial_t - \partial_{t'})^n (\partial_x - \partial_{x'})^m f(x, t) g(x', t')|_{x=x', t=t'}$$

These derivatives have many special properties which make the construction of soliton solutions to bilinear equations, such as (2.12), an elegant procedure. In the Hirota formalism

the one-soliton solution of the KdV equation is given by

$$\tau = 1 + e^{\eta} \quad (2.13)$$

where

$$\eta_i = k_i x - k_i^3 t + \phi_i \quad (2.14)$$

The two-soliton solution is a natural generalization of this and is given by

$$\tau = 1 + e^{\eta_1} + e^{\eta_2} + e^{\eta_1 + \eta_2 + A_{12}} \quad (2.15)$$

where

$$e^{A_{ij}} = \left(\frac{k_i - k_j}{k_i + k_j} \right)^2 \quad (2.16)$$

The quantity A_{12} is related to the phase shift which the two solitons experience as they collide. For completeness we give the expression for the N-soliton solution

$$\tau = \sum_{\mu_1=0}^1 \cdots \sum_{\mu_N=0}^1 \exp\left(\sum_{i>j} A_{ij} \mu_i \mu_j + \sum_{i=1}^N \mu_i \eta_i\right) \quad (2.17)$$

from which it can be seen that the phase shift experienced by a soliton which undergoes several collisions is merely the sum of the phase shifts from each individual collision, regardless of the order in which the collisions take place.

Together with the discovery of new techniques for constructing solutions, there has also been great progress in identifying those equations which possess solitons. Today there are many examples of integrable systems with soliton solutions, and many equations are known to have a whole hierarchy of integrable equations associated with them. However, the majority of soliton systems are confined to one space dimension, and in higher dimensions soliton theory is not so well understood. There are examples of integrable planar systems (ie where space is two dimensional) such as the Kadomtsev-Petviashvili^[17] (KP) and Davey-Stewartson^[18] equations, which are solvable by the IST, but most are simple generalizations of familiar examples from one space dimension. The KP equation

$$(u_t + 6uu_x + u_{xxx})_x + 3u_{yy} = 0 \quad (2.18)$$

is an example of an integrable equation in (2+1)-dimensions. It describes the propagation of waves in shallow water and is a two-dimensional version of the KdV equation. If we

impose the condition that u is independent of the space variable y then (2.18) clearly reduces to (2.1). From the point of view of the IST the spectral problem is obtained by promoting the spectral parameter λ to a differential operator ∂_y , and in this way a second space coordinate y is introduced. Although the IST can then be used to solve (2.18) the soliton solutions obtained are plane wave solitons, which are one-dimensional in character. Truly two-dimensional solitons (ie localised in all space directions) can only be obtained through other constructions, such as the Hirota method, and then only after certain limiting procedures have been made. It would therefore appear that such planar systems have a manifestly one-dimensional nature and may not be the most general extension of soliton equations to two space dimensions. In the following section we shall see how a unifying framework for one-dimensional integrable equations also produces integrable planar systems.

2.2 THE SELF-DUALITY EQUATIONS AND THE UNITY OF INTEGRABLE SYSTEMS

It has been conjectured^[19] that the self-dual Yang-Mills equations (sdYM) may provide a unifying framework for integrable systems, in that many integrable equations may be obtained as reductions of this one master equation. In this section we shall briefly review this work. Consider a Yang-Mills gauge theory with gauge group G which has Lie algebra \mathfrak{g} . Let spacetime M be four-dimensional with coordinates x^μ , where μ ranges over the values 0, 1, 2, 3. Let the metric be flat, and for the moment we shall leave the signature arbitrary.

The gauge potential A_μ is a 1-form on M taking values in \mathfrak{g} , and the field strength is $F_{\mu\nu} = \partial_\mu A_\nu - \partial_\nu A_\mu + [A_\mu, A_\nu]$.

The sdYM equations are given by

$$F_{\mu\nu} = \frac{1}{2} \epsilon_{\mu\nu\alpha\beta} F^{\alpha\beta} \quad (2.19)$$

where $\epsilon_{\mu\nu\alpha\beta}$ is the totally antisymmetric tensor with $\epsilon_{0123} = 1$.

This equation is integrable in the sense that it may be written as the compatibility condition of an overdetermined linear system, and has an infinite number of conservation laws. It is an important equation of particle physics, and occurs as a first order (in the gauge potential) system whose solutions automatically satisfy the second order Yang-Mills

equation

$$D_\mu F^{\mu\nu} = 0. \quad (2.20)$$

where $D_\mu = \partial_\mu - A_\mu$ is the covariant derivative.

(2.20) has a Lagrangian formalism and in a Euclidean spacetime (ie $M=\mathbf{R}^4$) solutions of the self-duality equations which have finite action are known as instantons.

There are two types of reduction that may be performed on the sdYM equations;

(i). Dimensional reduction - where the number of independent variables are reduced by factoring out by a subgroup of the Poincare group.

(ii). Algebraic reduction - where the number of dependent variables are reduced by imposing algebraic constraints on the dependent fields, in a way consistent with the equations.

In general, in order to obtain a particular integrable system requires a combination of both these reductions. As an example, we shall now show how the KdV equation may be obtained as a reduction of the sdYM equations.^[20]

Choose $M=\mathbf{R}^{2+2}$ with the metric given by

$$ds^2 = dx_0^2 - dx_1^2 - 2dx_2dx_3 \quad (2.21)$$

which has signature (2,2). The sdYM equations are equivalent to the compatibility condition of the following overdetermined linear system

$$\begin{aligned} [D_0 - D_1 + \lambda D_3]\Psi &= 0 \\ [D_2 - \lambda(D_0 + D_1)]\Psi &= 0 \end{aligned} \quad (2.22)$$

Take the gauge group G to be $SL(2,\mathbb{C})$. Reduce from (2+2)-dimensions to (1+1)-dimensions by factoring out by the timelike killing vector ∂_1 and the null killing vector ∂_2 . All fields are now functions of only the coordinates x_0 and x_3 . Next impose the algebraic constraints

$$\begin{aligned} A_2 &= \begin{pmatrix} 0 & 0 \\ 1 & 0 \end{pmatrix} \\ A_0 = -A_1 &= \frac{1}{2} \begin{pmatrix} q & 1 \\ \partial_0 q - q^2 & -q \end{pmatrix} \\ A_3 &= -\frac{1}{2} \begin{pmatrix} \partial_0(\partial_0 q - q^2) & -2\partial_0 q \\ 2w & -\partial_0(\partial_0 q - q^2) \end{pmatrix} \end{aligned} \quad (2.23)$$

where $4w = \partial_0^3 q - 4q\partial_0^2 q - 2(\partial_0 q)^2 + 4q^2\partial_0 q$

Finally, define

$$u = -2\partial_0 q \quad (2.24)$$

and after introducing the coordinates $x = x_0$, $t = \frac{1}{4}x_3$, the sdYM equation (2.19) becomes the KdV equation (2.1).

Many of the known integrable systems in (1+1)-dimensions can also be shown to be reductions of the sdYM equations, but some higher dimensional systems, such as the KP equation, do not as yet appear to fit into this scheme. There are indications that what may be required is an infinite dimensional gauge group. ^[21,22,23]

If we again begin with the sdYM equations in (2+2)-dimensions, but this time reduce by only a timelike killing vector, we obtain an integrable system in (2+1)-dimensions. Explicitly, take the metric to be

$$ds^2 = dx_0^2 - dx_1^2 - dx_2^2 + dx_3^2 \quad (2.25)$$

and reduce by imposing the condition that all fields are independent of the second time coordinate x_3 . Then the sdYM equation becomes

$$D_\mu \Phi = \frac{1}{2} \epsilon_{\mu\alpha\beta} F^{\alpha\beta} \quad (2.26)$$

where $\Phi = A_3$, and μ runs over 0,1,2. This is the Yang-Mills-Higgs-Bogomolny equation, which is hyperbolic and describes the time evolution of a Yang-Mills-Higgs system in (2+1)-dimensions. We shall study the soliton solutions of this equation in more detail in chapters VI and VII. A similar reduction of the self-duality equations in (4+0)-dimensions, ie $M=\mathbf{R}^4$, but this time by a spacelike vector, gives the Bogomolny equation for static monopoles in three space dimensions, ^[24] which has a similar form.

In order to obtain the KdV equation as a reduction of the sdYM equation the metric was taken to have signature (2,2). This signature of metric is used in all reductions to obtain integrable systems in (1+1)-dimensions. In order to obtain integrable static systems, such as the monopole equation, the metric is taken to have signature (4,0). The remaining possibility is therefore to consider a metric with signature (3,1). With this choice the self-duality equations only allow complex gauge groups, and not real forms

such as $SU(N)$. This is a severe limitation for relevance to particle physics, but in terms of soliton theory is not so restricting, and indeed studies of plane-wave soliton^{[25] [26]} solutions in this system have been made.

Methods from soliton theory, such as the IST and Bäcklund transformations, have been used^[27] to construct instanton solutions of the sdYM equation, and monopole solutions of the related Bogomolny monopole equation. A particularly useful technique is the twistor approach,^[28] which has been useful in constructing solutions of both these equations. It was shown^[29] that the instanton solutions of the sdYM equation correspond to certain holomorphic vector bundles over an associated complex manifold known as twistor space. By explicit construction of these bundles one can therefore obtain solutions to the sdYM equation. For an equation which is a reduction of sdYM, such as the monopole equation, this correspondence can also be reduced and used to construct solutions. The twistor method can be used on reductions of sdYM from $(2+2)$ -dimension, for example, to construct the soliton solutions of the sine-Gordon equation.^[30] In chapter VI we shall use twistor methods to construct soliton solutions of (2.26).

So far we have been dealing with soliton solutions of integrable systems. The usual definition of a soliton requires it to have certain properties.

- (i). That it be localised in space. Although in planar systems, such as the KP equation, solutions which are plane-waves, and therefore only localised in one space direction, are also known as solitons.
- (ii). That it behaves elastically under collision with other solitons.
- (iii). That it is stable against small perturbations.

The soliton concept has now become important in many scientific fields, most notably in elementary particle physics,^[31] and many localised objects have been named solitons, even though they may not satisfy all of the above conditions. From this point in our discussion we shall go along with a looser definition, and require that a soliton be a solution to a nonlinear equation which is localised in space and propagates with little change of shape. We shall require a stability to small perturbations but shall allow collisions to be inelastic. To the soliton theorist such structures may be called at most solitary waves, and in order to avoid confusion we shall attempt to make clear the properties of each of the solitons we consider.

2.3 SKYRMIONS

A soliton, being a localised structure which preserves its form during propagation and collision, appears like an ideal mathematical structure to describe a particle. The first appearance of solitons in particle physics was in the work of Skyrme,^[32] who used the sine-Gordon equation (2.10) as a toy model for a nonlinear meson field theory. This was in the days before quark theory and was an attempt at a unified description of hadrons (mesons and baryons), which were then the fundamental particles known in physics. The idea is that the field of the sine-Gordon equation is a meson field and the baryons (in particular the proton and neutron) occur as the solitons of the model. The baryon (or soliton) number, which is a fundamental conserved quantity, then has a natural interpretation in terms of the topological properties of the field, as described below. For the sine-Gordon field, ϕ , to have finite energy it must satisfy the boundary condition

$$\cos \phi = 1 \quad \text{at} \quad x = \pm\infty \quad (2.27)$$

Therefore,

$$\begin{aligned} \phi(x = +\infty, t) &= 2\pi n_+ \\ \phi(x = -\infty, t) &= 2\pi n_- \end{aligned} \quad (2.28)$$

where $n_{\pm} \in \mathbb{Z}$. Then

$$B = n_+ - n_- = \frac{1}{2\pi} \int_{-\infty}^{+\infty} \partial_x \phi \, dx \quad (2.29)$$

is an integer which is interpreted as the baryon (soliton) number. Because ϕ evolves continuously it must remain constant at $\pm\infty$, since from (2.28) it takes discrete values there, and so the baryon number is a conserved quantity. The sine-Gordon soliton may therefore be thought of as a topological soliton.

Skyrme performed numerical simulations of soliton scattering in the sine-Gordon equation, in order to simulate the scattering of baryon particles. He discovered the purely elastic scattering of sine-Gordon solitons and was able to construct an analytical expression for the exact two-soliton solution. In an attempt at a more realistic unified field theory he considered^[33] a nonlinear model in three space dimensions, involving an $SU(2)$ -valued field. This Skyrme model again places importance on the topological aspects of the theory and has topological solitons, known as Skyrmions, which are interpreted as baryons.

This classical solitonic approach to particle physics was, however, largely ignored. With quantum field theory, in which particles appeared as elementary excitations of a quantized field, the particle physicist did not appear to need the soliton. The propagation of a free particle is described by a quantized mode of a linear system, and not by a soliton solution of a nonlinear equation. Nonlinear interactions among quantum fields are described through perturbation theory, although it became increasingly apparent that a perturbative description of some phenomena was very difficult. At low energies, hadron physics is certainly non-perturbative and attention has focused upon the use of effective theories to describe the relevant physics. Following a recent observation by Witten,^[34] there has been renewed interest in the Skyrme model, and again an interpretation of baryons as the solitons in such a model is popular.

The Skyrme model is based upon the Lagrangian density

$$\mathcal{L} = -\frac{1}{2}\text{Tr}(\partial_\mu U \partial^\mu U^{-1}) - \frac{1}{16}\text{Tr}([\partial_\mu U \cdot U^{-1}, \partial_\nu U \cdot U^{-1}][\partial^\mu U \cdot U^{-1}, \partial^\nu U \cdot U^{-1}]) \quad (2.30)$$

where x^μ , $\mu = 0, 1, 2, 3$, are the spacetime coordinates with metric $\eta^{\mu\nu} = \text{diag}(-1, 1, 1, 1)$. U is a map $U : \mathbf{R}^{3+1} \rightarrow \text{SU}(2)$ and Tr denotes trace. For the configuration to have finite energy the boundary condition

$$U(\mathbf{x}) \rightarrow \mathbf{1} \quad \text{as} \quad |\mathbf{x}| \rightarrow \infty \quad (2.31)$$

must be imposed, where the vacuum has been taken to be $U = \mathbf{1}$, the 2 by 2 identity matrix. This boundary condition effectively compactifies space from \mathbf{R}^3 to S^3 , so that at a fixed time U is a map $U : S^3 \rightarrow \text{SU}(2)$. For such maps, since S^3 is the group manifold of $\text{SU}(2)$, the relevant identity is the homotopy group relation^[35]

$$\pi_3(S^3) = \mathbb{Z} \quad (2.32)$$

which implies that to each field configuration there may be associated an integer, known as the topological charge, which is conserved and represents the winding number of the field as a map from space to the target manifold. This winding number is interpreted as the baryon number and is given by

$$B = \frac{1}{24\pi^2} \int \epsilon_{ijk} \text{Tr}[(U^{-1} \partial_i U)(U^{-1} \partial_j U)(U^{-1} \partial_k U)] d^3 \mathbf{x} \quad (2.33)$$

where indices range over the values 1,2,3.

The static one-soliton solution (ie $B=1$) is known as the Skyrmion and has the form

$$U(\mathbf{x}) = \cos f(r) + i \frac{\sin f(r)}{r} \mathbf{x} \cdot \boldsymbol{\sigma} \quad (2.34)$$

where $r = |\mathbf{x}|$, $\boldsymbol{\sigma}$ are the usual Pauli matrices and $f(r)$ is a profile function, which has to be determined numerically,^[36] with the boundary conditions $f(0) = \pi$, $f(r) \rightarrow 0$, as $r \rightarrow \infty$. This Skyrmion is centered at the origin, but maybe moved to any position by a translation. The orientation may also be changed by conjugation of U by some fixed element of $SU(2)$. The Skyrmion is a stable structure and so satisfies our criterion for a soliton. The physical nucleons are obtained by promoting the position and orientation to dynamic variables which are then quantized.

Experimentally it is known that there is a bound state of a proton and neutron (the deuteron), and there is a vast amount of scattering data. To understand the low energy interaction of nucleons requires the study of multi-Skyrmion systems. Even the one-Skyrmion solution (2.34) can only be determined numerically and the study of a two-Skyrmion system has many difficulties. The fact that the model is a three-dimensional space system also means that numerical studies require powerful computers and large amounts of computing time. Some progress has been made^[37] on the numerical calculation of static multi-Skyrmion systems, and demonstrates the rich and novel structure of such solutions. The vast computing power required[†] to calculate static multi-Skyrmions makes a study of dynamics impractical unless new techniques or approximations can be used to truncate the full field theory. One such approximation, known as the slow motion approximation, has been used in the study of soliton dynamics in several systems and may prove of use here. To implement such an approximation, however, requires the identification of the full manifold of a two-Skyrmion solution. This has proved a difficult problem, although progress has been made through the use of some ingenious techniques.^[38] In chapter III we shall study the dynamics of Skyrmons in a two-dimensional space analogue of the Skyrme model. In this planar model the expression for a one-Skyrmion solution can be given in closed form and moreover has a simple form. This makes the identification of a suitable truncated two-Skyrmion manifold a much simpler and more tractable problem. For a planar system the comparison of such approximations with full field simulations can also be made, since the latter are just feasible with modern computing power.

† To determine the static Skyrmons of [37] required 170 hours CPU time on a CRAY-2 supercomputer

2.4 SIGMA MODELS AND LUMPS

The importance of the topological aspects of soliton theory has already been demonstrated, with the topological solitons of the sine-Gordon and Skyrme models of the last section. Topological soliton-like structures (known as lumps) occur in a large class of nonlinear systems known as σ -models. A σ -model is a nonlinear field theory, in which the field takes values in a Riemannian manifold \mathcal{M} , whose curvature is responsible for the nonlinearity of the theory. As an example, we shall consider the $O(3)$ σ -model, in $(2+1)$ -dimensions. The field of the $O(3)$ model is a real three vector which is constrained to have unit length, ie

$$\boldsymbol{\phi} = (\phi_1, \phi_2, \phi_3) \quad (2.35)$$

with the constraint

$$\boldsymbol{\phi} \cdot \boldsymbol{\phi} = 1 \quad (2.36)$$

The target manifold is therefore a two-sphere, ie $\mathcal{M} = S^2$. The name $O(3)$ refers to the symmetry of the model under rotations of $\boldsymbol{\phi}$ by a constant $O(3)$ matrix. The equations of motion are given by

$$\partial_\mu \partial^\mu \boldsymbol{\phi} + (\partial_\mu \boldsymbol{\phi} \cdot \partial^\mu \boldsymbol{\phi}) \boldsymbol{\phi} = 0 \quad (2.37)$$

where again the spacetime metric is the Minkowski metric $\eta^{\mu\nu} = \text{diag}(-1, 1, 1)$. This equation of motion is derived from the free field Lagrangian

$$\mathcal{L} = \frac{1}{4} \partial_\mu \boldsymbol{\phi} \cdot \partial^\mu \boldsymbol{\phi} \quad (2.38)$$

and the nonlinearities are due to the constraint (2.36).

The possibility of topological solitons, in two space dimensions, can again be seen from the homotopy relation

$$\pi_2(\mathcal{M}) = \pi_2(S^2) = \mathbb{Z} \quad (2.39)$$

This is a planar analogue of the relation (2.32), which allowed the possibility of topological solitons, the Skyrmions, to exist in three space dimension. The expression for the winding

number in the $O(3)$ model is

$$N = \frac{1}{8\pi} \int \epsilon_{ij} \phi \cdot (\partial_i \phi \wedge \partial_j \phi) d^2 x \quad (2.40)$$

where $i = 1, 2$ with $x^i = (x, y)$. This topological charge is the particle number and is analogous to the baryon number (2.33) for Skyrmions.

The static lump solutions are most easily written in terms of a complex field W , which is the stereographic projection of ϕ from the point $\phi_3 = 1$ onto the complex plane, ie

$$W = \frac{\phi_1 + i\phi_2}{1 - \phi_3} \quad (2.41)$$

which is an element of the coset space $\mathbb{C}\mathbb{P}^1$, where

$$\mathbb{C}\mathbb{P}^n = \frac{SU(n+1)}{SU(n) \times U(1)} \quad (2.42)$$

This alternative $\mathbb{C}\mathbb{P}^1$ description of the $O(3)$ model is possible because $\mathbb{C}\mathbb{P}^1$ is isometric to S^2 . The Lagrangian in the $\mathbb{C}\mathbb{P}^1$ formulation is

$$\mathcal{L} = \frac{\partial_\mu W \partial^\mu \bar{W}}{(1 + |W|^2)^2} \quad (2.43)$$

The static lumps (anti-lumps) are given by ^[39,40] W a holomorphic (anti-holomorphic) function of $z = x + iy$. For finite energy W is required to be a rational function, and the degree of this rational function is equal to the topological charge N . The energy of a static N -lump solution is given by

$$E = 2\pi N \quad (2.44).$$

The S^2 target space may have arbitrary orientation in internal space without affecting the energy. The choice of orientation corresponds to fixing three overall phases, thereby removing three real degrees of freedom from the solution. Up to this choice of orientation the most general one-lump solution is given by

$$W = \lambda(z - a) \quad (2.45)$$

where a is a complex constant which determines the position of the lump in the complex z -plane, and λ is a real constant which determines the size-scale of the lump. The maximum

of the energy density occurs at $z = a$, at which it takes the value $2\lambda^2$. The scale λ is therefore a measure of the height of the lump. Exactly half the total energy of the lump is contained within a radius λ^{-1} , which is therefore also a measure of the width of the lump. The \mathbb{CP}^1 (or equivalently $O(3)$) model is Lorentz invariant, ie (2.43) has an $SO(2,1)$ spacetime symmetry. This allows a static lump to be Lorentz boosted in order to obtain a lump solution which moves at constant velocity. Explicitly the Lorentz boost is achieved through the replacement

$$z \rightarrow z + kt + k^2 \bar{z} \quad (2.46)$$

where k is a complex constant which determines the velocity of the lump in the z -plane. If a static N -lump solution is Lorentz boosted then all the lumps move with the same velocity. Unlike the integrable examples of section 1, there is no solution in closed form which represents multi-lumps which move with arbitrary *independent* velocities. The \mathbb{CP}^1 model is integrable in $(2+0)$ -dimensions, where there is a Lax pair formulation, but the introduction of time dependence destroys the integrability. The study of the dynamics of \mathbb{CP}^1 lumps is therefore a highly non-trivial problem^[41,42] which often requires the use of numerical and computing techniques.

The \mathbb{CP}^1 model is conformally invariant in $(2+0)$ -dimensions, which is reflected in the fact that the static one-lump (2.45) can have an arbitrary size λ . The total energy is independent of this size, as shown by (2.44). The topological nature of the lumps prevents decay to the vacuum, since the vacuum has zero topological charge. However, the conformal invariance of the model leads to the lumps being unstable. Using numerical simulations it has been shown^[43] that under perturbations the size of the lump tends either to shrink towards zero or to grow without limit. It is this instability that prevents the lumps from satisfying our definition of a soliton. The Skyrmions of the last section are solitons, since the Skyrmion does not suffer from this type of instability. This is due to the fact that the Skyrme model in $(3+0)$ -dimensions is not scale invariant and the second term in (2.30) (known as the Skyrme term) introduces a finite preferred scale. In chapter III we shall study a modification of the \mathbb{CP}^1 model in which a Skyrme-like term is introduced. The lump then becomes a planar analogue of the Skyrmion, and the instability is removed, making it a true soliton.

The \mathbb{CP}^1 model and the $O(3)$ model are equivalent, but they have inequivalent gen-

eralizations. The $\mathbb{C}\mathbf{P}^1$ model generalizes to a $\mathbb{C}\mathbf{P}^{n-1}$ target manifold. Write

$$\mathbf{P} = \frac{1}{(1 + |W|^2)} \begin{pmatrix} 1 & W \\ \bar{W} & |W|^2 \end{pmatrix} \quad (2.47)$$

which is a one-dimensional hermitian projector

$$\mathbf{P} = \mathbf{P}^\dagger = \mathbf{P}^2. \quad (2.48)$$

The equation of motion of the $\mathbb{C}\mathbf{P}^1$ model in terms of this projector formalism is

$$[\square\mathbf{P}, \mathbf{P}] = 0. \quad (2.49)$$

where $\square = \partial_\mu \partial^\mu$ is the wave operator in (2+1)-dimensions. The $\mathbb{C}\mathbf{P}^{n-1}$ σ -model is obtained by simply increasing the rank of \mathbf{P} , so that it is an $n \times n$ hermitian projector.

In the $O(n)$ σ -model the target manifold is S^{n-1} . The Lagrangian is again the free field Lagrangian (2.38), where ϕ is a real n -component vector, constrained to unit length. Consider the $O(4)$ model, and write

$$J = \mathbf{1}\phi_0 + i\sigma \cdot \phi \quad (2.50)$$

where σ are the usual Pauli matrices. Then $J \in \text{SU}(2)$, and the equation of motion becomes

$$\partial_\mu (J^{-1} \partial^\mu J) = 0. \quad (2.51)$$

This is the $\text{SU}(2)$ Chiral model, and has the Lagrangian density

$$\mathcal{L} = -\frac{1}{2} \text{Tr}(\partial_\mu J \partial^\mu J^{-1}). \quad (2.52)$$

Note that this is the first term of the Skyrme model (2.30). The additional Skyrme term is added to this σ -model action in order to allow the existence of stable topological solitons. The planar model of chapter III is constructed in just this way, but with the $O(3)$, rather than the $O(4)$, model used as the basic Lagrangian, in order to match the topological properties of the target manifold to the number of space dimensions.

By, for example, setting $\phi_0 = 0$ we can restrict the $O(4)$ model to a totally geodesic $O(3)$ subspace. In terms of the $\text{SU}(2)$ Chiral formulation this corresponds to restricting J to an anti-hermitian submanifold, ie $J = -J^\dagger$. With this restriction the $O(4)$ and $O(3)$ models are equivalent, so that solutions can be obtained through an embedding procedure. This is used in chapter VII in the study of soliton scattering in an integrable modification of the $\text{SU}(2)$ chiral model.

CHAPTER III.

The Dynamics of Planar Skyrmions

3.1 INTRODUCTION

There are many examples where solitons play an important role in classical field theories. In three spatial dimensions they include BPS monopoles and Skyrmions, while in planar systems there are vortices of the abelian Higgs model and more general extended structures in the nonlinear σ -models. The above examples in (3+1) and (2+1)-dimensions all have a Lorentz invariant Lagrangian formulation, but are not integrable. It is not known whether an integrable and Lorentz invariant Lagrangian model exists in dimensions higher than (1+1).

In this chapter we study a Lorentz invariant, non-integrable, planar model^[44] which has stable soliton solutions, and has links with all the main non-integrable examples given earlier. The model is similar to monopoles and vortices in that parameters exist in the Lagrangian which determine the size of the extended structure. Furthermore when a particular limit of these parameters is taken (this corresponds to the BPS limit in the case of monopoles) the force between extended structures vanishes. The link with other examples will be clear when the model is given explicitly, and we shall see that the model is a planar analogue of the Skyrme model. It also contains the $O(3)$ σ -model as a limiting case.

An obvious motivation for the study of the model stems from its connection to so many of the important Lorentz invariant non-integrable soliton systems, and it may prove useful in any attempt at a general description of models of this form. The model is also a useful test-bed for techniques to study the dynamics of Skyrmions in three-dimensional space, where Skyrmions are interpreted as baryons, and provide a good approximation to a description of low energy hadron physics.

3.2 PLANAR SKYRMIONS

The model we study is based upon the \mathbb{CP}^1 (or equivalently the $O(3)$) σ -model in (2+1)-dimensions. Recall from chapter II that the \mathbb{CP}^1 model is defined in terms of a complex scalar field W and is given by the Lagrangian density

$$\mathcal{L} = \frac{\partial_\mu W \partial^\mu \bar{W}}{(1 + |W|^2)^2} \quad (3.1)$$

where the metric is the Minkowski metric $\eta^{\mu\nu} = \text{diag}(-1,1,1)$. As described earlier, the \mathbb{CP}^1 model has localised lump solutions, but these lumps are unstable. In an attempt to remove the instability associated with \mathbb{CP}^1 lumps a modification of the model was introduced^[44], following the ideas of Skyrme^[33], and involving the introduction of a term quartic in derivatives. In (3+1)-dimensions the Skyrme term is sufficient to stabilize the soliton (Skyrmion), by introducing a scale into the model so that the Skyrmion has a fixed size. However, in (2+1)-dimensions it is not sufficient and a potential term had also to be introduced.

Explicitly, the modified model is defined in terms of a complex scalar field W and is given by^[44] the Lagrangian density

$$\mathcal{L} = \frac{\partial_\mu W \partial^\mu \bar{W}}{(1 + |W|^2)^2} + \frac{8\theta_1 ((\text{Im}(\bar{W}_t W_x))^2 + (\text{Im}(\bar{W}_t W_y))^2 - (\text{Im}(\bar{W}_x W_y))^2) + 4\theta_2}{(1 + |W|^2)^4} \quad (3.2)$$

where θ_1 and θ_2 are two real and positive parameters of the theory. Here Im denotes the imaginary part and subscripts denote partial differentiation.

The first term is the Lagrangian of the \mathbb{CP}^1 model, the term proportional to θ_1 is the analogue in (2+1)-dimensions of the Skyrme term, and the final term is the required potential term. It should be noted that this Lagrangian still maintains the desirable property of Lorentz invariance. The lumps of this model have the soliton property of stability to small perturbations, and we shall refer to such structures as planar Skyrmons. It is the study of the interaction between planar Skyrmons which is the main topic of this chapter.

As our investigation reported here is concerned with the Skyrmon solutions of the model (3.2) it is more convenient to introduce the complex variables z and \bar{z} defined by $z = x + iy$ and $\bar{z} = x - iy$

Skyrmion solutions correspond to W being a holomorphic function of z , and so without loss of generality we may assume that W is of this type. This allows the Lagrangian density to be written in the more compact form

$$\mathcal{L} = (|W_t|^2 - 2|\partial W|^2) \frac{1}{(1 + |W|^2)^2} + 4(2\theta_1|\partial W|^2(|W_t|^2 - |\partial W|^2) - \theta_2) \frac{1}{(1 + |W|^2)^4} \quad (3.3)$$

where ∂ denotes partial differentiation with respect to z .

The most general ansatz for a static one Skyrmion configuration is

$$W = \lambda(z - b) \quad (3.4)$$

where λ and b are arbitrary complex numbers. The model has a global $U(1)$ symmetry that we shall use to choose λ to be real. It can easily be checked that the equations of motion resulting from the Lagrangian are satisfied only if $\lambda = \lambda_c$ where

$$\lambda_c = \left(\frac{\theta_2}{2\theta_1} \right)^{\frac{1}{4}} \quad (3.5)$$

which we shall term the canonical height, for the reason to be explained below.

The energy density of the ansatz (3.4) has a maximum at $z = b$, at which it takes the value

$$\mathcal{E}_{max} = 2\lambda^2 + 8\theta_1\lambda^4 + 4\theta_2 \quad (3.6)$$

We shall say that (3.4) describes a Skyrmion of height λ with position b . Approximately half the total energy of the Skyrmion is contained within a radius λ^{-1} which is therefore also a measure of the width of the Skyrmion.

The total energy of the ansatz (3.4) is found to be

$$E(\lambda) = 2\pi \left(1 + \frac{4}{3}\theta_1\lambda^2 + \frac{2}{3}\frac{\theta_2}{\lambda^2} \right) \quad (3.7)$$

This clearly demonstrates the stabilising nature of each of the terms. The Skyrme term contains a λ factor in the numerator and so prevents the height from becoming infinite, whereas the potential term contains a λ factor in the denominator and so prevents the height becoming zero.

A scale has thus been introduced into the model and the Skymion now has a fixed height. The mass of a static Skymion is given by

$$M = E(\lambda_c) = 2\pi\left(1 + \frac{8}{3}\sqrt{\frac{\theta_1\theta_2}{2}}\right) \quad (3.8)$$

A candidate for a static two Skymion solution would contain quadratic powers in z , but unlike the \mathbb{CP}^1 model, no such solution has been found. Obviously the superposition of a pair of static one Skymion solutions may be considered but since this is not a solution it implies that this structure will evolve in time. It is the investigation of the interaction between the two such Skymions that shall form the basis of our discussion.

3.3 A COLLECTIVE COORDINATE APPROACH

The majority of investigations concerning the scattering of extended structures are based upon the method of Manton.^[45] This involves a truncation of the full field theory to a finite dimensional system where motion is then confined to a manifold \mathcal{M} determined by this truncation. For models in which there are no static forces between extended structures the dynamics of the system then follows from consideration of the geodesics in this manifold, where the metric is determined by the form of the kinetic energy. Such a method has been used in the study of BPS monopoles^[46] and also vortices^[47] at critical coupling. A justification of this procedure is given by consideration of the nature of this manifold, and the assumption that the motion is confined to a region where the potential energy is close to the lower bound induced by the topological nature of the field configuration. For the model considered here static forces do exist between Skymions, but these forces are weak. In such a situation the truncation of the model to a manifold \mathcal{M} may still be given some justification but now \mathcal{M} has both a non-trivial metric and a non-trivial potential energy function. One of the aims of this paper is to illustrate that such a collective coordinate method is still justified.

In order to study the interaction between two Skymions we consider the configuration where the Skymions lie on the real axis, are of equal height, and are equidistant from the origin. There is little loss of generality here since fixing the centre of mass of the system has no effect upon the interaction. The model is truncated to a two dimensional manifold

by assuming that at all times the Skyrmions are well approximated by an ansatz

$$W = Cz^2 - D \quad (3.9)$$

where C and D are two real parameters related to the height and separation of the Skyrmions. These parameters are the collective coordinates which provide an explicit parametrization of \mathcal{M} .

For two Skyrmions which are well separated (i.e. have minimal overlap) a product ansatz is a good approximation to the configuration, and takes the form

$$W = \frac{\lambda}{2b}(z^2 - b^2) \quad (3.10)$$

where λ is the height of each of the Skyrmions which are positioned at the points $(+b,0)$ and $(-b,0)$ in the (x,y) plane. By an appropriate comparison of these two ansätze an interpretation of C and D in terms of the position and heights of the Skyrmions can be made. Recall that λ^{-1} is a measure of the Skyrmions width and so this interpretation of C and D is valid only within the region $b > \lambda^{-1}$. Outside this region the energy density no longer resembles two distinct Skyrmions and must be examined for each value of C and D in order to obtain a physical interpretation of these parameters.

The C and D variables of the ansatz are now allowed to be time dependent. Substituting (3.9) into the Lagrangian density and integrating gives the total Lagrangian

$$L = E\dot{C}^2 + F\dot{C}\dot{D} + G\dot{D}^2 - V \quad (3.11)$$

where E, F, G, V are functions of C and D and involve integrating the complex variable z over the whole complex plane. Dot denotes differentiation with respect to the time variable t .

This is the effective Lagrangian for the model, and leads to the Euler-Lagrange equations.

$$\begin{aligned} \frac{d}{dt} \left(\frac{\partial T}{\partial \dot{C}} \right) - \frac{\partial T}{\partial C} + \frac{\partial V}{\partial C} &= 0 \\ \frac{d}{dt} \left(\frac{\partial T}{\partial \dot{D}} \right) - \frac{\partial T}{\partial D} + \frac{\partial V}{\partial D} &= 0 \end{aligned} \quad (3.12)$$

Note that if the motion is confined to a region where the potential varies little above the topological lower bound, then the terms involving the derivative of the potential

may be ignored. This leads us back to the geodesic motion with the metric determined by the kinetic energy. With the above system of equations the dynamics are known if the functions E, F, G, V together with their derivatives can be found. Recall that these functions involve calculating integrals over the complex plane. Unfortunately these integrals can not be done analytically. Thus in order to evolve the system we must resort to numerical integration methods.

The results of the next section were obtained using an AMDAHL 5860 with the MTS operating system at Durham, where extensive use was made of the NAG numerical libraries. The time evolution of the equations (3.12) were implemented using a fourth-order Runge-Kutta method. Checks on numerical errors were performed in a number of ways, including checks on total energy conservation, and repeating simulations with varying stepsizes for the evolution parameters.

A final point regards the choice of the parameters θ_1 and θ_2 of the model, which were taken to be $\theta_1 = 1.9531 \times 10^{-3}$ and $\theta_2 = 1.0$. From section 2, this implies a canonical height of $\lambda_c = 4.0$. The choice of these particular values is motivated by the requirement that the canonical height be of a reasonable value. Also the parameters should be such that the energy of the Skyrme and potential terms should be a small percentage of the total energy in order to justify the model to be a small perturbation of the \mathbb{CP}^1 model.

The general features of the model are not dependent upon the choice of these parameters, with the analytical calculations of section 5 valid for all values of θ_1 and θ_2 . Specific values will, however, be used in order to compare with the numerical simulations.

3.4 SKYRMION SCATTERING

We know from the general discussion of section 2, that there are no static two Skyrmion configurations. This implies that a force exists between Skyrmons, and in order to investigate this force we need to examine the evolution of two Skyrmons with varying initial conditions. We shall be dealing with two Skyrmons that lie on the real axis, equidistant from the origin and of equal height. This is exactly the situation described in the previous section, and the same notation will be used here to describe the configuration in terms of a position b and a height λ as described by the ansatz (3.9).

We begin by studying Skyrmons with the initial values $b = 0.5$ and $\lambda = \lambda_c = 4.0$. This particular choice of b is motivated by the requirement that the Skyrmons be distinct

(ie. their overlap is minimal) but that they be within a reasonable range of each other so that any interaction forces will be easily observed. Fig 3.1 shows the resulting motion.

It is clearly evident that there is a weak repulsion between two Skyrmions which results in their separation becoming infinite. The Skyrmions move with an almost linear trajectory once their separation is beyond a certain value, which indicates the short range nature of the force. The most interesting feature is that the height appears to oscillate with decreasing amplitude around a value which is larger than the canonical height λ_c but which decreases towards λ_c with increasing separation. This suggests that the interaction between Skyrmions results in a preferred height $\lambda_p(b)$ which is dependent upon the separation of the Skyrmions (recall the separation between Skyrmions is $2b$) with the property that $\lambda_p(\infty) = \lambda_c$.

For the initial position $b = 0.5$ we can attempt to find this value since it will be the initial value of λ for which the resulting oscillation of height is minimised. By trial and error we find the value $\lambda_p(0.5) = 4.2$. The resulting motion for such an initial height is shown in Fig 3.2.

We see that the height no longer oscillates but decreases smoothly towards the value λ_c . The lack of oscillation suggests that for this evolution the height at a given position will be a good approximation to $\lambda_p(b)$. In Fig 3.3a we plot the height against position for this simulation. The qualitative behaviour of $\lambda_p(b)$ may be examined by finding the value of λ which minimises the total potential energy at a given position b . Numerical integration of the potential energy gives the results shown in Fig 3.3b which agree quite well with the results of the simulation shown in Fig 3.3a.

From these and other similar studies the following conclusions are drawn. We find that the dominant force between Skyrmions is a weak repulsion. For Skyrmions which are well separated their height plays little role in the dynamics of the system. If the height of individual Skyrmions is not at the canonical value then it oscillates about this value with decreasing amplitude until the canonical value is reached. For Skyrmions which are within close range of each other their interaction results in a preferred height which differs from the canonical height and is position dependent. In the case in which Skyrmions are not at their preferred height then oscillation of height is around this preferred value and can have an effect upon the dynamics of the Skyrmions. However, this effect is short lived and once the preferred height has been reached the height of the Skyrmion once again has little effect upon its motion.

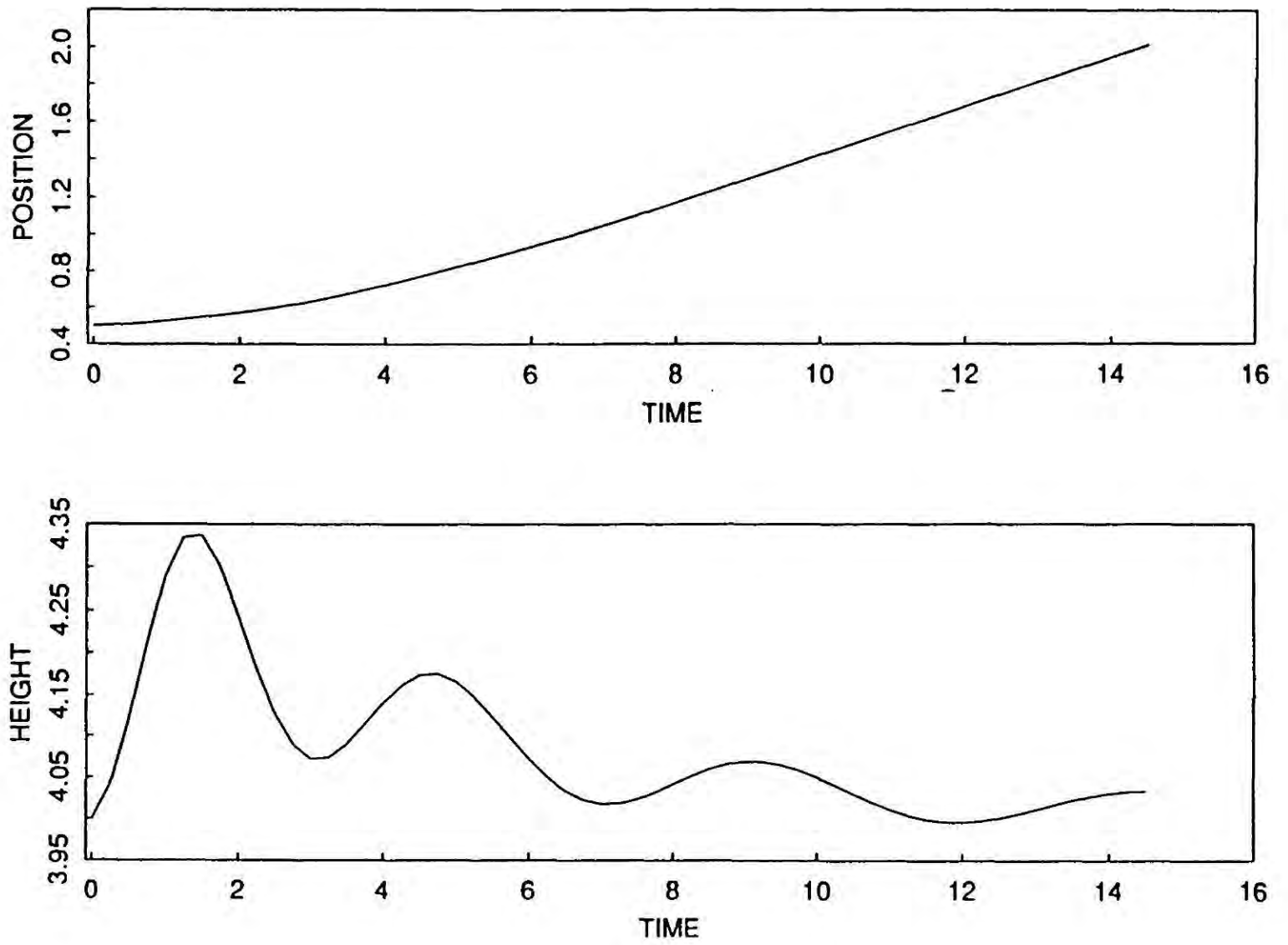


Fig 3.1 Time evolution of height λ and position b with initial conditions $b = 0.5$ and $\lambda = \lambda_c = 4.0$.

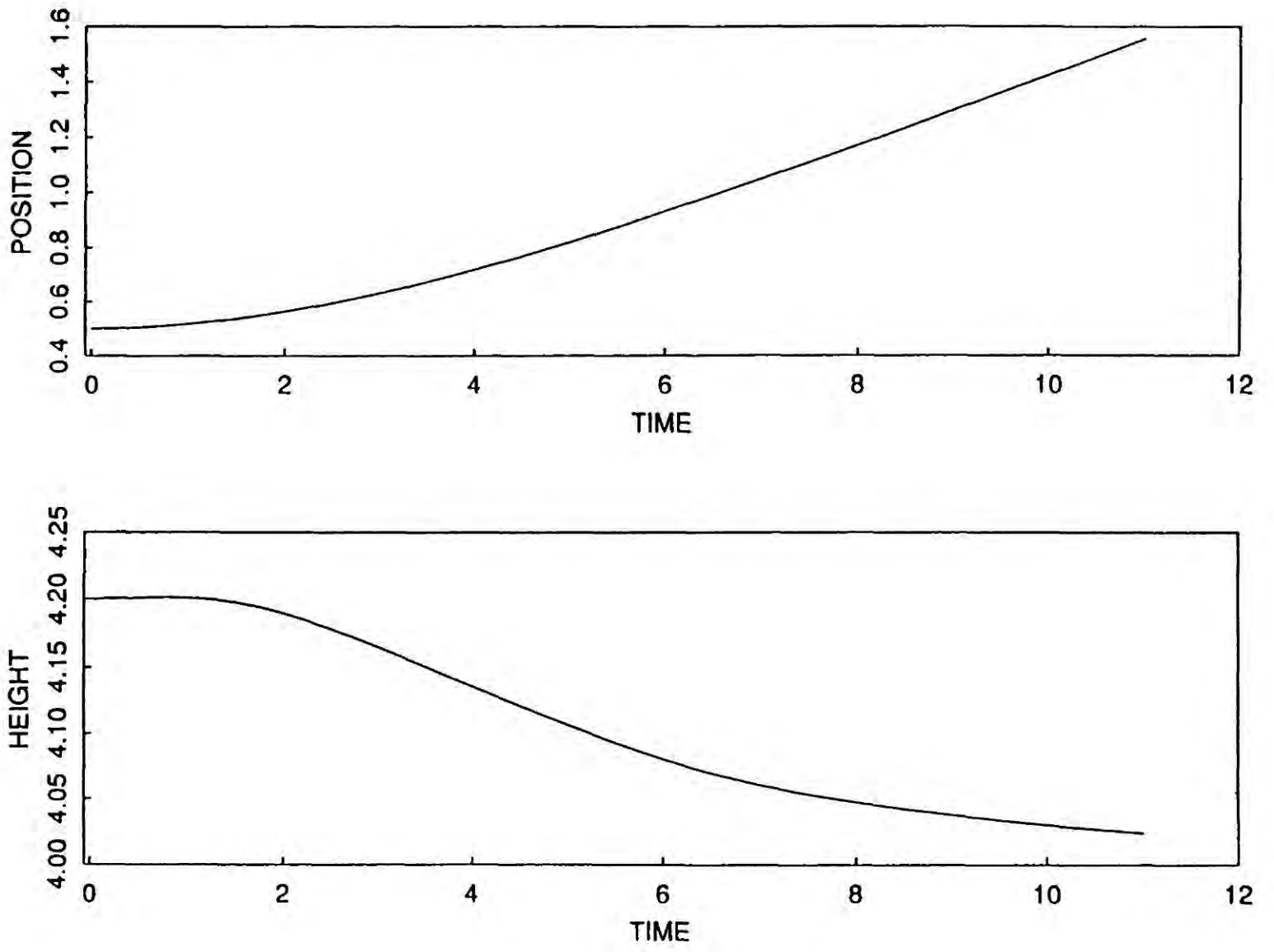


Fig 3.2 Time evolution with initial conditions $b = 0.5$ and $\lambda = 4.2$.

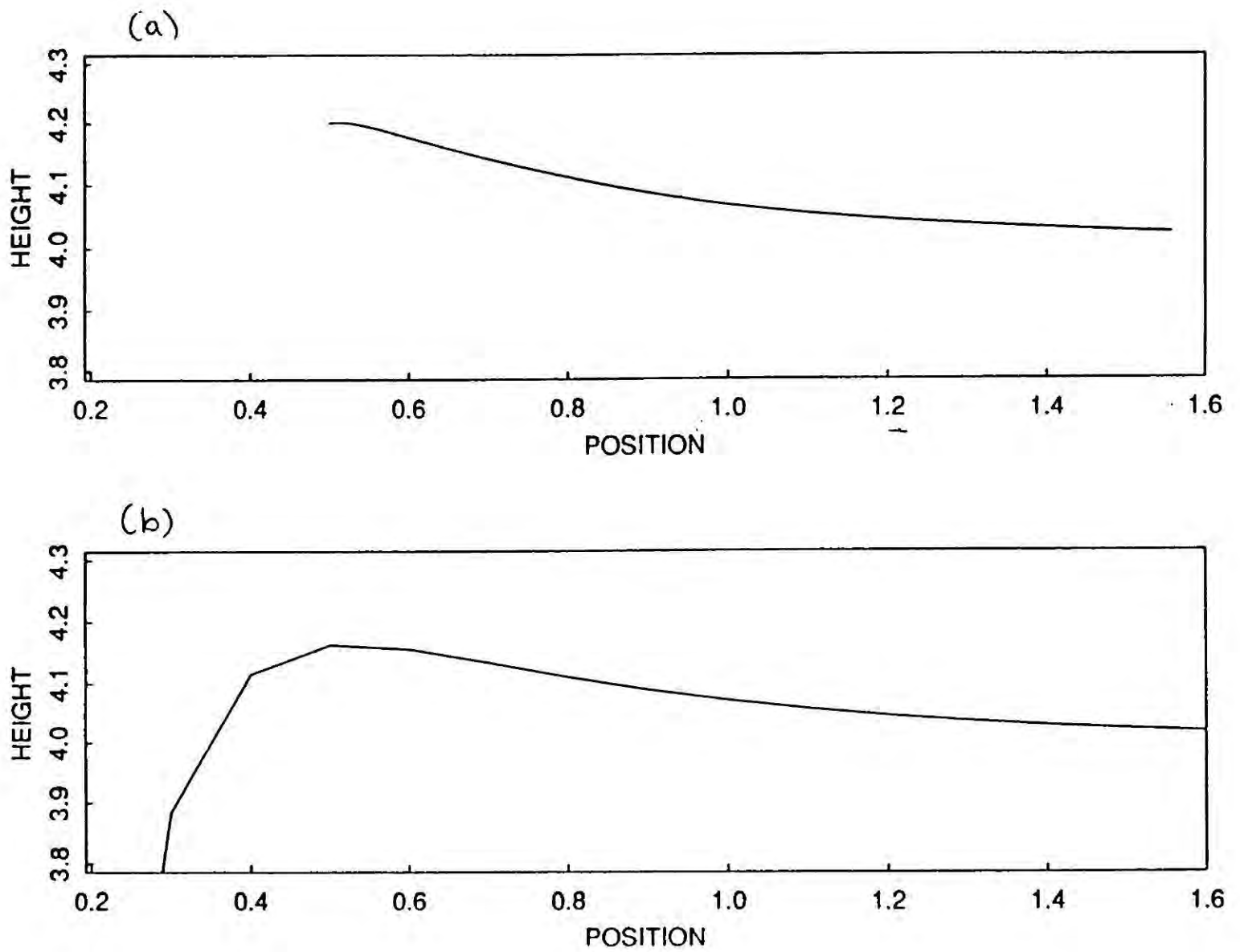


Fig 3.3 (a) Plot of λ against b for the simulation with initial conditions $b = 0.5$ and $\lambda = 4.2$.

(b) Numerical approximation for $\lambda_p(b)$ (ie the value of λ for which the total potential energy is minimised.)

We shall now study the head-on collision of two Skyrmions. The discussion of the previous section implies that if we begin with Skyrmions that are not of the preferred height then there will be an initial period in which the height of the Skyrmions will oscillate. However, once this oscillation has ceased the motion of the Skyrmions will be unaffected by height considerations, so with little loss of generality we may consider Skyrmions which begin well separated and have canonical height.

Fig 3.4a shows the resulting motion of the initial conditions $b = 2.0$, $\lambda = \lambda_c = 4.0$ and in which the Skyrmions are given an initial velocity $v = 0.2$ towards each other.

The position decreases to a minimum non-zero value before increasing again. Note that the trajectory is almost linear until the separation reaches a certain small value, which again demonstrates the short range nature of the repulsive force. Clearly the repulsion of the Skyrmions is sufficient to overcome the applied initial motion and the Skyrmions scatter back-to-back. It is interesting to plot the height against position for this simulation, which is shown in Fig 3.4b. The two superimposed curves represent the initial motion of the Skyrmions towards each other, followed by their motion as they scatter back-to-back. Again this demonstrates that the height is playing little role in the motion of the Skyrmion but is clearly following the preferred height curve (cf Fig 3.3).

Now consider the same initial position and height but where the initial velocity is increased to $v = 0.3$. In this case the height again adjusts to the preferred value as a function of separation. However, in this case the Skyrmions do not reach a minimum separation but instead collide. Recall the discussion of section 3 where we noted that a product ansatz is not a good description of the field configuration for two Skyrmions which are not distinct (ie. $b < \lambda^{-1}$), so a description of the Skyrmions in terms of a height and position is not relevant for some portion of this simulation. We must therefore examine the energy density of the configuration during this simulation in order to have a physical interpretation of the parameter values.

Fig 3.5 shows the energy density of the configuration at varying times. We see that the Skyrmions do not remain distinct throughout the evolution but form a radially symmetric ring-like structure. It is from this structure that the two new Skyrmions emerge at right angles to the original direction of motion. This is an inelastic scattering event with each of the new Skyrmions having gained their energy equally from both the initial Skyrmions. This phenomenon of 90° scattering is common to many of the studies of extended structures such as BPS monopoles^[46] and vortices^[47] at critical coupling. What is

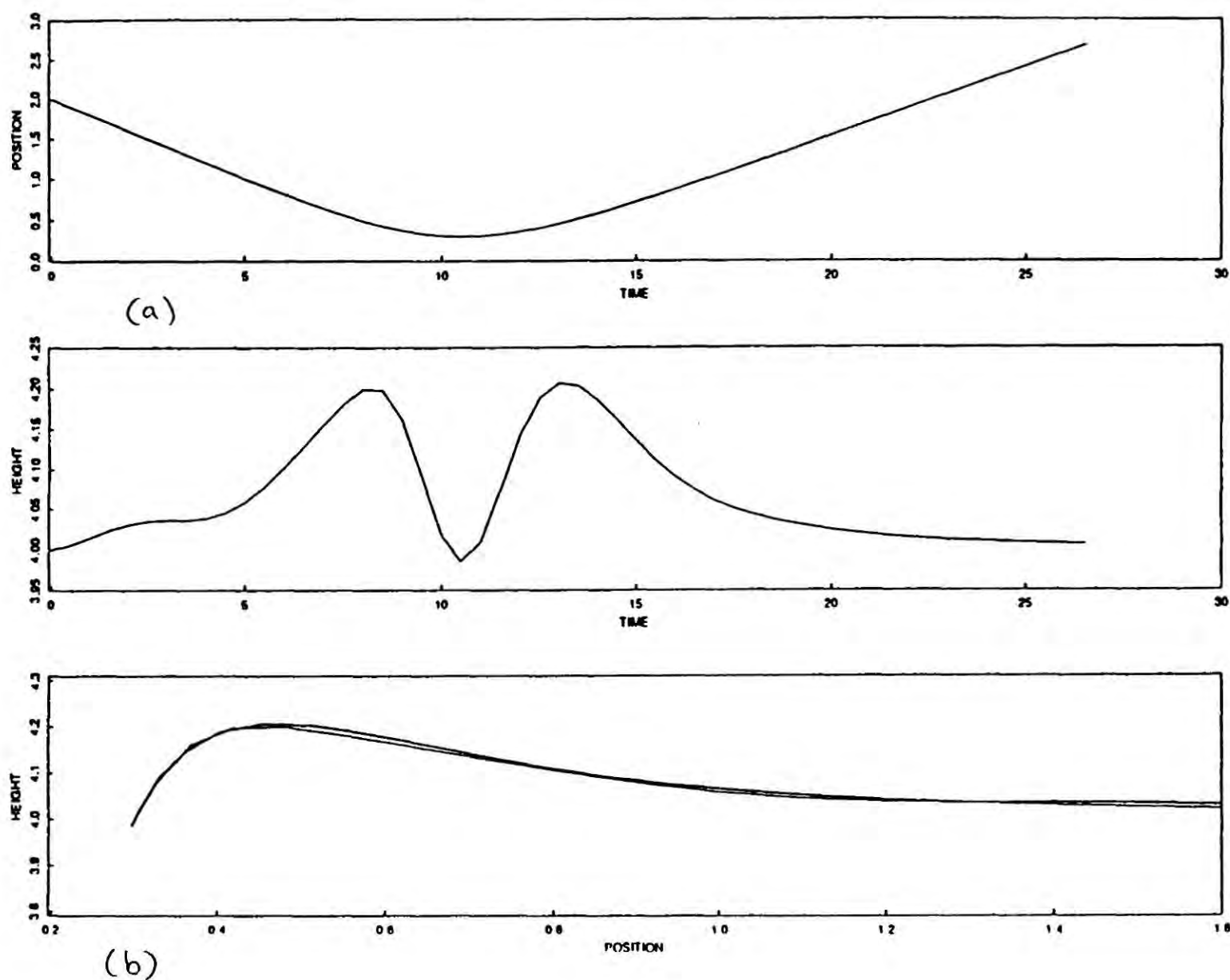


Fig 3.4 (a) Time evolution with initial conditions $b = 2.0$, $\lambda = \lambda_c = 4.0$ and initial velocity $v = 0.2$.

(b) Plot of λ against b for the same simulation.

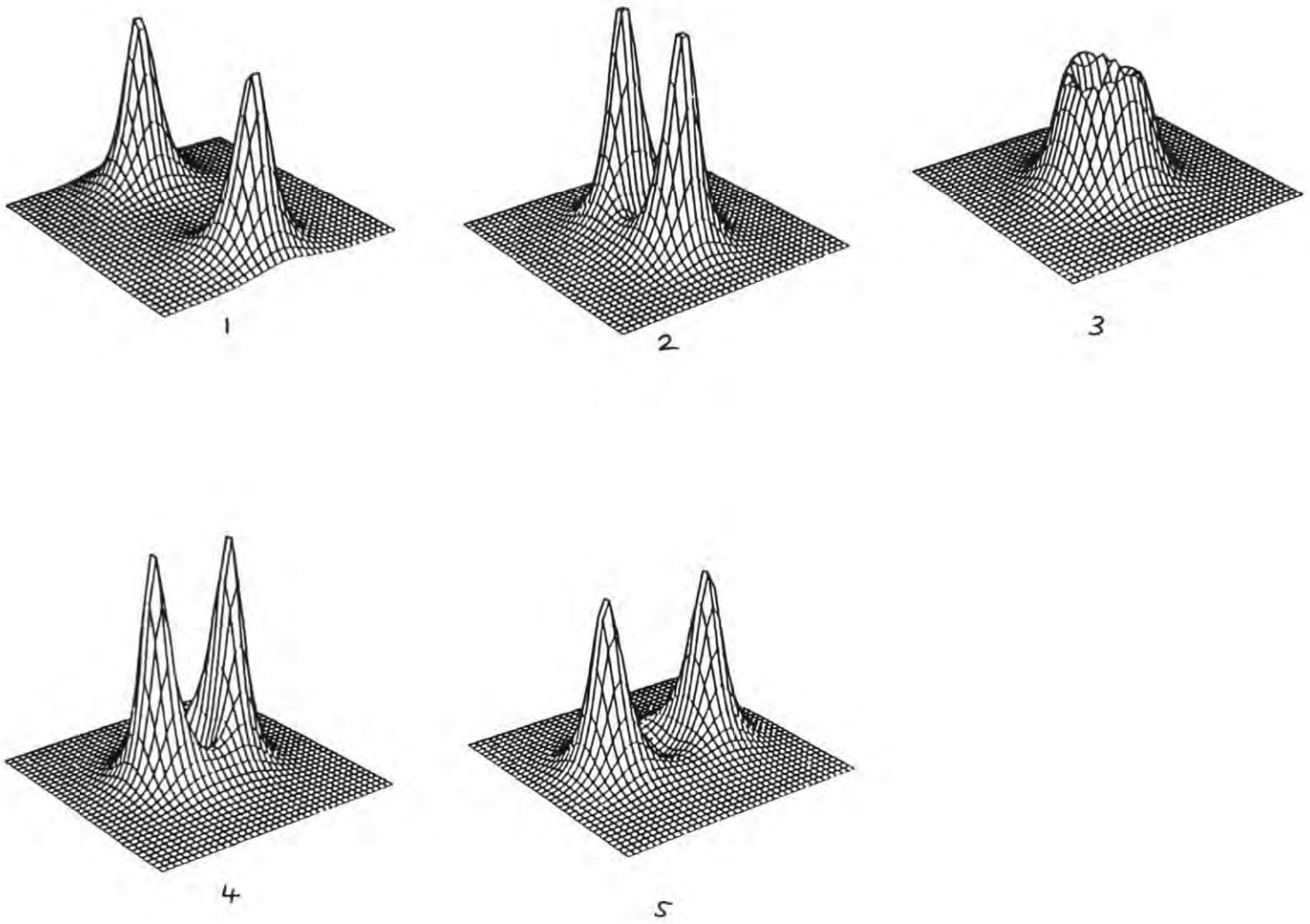


Fig 3.5 Energy density of the configuration at increasing time, with initial conditions $b = 2.5$, $\lambda = \lambda_c = 4.0$ and initial velocity $v = 0.3$.

new about this model is the existence of a critical velocity v_{cr} for which Skyrmions with a collision velocity $v < v_{cr}$ scatter back-to-back whereas Skyrmions with $v \geq v_{cr}$ scatter at right angles to the original direction of motion.

In the above numerical simulations the critical velocity was found to be $v_{cr} = 0.21$. In the following section an analytical expression for the critical velocity v_{cr} in terms of the parameters θ_1 and θ_2 of the model will be given.

3.5 DERIVATION OF CRITICAL VELOCITY

The ring structure observed in 90° scattering may be described by a radially symmetric ansatz

$$W = \lambda_r z^2 \quad (3.13)$$

where λ_r is a positive real number that we shall refer to as the ring parameter, and describes both the radius and height of the ring.

In view of the above discussion, it should be possible to calculate the ring parameter, since it will be the value of λ which minimises the potential energy of the ansatz (3.13). The potential energy is given by

$$V = \int d^2z \frac{2|\partial W|^2}{(1+|W|^2)^2} + \frac{(8\theta_1|\partial W|^4 + 4\theta_2)}{(1+|W|^2)^4} \quad (3.14)$$

Now, since the ansatz is radially symmetric, the integration of the potential energy may be performed, with the result

$$V(\lambda) = 4\pi\left(1 + 2\pi\theta_1\lambda + \frac{5\pi\theta_2}{16\lambda}\right) \quad (3.15)$$

Then

$$\frac{dV}{d\lambda}(\lambda_r) = 0 \quad \Rightarrow \quad \lambda_r^2 = \frac{5\theta_2}{32\theta_1} \quad (3.16)$$

and by (3.5)

$$\lambda_r^2 = 5\left(\frac{\lambda_c}{2}\right)^4 \quad (3.17)$$

ie. the ring parameter is determined by the canonical height of the model.

With the parameter values used in our simulations, $\lambda_c = 4.0$, which therefore implies that $\lambda_r = 8.9$. The value found in the numerical simulation of scattering was $\lambda_r = 9.1$, which compares favourably with the analytical value, and gives further credibility to the effective Lagrangian model.

The energy of this ring structure is then given by

$$E_{ring} = V(\lambda_r) = 4\pi\left(1 + 2\pi\sqrt{\frac{5\theta_1\theta_2}{32}}\right) \quad (3.18)$$

Now for two Skymions at infinity, with canonical height, and each Skymion having a velocity v the total energy of the Skymions is

$$E_{2\infty} = 2M\gamma \quad (3.19)$$

where M is the rest mass of a Skymion, as given by (3.8), and γ is the usual Lorentz factor $\gamma = (1 - v^2)^{-\frac{1}{2}}$.

Now in order to achieve 90° scattering the Skymions must have an initial energy which is at least equal to the energy of the ring-like structure. The value of the velocity at which these two energies are equal will therefore be the critical velocity of the model.

$$E_{2\infty} = E_{ring} \quad (3.20)$$

then gives

$$v_{cr}^2 = \frac{2\psi(3\pi\sqrt{5} - 16)(12 + (3\pi\sqrt{5} + 16)\psi)}{3(2 + \pi\sqrt{5}\psi)^2} \quad (3.21)$$

where ψ is given in terms of the parameters of the model by $2\psi^2 = \theta_1\theta_2$.

With the theta values used in the numerical simulations equation (3.21) gives a critical velocity of $v_{cr} = 0.217$, which is slightly higher than the value found in section 4. However, the expression (3.21) is for the critical velocity of Skymions which are initially at infinite separation, and there will be a weak dependence upon initial separation, since the Skymions will also have a slight potential energy due to their interaction. However, the repulsive force between Skymions is very weak and so it is to be expected that Skymions which are initially well separated will have a critical velocity which is only slightly lower than that given by (3.21).

The existence of a critical velocity is in contrast to the pure \mathbb{CP}^1 model where both analytical^[41] and numerical^[42] studies indicate that any positive initial value for the collision velocity is sufficient to ensure that the lumps will collide. Note that in the limit $\theta_1\theta_2 \rightarrow 0$ then $v_{cr} \rightarrow 0$, so that we reproduce the result that the pure \mathbb{CP}^1 model has no critical velocity. It is important to note the similarities and to find any differences between the modified model and the pure \mathbb{CP}^1 model since, as discussed in section 2, a motivation for the model was an attempt to introduce a preferred height for the \mathbb{CP}^1 lumps. Although this has been achieved, we need to be aware of the side-effects of breaking the conformal invariance which is present in (2+0) dimensions.

In the limit in which $\theta_1\theta_2 \rightarrow \infty$ then $v_{cr}^2 \rightarrow 1 - \frac{256}{45\pi^2}$ ie $v_{cr} \approx 0.65$, so that both back-to-back and 90° scattering can still take place. Increasing θ_1 and θ_2 also has the effect of increasing the frequency of oscillations of Skyrmions which are not of the preferred height, and so the Skyrmions now stabilise after a shorter period of time. This is to be expected since the theta terms were introduced in order to stabilise the Skyrmion and so one would expect their effect to be more pronounced as their contribution to the total energy is increased.

3.6 COMPARISON WITH OTHER METHODS

It may seem surprising that such a rich structure occurs when the truncation of the model appears so severe, and one may wonder to what extent the truncation of the model contributes to this behaviour. However, the truncation would appear to be valid since the numerical results described here have also been obtained using a numerical evolution of the full field equations^[48]. The results are not only qualitatively similar but there is also good agreement for specific values such as the critical velocity for scattering. The formula (3.21) fits very well their study of the dependence of the critical velocity upon the parameters θ_1 and θ_2 of the model.

An advantage of evolving the full field equations is that, in addition to being able to study the energy density associated with the Skyrmions, all other energy involved in the process can also be observed. Such simulations show that radiation in the form of a ring of energy is emitted by each Skyrmion as it changes its height. Fortunately this radiation is a small percentage of the total energy of the system and has little effect upon the dynamics of the Skyrmions. A major disadvantage of evolution of the full field equations is the immense computing time required to evolve the system.

3.7 CONCLUSION

Using a collective coordinate method the interaction of Skyrmions in a modified \mathbb{CP}^1 model has been studied. Static Skyrmions resemble lumps of the \mathbb{CP}^1 model but have a fixed scale. This scale has effects upon the interaction of the Skyrmions and leads to properties such as a critical velocity for scattering.

An obvious analogy can be made between Skyrmions of this model and Skyrmions in (3+1)-dimensions, which provide a good approximation to a description of low energy hadron physics. Do the results here have relevance to the study of nucleon interactions in such a model ?

Another more subtle analogy can be made with monopoles in (3+1) dimensions. In this model the force between two monopoles is removed by taking the BPS limit, which corresponds to a massless Higgs field which is then able to counteract the infinite range magnetic force. In our model this corresponds to taking the limit of vanishing θ_1 and θ_2 , in which case there is no force between Skyrmions and no critical velocity for scattering. Hence an open question is whether the results of this chapter are relevant to the study of monopoles other than in the BPS limit.

CHAPTER IV.

Solitons from Instantons

4.1 INTRODUCTION

As described in chapter *II* the Skyrme model^[33] is a nonlinear field theory which provides an effective description of low energy hadron physics. The soliton solution of the model is known as the Skyrmion, the quantum states of which describe nucleons. In order to quantize the Skyrme model it is required to truncate the full field theory to a finite dimensional system. Such a truncation is also required before the approximation used in chapter *III*, to study the dynamics of planar Skyrmions, could be applied to the study of Skyrmion dynamics in (3+1)-dimensions. To perform this truncation, and yet still include the most important degrees of freedom, is a difficult task. Recently progress has been made^[38] by observing that computing the holonomy of $SU(2)$ instantons in \mathbf{R}^4 generates configurations in \mathbf{R}^3 which are good approximations to solitons (Skyrmions) of the Skyrme model. Although this procedure clearly works, a deeper understanding of why this should be the case is still lacking.

In this chapter we briefly review the main idea of this work and then go on to show in detail how the procedure of computing the holonomy of instantons to generate soliton configurations is not limited to this one example. It is shown that computing the holonomy of CP^1 instantons in \mathbf{R}^2 generates configurations in \mathbf{R} which are good approximations to sine-Gordon solitons (kinks). To conclude the chapter we note a curious observation, between the instanton generated Skyrmions and kinks, that motivates a simple procedure through which Skyrme fields may be derived from sine-Gordon kinks. We find that the energy of such a kink generated Skyrmion is slightly nearer to the true Skyrmion energy than that of previous approximations.

4.2 SKYRMIONS FROM INSTANTONS

The Skyrme field, $U(\mathbf{x})$, at fixed time is a map $U : \mathbf{R}^3 \rightarrow SU(2)$, with $U \rightarrow 1$ as $|\mathbf{x}| \rightarrow \infty$, required for finite energy. This boundary condition implies that U has a well-defined degree, which is identified with the baryon number B . The energy of a static Skyrme field is given by

$$E = \int d^3x \left\{ -\frac{1}{2} \text{Tr}(\partial_i U \partial_i U^{-1}) - \frac{1}{16} \text{Tr}[\partial_i U U^{-1}, \partial_j U U^{-1}]^2 \right\} \quad (4.1)$$

and there is a topological bound on the total energy

$$E \geq 12\pi^2 |B| \quad (4.2)$$

The Skyrme field is the $B = 1$ minimal energy solution of the field equations and has the form (in standard orientation and centred at the origin)

$$U(\mathbf{x}) = \exp[if(r)\hat{\mathbf{x}} \cdot \boldsymbol{\sigma}] \quad (4.3)$$

where $r = |\mathbf{x}|$ and $\boldsymbol{\sigma}$ are the usual Pauli matrices. Here $f(r)$ is a profile function with the boundary conditions $f(0) = \pi$ and $f(r) \rightarrow 0$ as $r \rightarrow \infty$. This profile function has been determined numerically^[36] and gives the Skyrme energy to be $E = 1.232 \times 12\pi^2$.

Atiyah and Manton have shown [38] how to generate Skyrme fields by computing the holonomy of $SU(2)$ Yang-Mills instantons in \mathbf{R}^4 along lines parallel to the time-axis. The Skyrme field is given by

$$U(\mathbf{x}) = \mathcal{P} \exp\left[-\int_{-\infty}^{+\infty} A_4(\mathbf{x}, x_4) dx_4\right] \quad (4.4)$$

where \mathcal{P} denotes path-ordering and A_μ is a Yang-Mills instanton field in \mathbf{R}^4 .

A charge 1 instanton, with scale λ , generates a Skyrme field of the form (4.3) with a profile function given by

$$f(r) = \pi \left[1 - \left(1 + \frac{\lambda^2}{r^2} \right)^{-\frac{1}{2}} \right]. \quad (4.5)$$

This Skyrme field has minimum energy when $\lambda^2 = 2.11$ at which it takes the value $E = 1.24320 \times 12\pi^2$, which is within 1% of the numerically determined value. The approximation is therefore very good and it would be surprising if a better approximation

could be found. A modification of this procedure involving thermal instantons^[49] produced a profile function with energy $E = 1.24306 \times 12\pi^2$ which is therefore very slightly lower.

Having very briefly described how instanton holonomies generate Skyrme fields we now study a 2-dimensional analogue of this procedure which generates sine-Gordon kink fields.

4.3 KINKS FROM INSTANTONS

The well known sine-Gordon model is a field theory in (1+1)-dimensions involving a real field $\phi(x^\mu)$, where $x^\mu = (t, x)$ are the spacetime coordinates with metric $\eta^{\mu\nu} = \text{diag}(1, -1)$. The Lagrangian density is given by

$$\mathcal{L}_{SG} = \frac{1}{8} \partial_\mu \phi \partial^\mu \phi + \frac{1}{4} (\cos \phi - 1) \quad (4.6)$$

and leads to the equation of motion

$$\partial_\mu \partial^\mu \phi + \sin \phi = 0. \quad (4.7)$$

Kinks (solitons) are solutions to (4.7) which have finite energy, so that the field $\phi(x)$ at fixed time must tend to an integer multiple of 2π as $x \rightarrow \pm\infty$. The quantity

$$Q = \frac{1}{2\pi} \int_{-\infty}^{+\infty} \partial_x \phi \, dx \quad (4.8)$$

is therefore a conserved topological charge. It is integer valued and gives the kink number of the configuration. It can be shown that for a charge Q configuration the total energy E satisfies the Bogomolny like bound

$$E \geq 2Q. \quad (4.9)$$

The charge one and two kink solutions were first given in ref [50]. The static one-kink solution located at the origin is given by

$$\phi = 4 \arctan(e^x) \quad (4.10)$$

and saturates the bound (4.9) so that it has energy $E = 2$.

There are no static two-kink solutions to the sine-Gordon equation; however two-kink solutions in which either kinks have arbitrary velocity (but at least one non-zero) can be constructed. The solution

$$\phi = 4 \arctan\left(\frac{v \sinh(\gamma x)}{\cosh(\gamma vt)}\right) \quad (4.11)$$

where $\gamma = (1 - v^2)^{-\frac{1}{2}}$ is the usual Lorentz factor, is a two-kink solution in which the kinks approach along the x -axis with velocity v , scatter elastically at $t = 0$, and emerge from the interaction with only a phase shift. It has energy $E = 4\gamma$.

We shall now show how to generate approximations to the one and two-kink solutions (4.10) and (4.11) from $\mathbb{C}\mathbb{P}^1$ instantons in \mathbb{R}^2 by computing the holonomy along lines parallel to one of the coordinate axes.

There are several formulations of the $\mathbb{C}\mathbb{P}^1$ σ -model and the one we shall use here is the gauge field formulation.^[31] The $\mathbb{C}\mathbb{P}^1$ σ -model in (2+0)-dimensions is defined in terms of a 2-component column vector Z , which is a function of the euclidean spacetime coordinates $x^\mu = (x^0, x^1)$, and is constrained to satisfy the condition

$$Z^\dagger Z = 1. \quad (4.12)$$

The action density has a U(1) gauge symmetry and is given by

$$\mathcal{L}_{CP} = \text{Tr}(D_\mu Z)^\dagger (D^\mu Z) \quad (4.13)$$

where Tr denotes trace and D_μ are the covariant derivatives

$$D_\mu = \partial_\mu - A_\mu \quad (4.14)$$

with the composite gauge fields being purely imaginary and defined by

$$A_\mu = Z^\dagger \partial_\mu Z. \quad (4.15)$$

The equation of motion resulting from (4.13) is

$$[\partial_\mu \partial^\mu \mathbf{P}, \mathbf{P}] = 0 \quad (4.16)$$

where \mathbf{P} is the one-dimensional hermitian projector

$$\mathbf{P} = Z Z^\dagger. \quad (4.17)$$

The instantons are finite action solutions to (4.16) and as described in section 2.4 are

most easily written using the W parametrization

$$Z = \frac{1}{\sqrt{1 + |W|^2}} \begin{pmatrix} 1 \\ W \end{pmatrix} \quad (4.18)$$

where they are given by W a rational function of $x_+ = x_0 + ix_1$.

The target manifold is $\mathbb{C}\mathbb{P}^1$, which is isometric to S^2 , so that due to the homotopy relation

$$\pi_2(S^2) = \mathbb{Z} \quad (4.19)$$

each finite action field configuration has an associated integer winding number (the topological charge). This winding number is the instanton number of the configuration and is given by

$$N = \frac{1}{\pi} \int \frac{\text{Im}(\partial_0 W \partial_1 \bar{W})}{(1 + |W|^2)^2} d^2 x \quad (4.20)$$

where Im denotes the imaginary part. For instanton fields the degree of the rational function $W(x_+)$ is equal to the instanton number N .

In analogy with the procedure of the previous section we shall now consider the holonomy parallel to the x_1 coordinate axis ie

$$U(x_0) = \exp\left(\int_{-\infty}^{+\infty} A_1 dx_1\right) \quad (4.21)$$

which is a $U(1)$ -valued field.

In order to obtain a real-valued field from $U(x)$ (from now on we shall drop the subscript on x_0) we define

$$e^{i\tilde{\phi}(x)} = (-1)^N U(x) \quad (4.22)$$

where the prefactor involving the instanton number is required to give $\tilde{\phi}(x)$ the correct topological properties.

Then from general considerations it can be shown that an N -instanton solution generates a sine-Gordon configuration, $\tilde{\phi}(x)$, which has soliton number $Q = N$. Such configurations are therefore candidates for approximations to sine-Gordon soliton solutions at fixed time.

Using the parametrization (4.18) and combining the formulae already given we obtain the direct relation

$$\tilde{\phi}(x) = N(\text{mod}2)\pi + \int_{-\infty}^{+\infty} \frac{\text{Im}(\bar{W}\partial_1 W)}{(1+|W|^2)} dx_1 \quad (4.23)$$

For the $N = 1$ instanton solution we take

$$W = \lambda x_+ \quad (4.24)$$

where λ is an arbitrary real scale parameter. We may in addition shift x_+ by a complex constant, the imaginary part of which is irrelevant due to the invariance of (4.23) to shifts in x_1 , and the real part of which gives the position of the generated kink configuration. This generates the field

$$\tilde{\phi}(x) = \pi \left(1 + \frac{\lambda x}{\sqrt{1 + \lambda^2 x^2}} \right) \quad (4.25)$$

As in the previous section, since the instantons are scale invariant (whereas the sine-Gordon theory has a fixed scale), we are left with an additional parameter, λ , which we can vary to minimise the energy of (4.25). We find that the energy is minimised at $\lambda = 0.695$, at which it takes the value $E = 2 \times 1.010$. The energy is therefore within 1% of the energy of the exact one-kink solution (4.10). In Fig 4.1 we show a plot to compare the exact one-soliton solution (4.10) with the generated approximation (4.25).

We now consider charge 2 instantons, which may be written in the form

$$W = \frac{\lambda^2(x_+ - a_1)(x_+ - a_2)}{\alpha x_+ + 1} \quad (4.26)$$

Again using the invariance of (4.23) we may choose a_1 to be real and the scale parameter, λ , to be real, without loss of generality. The complex constant α determines the relative scale of the two instantons, together with their relative orientation in target space.

For simplicity we shall consider the case in which both generated kinks are at the origin ($a_1 = a_2 = 0$) and have equal scale ($\alpha = 0$). We then obtain

$$\tilde{\phi}(x) = \frac{\sqrt{2}\pi\lambda x \sqrt{\sqrt{1 + \lambda^4 x^4} + \lambda^2 x^2}}{\sqrt{1 + \lambda^4 x^4}} \quad (4.27)$$

The energy of (4.27) is minimised at $\lambda = 0.318$, at which it takes the value $E = 4 \times 1.054$. This is within 6% of the bound (4.9), which is only obtained by the exact two-kink

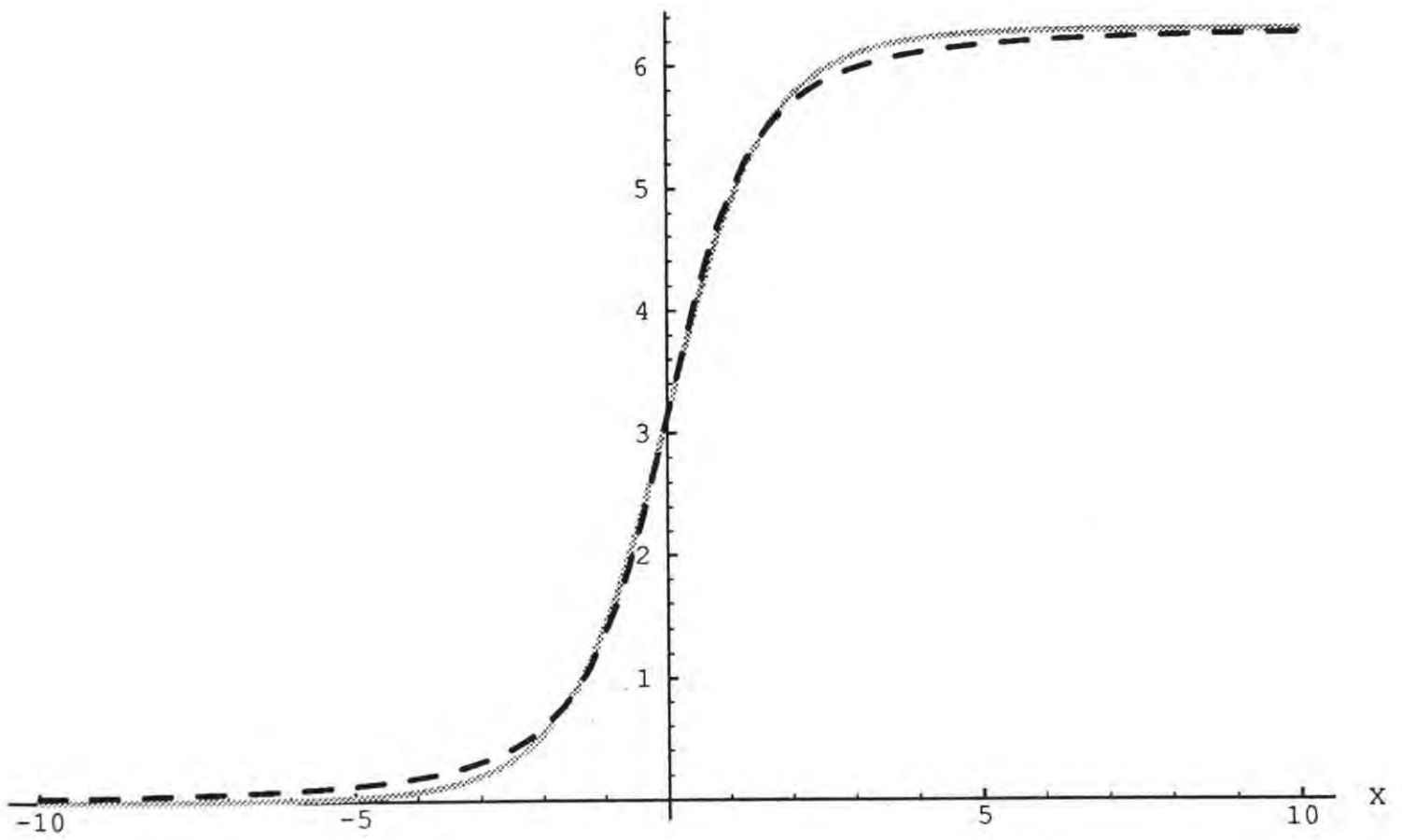


Fig 4.1 Comparison of the static one-kink solution $\phi(x)$ (continuous curve) with the generated approximation $\tilde{\phi}(x)$ (dashed curve).

solution (4.11) in the singular limit $v \rightarrow 0$. We shall now compare this function with the exact solution (4.11) at $t = 0$. It is interesting to attempt to find the particular two-kink solution which (4.27) approximates at $t = 0$. It may be that if the approximation were to be taken as initial data then the radiation component of the resulting evolution would be small. This suggests that we should compare the approximation with the exact solution which has the same energy. The velocity in the exact solution is therefore determined from $E = 4\gamma = 4 \times 1.054$, which gives $v = 0.32$. In Fig 4.2 we compare the approximation with the exact solution with $v = 0.32$.

It can be seen that this is a good fit. However, the field (4.27) does not provide a good approximation to the two-kink solution (4.11) for velocities which are lower than this value, since the energy of (4.27) is too large.

By allowing a_1 and a_2 in (4.26) to be non-zero it is possible to generate fields with reduced energies. If we choose $a_1 = -a_2 = a$, where a is a real constant, then we generate the following field. For notational convenience we define $\zeta \equiv 4\lambda^4 a^2 x^2 - 1$

$$\tilde{\phi}(x) = \begin{cases} \frac{\pi\lambda x}{\sqrt{\zeta}} \left(\frac{\sqrt{\zeta+2\lambda^2 a^2}}{\sqrt{\lambda^2(x^2+a^2)+\sqrt{\zeta}}} + \frac{\sqrt{\zeta-2\lambda^2 a^2}}{\sqrt{\lambda^2(x^2+a^2)-\sqrt{\zeta}}} \right) & \text{if } \zeta \geq 0 \\ \frac{\sqrt{2}\pi\lambda x}{\zeta\sqrt{\lambda^4(x^2+a^2)^2+\zeta^2}} \times \\ \left\{ \zeta\sqrt{\sqrt{\lambda^4(x^2+a^2)^2+\zeta^2} + \lambda^2(x^2+a^2)} \right. \\ \left. + 2\lambda^2 a^2 \sqrt{\sqrt{\lambda^4(x^2+a^2)^2+\zeta^2} - \lambda^2(x^2+a^2)} \right\} & \text{if } \zeta < 0 \end{cases} \quad (4.28)$$

The energy of (4.28) is minimised at $\lambda = 0.296$, $a = 3.16$, at which it takes the value $E = 4 \times 1.0032$. Again we compare this with the exact solution with the same energy. $E = 4\gamma = 4 \times 1.0032$, gives $v = 0.079$. In Fig 4.3 we compare the approximation (4.28) with the exact solution with $v = 0.079$. Again it can be seen that this is a very good fit.

Finally, note that by allowing arbitrary a_1, a_2 and α in (4.26) we could generate many more sine-Gordon fields with perhaps reduced energies.

We have shown that the procedure of computing the holonomy of instanton fields to generate soliton configurations is not limited to four dimensions, but also has a two dimensional analogue. In the lower dimensional version the procedure has a much simpler form; the gauge group is abelian and the expressions are more tractable. By studying this simpler version it is hoped that a deeper understanding of why this procedure works may be found.

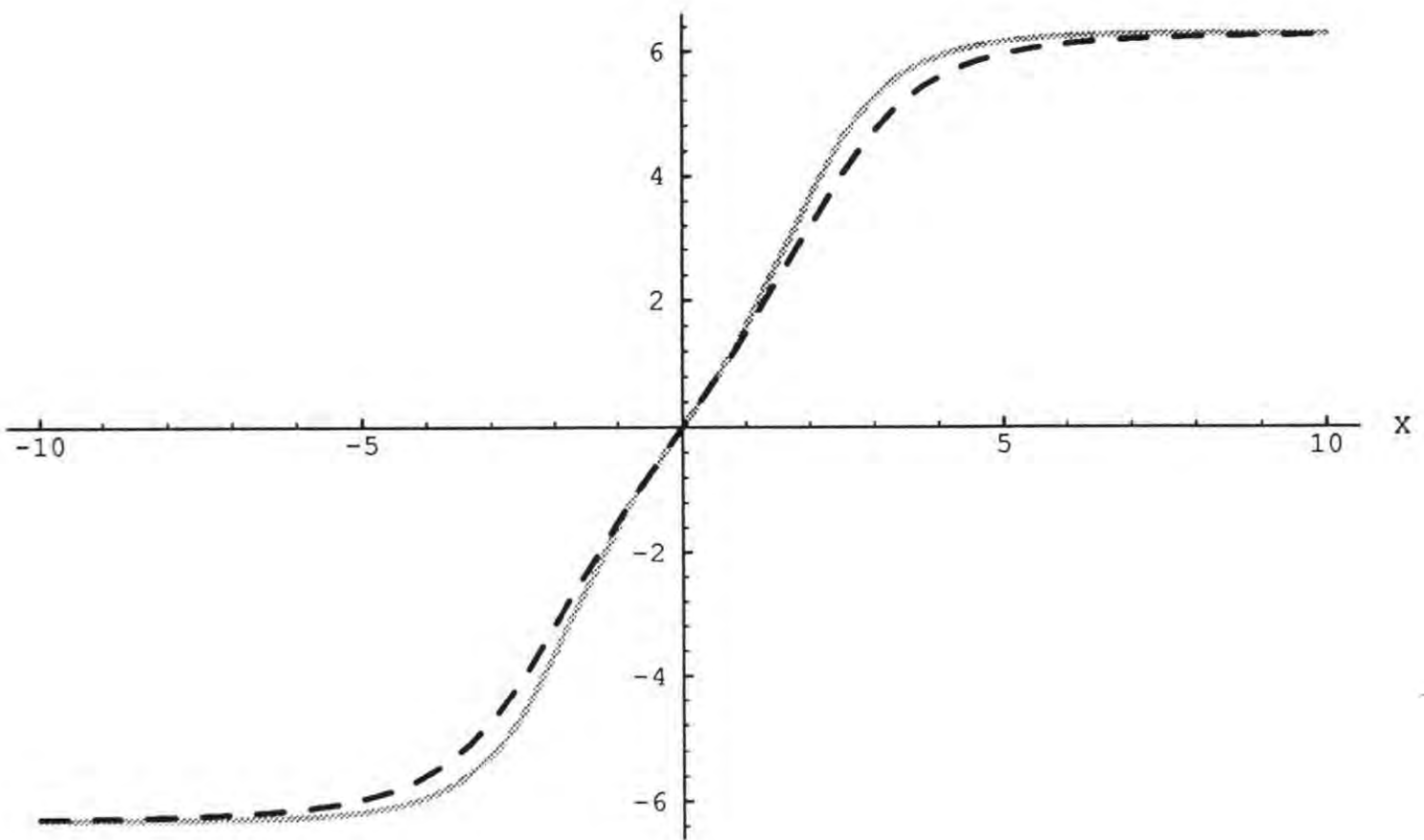


Fig 4.2 Comparison of the two-kink solution $\phi(x)$ with soliton speed $v = 0.32$ (continuous curve) against the generated approximation $\tilde{\phi}(x)$ (dashed curve).

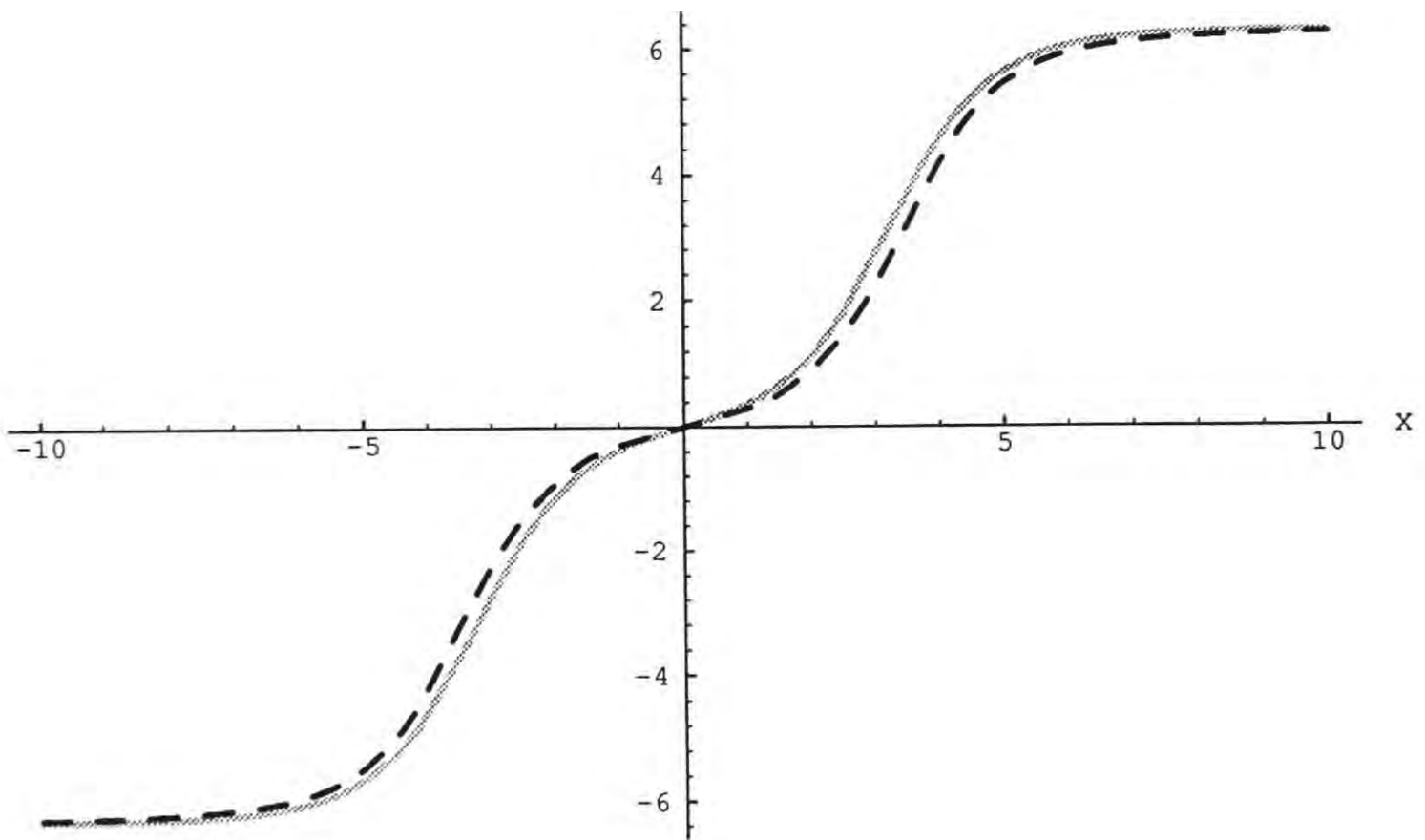


Fig 4.3 Comparison of the two-kink solution $\phi(x)$ with soliton speed $v = 0.079$ (continuous curve) against the generated approximation $\tilde{\phi}(x)$ (dashed curve).

A better fit to sine-Gordon solitons might be obtained using the construction described here applied to the gauge potentials of vortex solutions of the abelian Higgs model, since they have an exponential rather than power law asymptotic behaviour. However, the static vortex solutions, although known to exist, are not known in closed form. The procedure would therefore have to be performed numerically, thereby losing some of the elegance of the simple procedure described here. An alternative to this numerical construction may be to apply this procedure to vortex solutions of the abelian Higgs model defined in a spacetime of constant negative curvature; since the vortex solutions can then be given^[51] in closed form.

4.4 SKYRMIONS FROM KINKS

Suppose we make the sign modification to (4.21) so that

$$U(x_0) = \exp\left(-\int_{-\infty}^{+\infty} A_1 dx_1\right) \quad (4.29)$$

and again

$$e^{i\tilde{\phi}(x)} = (-1)^N U(x) \quad (4.30)$$

then a charge $N = 1$ instanton, with scale λ , generates an approximation

$$\tilde{\phi}(x) = \pi\left[1 - \left(1 + \frac{\lambda^2}{x^2}\right)^{-\frac{1}{2}}\right] \quad (4.31)$$

to the true sine-Gordon anti-kink $Q = -1$ solution

$$\phi(x) = 4\arctan(e^{-x}) \quad (4.32)$$

Now observe that the anti-kink approximation (4.31) and the Skyrme profile approximation (4.5) are identical if we replace x by r . Since (4.31) is an approximation to the sine-Gordon anti-kink (4.32) this motivates the choice of a sine-Gordon anti-kink field as

the Skyrmion profile function is

$$f(r) = 4\arctan(e^{-r}). \quad (4.33)$$

which gives the simple Skyrme field

$$U(\mathbf{x}) = \frac{-1 + \sinh^2 r + 2i\hat{\mathbf{x}} \cdot \boldsymbol{\sigma} \sinh r}{\cosh^2 r} \quad (4.34)$$

with energy $E = 1.24035 \times 12\pi^2$, which is less than the instanton generated approximations. Moreover, unlike the instanton, the sine-Gordon anti-kink has a fixed scale, so there are no arbitrary scale parameters which have to be fixed by hand in order to minimise the energy. A scale for the anti-kink can be introduced artificially through the replacement $r \rightarrow \lambda r$, in (4.33). The minimum energy then occurs when $\lambda = 1.02$, which is very close to the natural anti-kink scale, with the energy slightly reduced to $E = 1.24013 \times 12\pi^2$.

In both the numerical and instanton generated Skyrmons the profile function has a r^{-2} asymptotic decay. This is in contrast to the anti-kink profile function (4.33), which has an exponential decay for large r . Such an exponential asymptotic behaviour of the profile function is obtained when the Skyrme Lagrangian (4.1) is modified through the addition of a chiral symmetry breaking term^[52] which corresponds to a theory in which the underlying pion fields are massive. Although the calculation of the Skyrmon energy is fairly insensitive to the asymptotic decay of the profile function, other physical quantities of the Skyrmon are much more sensitive to this property, and in particular some quantities are finite only in the latter case. This suggests that the anti-kink generated Skyrme field may have relevance in the physically more realistic case of massive pions.

The minimal energy Skyrmon in the $B = 2$ sector is not spherically symmetric but has an axial symmetry^[53] with energy $E = 1.18 \times 24\pi^2$, which is less than that of two well-separated Skyrmons. The energy density of this solution is concentrated in a toroidal region. Among fields with a spherically symmetric energy density there are two ways to obtain $B = 2$ Skyrme fields. The first is to alter the boundary condition on the profile function so that $f(0) = 2\pi$. Such a field has energy^[54] $E = 1.83 \times 24\pi^2$, which is greater than that of two well-separated Skyrmons. We can generate an approximation to this Skyrme field by using the anti-kink profile function

$$f(r) = 8\arctan(e^{-r}). \quad (4.35)$$

which has energy $E = 1.90 \times 24\pi^2$. Again we can introduce a scale through the replacement

$r \rightarrow \lambda r$, in (4.35), upon which the energy is minimised when $\lambda = 0.92$ and takes the value $E = 1.89 \times 24\pi^2$. The second method of obtaining $B = 2$ Skyrme fields is to leave the boundary condition on the profile function unchanged but to have the Skyrme field rotate twice as rapidly as the radial vector \hat{x} under a change in the azimuthal angle around an axis⁽⁵⁵⁾. Explicitly,

$$U = \exp\{if(r)(\sigma_1 \sin \alpha \cos 2\varphi + \sigma_2 \sin \alpha \sin 2\varphi + \sigma_3 \cos \alpha)\} \quad (4.36)$$

where $(x, y, z) = (\rho \cos \varphi, \rho \sin \varphi, z)$ and $\tan \alpha = \frac{\rho}{z}$. A numerical procedure to find $f(r)$ that minimises the energy of (4.36) produces⁽⁵⁵⁾ $E = 1.32 \times 24\pi^2$. If we use choose $f(r)$ to be the anti-kink (4.33) then the field (4.36) has energy $E = 1.41 \times 24\pi^2$, although introducing a scale $\lambda = 0.78$ reduces the energy to $E = 1.36 \times 24\pi^2$.

In conclusion, we see that through a very simple identification procedure we are able to obtain spherically symmetric Skyrmions from kinks. These Skyrmions have energy which is only very slightly above that of the true Skyrmion and may be a signal to a deeper relationship between the Skyrme and sine-Gordon theories, particularly since the scales in the two models appear to be related. By considering multi-kink and kink-antikink fields we may be able to generate other interesting spherically symmetric Skyrme fields. It would be interesting to see if a similar identification could be found for the axisymmetric minimal energy Skyrmion in the $B = 2$ sector. Finally, given the simple form of the Skyrme field (4.34), together with the accuracy with which it approximates the true Skyrmion, it may be possible to find a modified Skyrme model in which (4.34) is an exact solution. Since the Skyrme model is only an approximate description of low energy hadron physics it would be interesting if such a modification could be found.

4.5 CONCLUSION

In this chapter we have shown that the procedure of computing instanton holonomies to generate soliton approximations is a general method which is not limited to the single example previously known. It is hoped that by studying these simpler examples we may be able to shed some light on this (still mysterious) technique. For example, it would be very interesting to determine the equations for which the soliton approximations are exact solutions. This is a difficult task for the generated $SU(2)$ Skyrme fields in 3-dimensions but should be greatly simplified for the real-valued kink field in 1-dimension.

By obtaining Skyrme fields from kinks we have demonstrated that there appear to be many (as yet unexplained) connections between solitons and instantons in varying spacetime dimensions. As a final point, note that the $\mathbb{C}\mathbb{P}^1$ model in \mathbf{R}^2 may be obtained as a dimensional reduction of the $SU(2)$ self-dual Yang-Mills equations in \mathbf{R}^4 , so that we may also be able to interpret the sine-Gordon generated kinks as having been obtained (in some way) from holonomies of self-dual Yang-Mills fields.

CHAPTER V.

Classical and Quantum Kink Scattering

5.1 INTRODUCTION

There are many examples in which solitonic structures are important phenomena in both classical and quantum field theory. In a range of space dimensions they include monopoles, Skyrmions, lumps, vortices and kinks. Most of the physically interesting theories which possess soliton solutions are, however, non-integrable upon the introduction of time dependence, even if they are integrable in the static case. This makes the study of soliton dynamics, even at the classical level, a difficult task which invariably requires the use of approximations or numerical simulations.

The majority of investigations on soliton dynamics are based upon the method of Manton.^[45] As described in chapter *III* this involves a truncation of the full field theory to a finite dimensional system where motion is then confined to a manifold \mathcal{M} determined by this truncation. Quantization of this finite dimensional system then allows the investigation of quantum soliton scattering in the theory. This method has been used in the study of classical and quantum monopole scattering^[46,56], vortex scattering^[47,57,58], classical lump scattering^[41,42] and many other systems. For solitons in 3-dimensional space, such as monopoles, this is the only practical method currently known for studying dynamics. In 2-dimensional space, where vortices and lumps occur, some numerical simulations^[59,60] of classical soliton scattering are just possible with modern computers and allow some comparison to be made with the collective coordinate approximation; thereby providing some indication as to its accuracy. These few results demonstrate that the approximation does surprisingly well in these cases.

Turning now to the situation in which weak forces exist between static solitons (which is the case for Skyrmions, non-BPS monopoles and vortices which are not at critical coupling) then the truncation of the model to a manifold \mathcal{M} may still be performed but now \mathcal{M} has both a non-trivial metric and a non-trivial potential energy function. The dynamics is therefore more complicated, in particular it is no longer given by geodesic

motion in \mathcal{M} , and the validity of the approximation is less clear. However, this method was applied to the study of soliton scattering in the planar Skyrme model in chapter III in which weak forces exist between static solitons, and was again found to be a surprisingly good approximation when tested against numerical simulations.

In this chapter we test the collective coordinate approximation by applying it to the study of classical and quantum kink scattering in the sine-Gordon model in (1+1)-dimensions. This model is integrable both at the classical and quantum level and therefore allows a test of the collective coordinate approximation to be made, thereby providing useful information regarding the validity of the approximation for studying classical and quantum soliton scattering.

5.2 SINE-GORDON KINKS

The sine-Gordon model was described in the previous chapter and is given by the Lagrangian density

$$\mathcal{L} = \frac{1}{8} \partial_\mu \phi \partial^\mu \phi + \frac{1}{4} (\cos \phi - 1). \quad (5.1)$$

The static one-kink solution located at the origin is given by

$$\phi = 4 \arctan(e^x). \quad (5.2)$$

One-kink solutions may also be obtained from (5.2) by the replacement $\phi(x) \rightarrow -\phi(-x)$, or by the addition of an integer multiple of 2π . The solution

$$\phi = 4 \arctan\left(\frac{u \sinh(\gamma x)}{\cosh(\gamma ut)}\right) \quad (5.3)$$

is a two-kink solution in which the kinks scatter elastically with a phase shift given by

$$\delta = \frac{2 \log(u^{-1})}{\gamma} \quad (5.4)$$

The positions of the kinks are strictly only defined when the separation between the two kinks is large, since as the kinks approach each other they lose their individual identities.

We define the positions $x = \pm a$ of the kinks for all separation by

$$\phi(x = a) = \pi \quad (5.5)$$

so that for the two-kink solution (5.3) we have

$$a = \pm \frac{\operatorname{arcsinh}(u^{-1} \cosh(\gamma ut))}{\gamma}. \quad (5.6)$$

Note that since we are considering the scattering of identical kinks then we can not distinguish between forward and backward scattering. However, by considering the scattering of non-identical kinks⁽⁶¹⁾ we find that the most natural interpretation is that of forward scattering. If we choose the sign in (5.6) so that we define $a \geq 0$ for all t then we interpret a as describing a kink at $x = -a$ for $t < 0$ which emerges with an unchanged velocity as a kink at $x = +a$ for $t > 0$; with a similar interpretation for the second kink.

5.3 THE COLLECTIVE COORDINATE APPROXIMATION

We now introduce the collective coordinate approximation for the sine-Gordon two-kink system. For theories in which there are no forces between static solitons the parameter space of static N -soliton solutions provides a natural set of collective coordinates which essentially give an explicit parametrization of the manifold \mathcal{M} . When there are forces between static solitons (as there are in the sine-Gordon model) then an alternative method for identifying the collective coordinates, and hence the manifold \mathcal{M} , must be found. The simplest method is to obtain an ansatz that describes an N -soliton configuration by patching together N copies of a single soliton solution. The collective coordinates are then the parameters that appear in the ansatz. This will adequately describe the N -soliton system when the separation between the solitons is large and the inter-soliton forces are weak. It is then hoped that such a set of collective coordinates also provides an adequate description of the configuration when soliton separations are small. In some systems this is indeed the case, although a notable exception is the Skyrme model where an adequate approximation to the minimal energy two-Skyrmion solution cannot be obtained through this procedure. This leads us to the second method of obtaining a suitable set of collective coordinates. This is the method described in the previous chapter involving the calculation of instanton holonomies. Computing such holonomies allows a suitable set of collective coordinates and hence a manifold \mathcal{M} to be found. In the previous chapter it was shown

how this procedure involving the holonomy of \mathbb{CP}^1 instantons on \mathbb{R}^2 could be used to generate sine-Gordon kink fields. For the kink scattering we wish to study in this chapter a suitable truncation is explicitly given there, in which \mathcal{M} is a 2-dimensional manifold. The physical interpretation of the collective coordinates is that they correspond to the separation and size of the kinks. Although we could use this manifold the complexity of the formulae involved makes the procedure cumbersome. We therefore choose to obtain a two-kink field by patching together two one-kink solutions in the following way

$$\begin{aligned}\tan\left(\frac{\phi}{4}\right) &= e^{(x-a)} - e^{-(x+a)} \\ &= 2e^{-a} \sinh x\end{aligned}\tag{5.7}$$

where $a \in \mathbb{R}^+$ is the collective coordinate, so that \mathcal{M} is one-dimensional. The first term represents a kink located at $x = a$ which increases from 0 to 2π as x increases from $-\infty$ to $+\infty$. The second term represents a kink located at $x = -a$ which increases from -2π to 0 as x increases from $-\infty$ to $+\infty$. When a is large (5.7) therefore represents two well-separated kinks. Note that this patching argument requires that we must have $a > 0$ for the tail of the kink at $x = a$ to match up correctly with the head of the kink at $x = -a$. However, (5.7) is a perfectly well behaved function for all a including $a \leq 0$ so one may wonder why we do not take \mathcal{M} to be \mathbb{R} instead of \mathbb{R}^+ . We shall see later that the region $a \leq 0$ is never accessible for kinematical reasons.

To perform the truncation to a one-dimensional system we now substitute the ansatz (5.7) into the Lagrangian density (5.1) and integrate over x . The result is the one-dimensional system given by the Lagrangian

$$L = \frac{1}{2}g(a)\dot{a}^2 - V(a)\tag{5.8}$$

where dot denotes differentiation with respect to t . Here $g(a)$ is the metric on \mathcal{M}

$$g(a) = 32e^{-2a} \int_0^\infty \frac{\sinh^2 x}{(1 + 4e^{-2a} \sinh^2 x)^2} dx\tag{5.9}$$

and $V(a)$ is the potential

$$V(a) = 16e^{-2a} \int_0^\infty \frac{\sinh^2 x + \cosh^2 x}{(1 + 4e^{-2a} \sinh^2 x)^2} dx\tag{5.10}$$

In Fig 5.1 we plot the metric and potential functions.

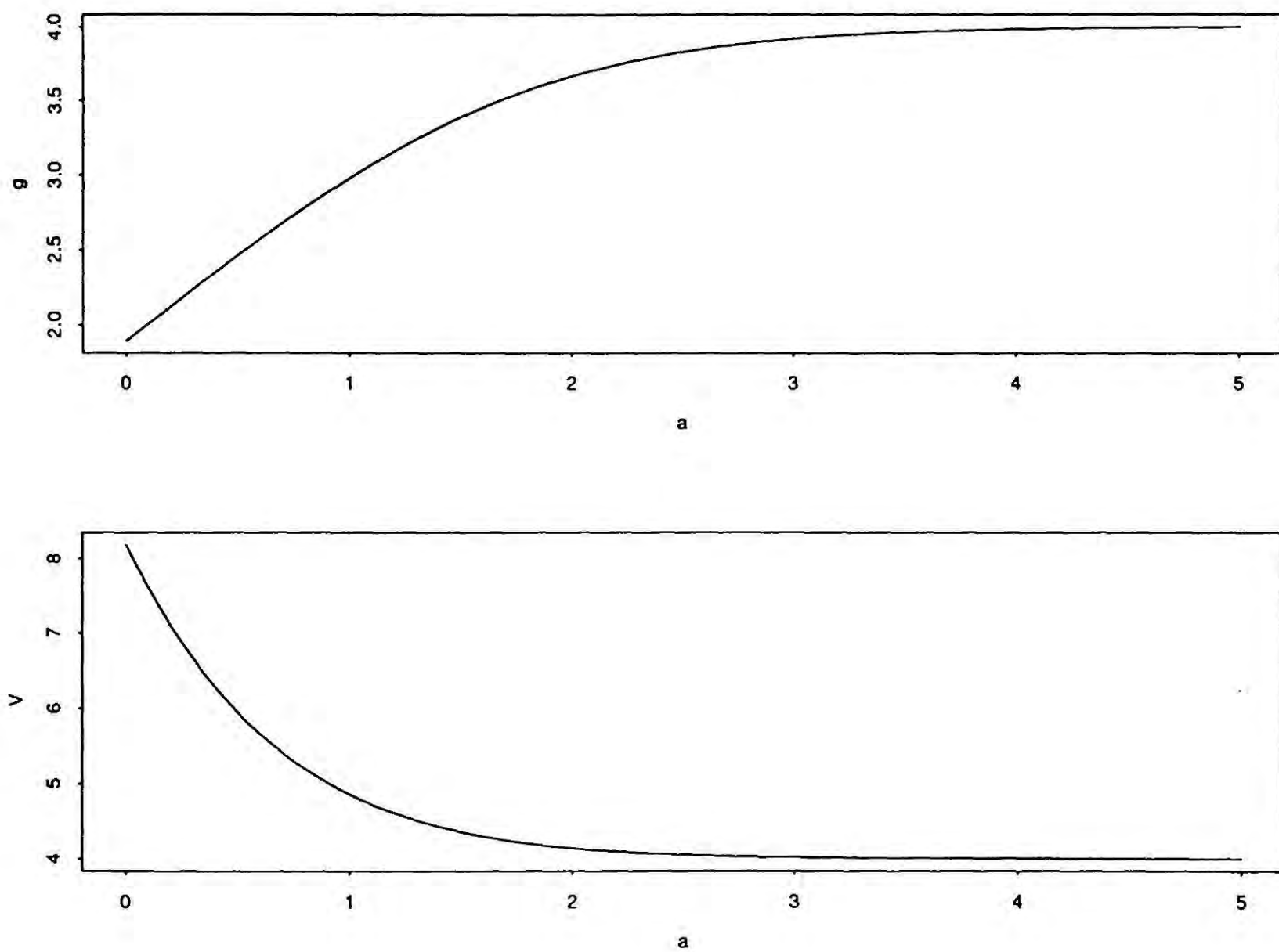


Fig 5.1 Plot of (a) metric g and (b) potential V , as a function of kink position a .

We see that $g(a) \rightarrow 4$ and $V(a) \rightarrow 4$ as $a \rightarrow \infty$, which is to be expected since each individual kink has a mass equal to 2, so that the total mass of the system is 4.

In the next section we consider the dynamical system given by the Lagrangian (5.8) to study kink scattering.

5.4 CLASSICAL KINK SCATTERING

The equation of motion derived from the Lagrangian (5.8) is simply

$$g\ddot{a} + \frac{1}{2} \frac{dg}{da} \dot{a}^2 + \frac{dV}{da} = 0 \quad (5.11)$$

which we can interpret as a particle with position $a(t)$ moving in a potential $V(a)$, with a variable mass $g(a)$. The initial conditions for kink scattering with a velocity u are $a(t=0) = a_0$ and $\dot{a}(t=0) = -u$. The total energy of the system is

$$E = \frac{1}{2}g(a_0)u^2 + V(a_0) \quad (5.12)$$

so that the turning point of the motion, a_1 , is given by $V(a_1) = E$. We can simply solve the equation of motion (5.11) by quadrature to obtain $a(t)$ implicitly as

$$t(a) = \int_a^{a_0} \sqrt{\frac{g(\alpha)}{2(E - V(\alpha))}} d\alpha \quad (5.13)$$

which is valid for $0 \leq t \leq t_1$, where t_1 is the turning time $t_1 = t(a_1)$. The position for $t > t_1$ is determined by the fact that the motion is symmetric about t_1 ie, $a(t - t_1) = a(t_1 - t)$.

The phase shift is given by

$$\delta = 2(a_0 - ut_1) \quad (5.14)$$

in the limit in which $a_0 \rightarrow \infty$ with t_1 appropriately determined by the dynamics as given by (5.13).

In practise to compare with the exact two-kink solution (5.3) we need only choose a_0 to be sufficiently large so that $g(a_0)$ and $V(a_0)$ are within a desired accuracy of their asymptotic values $g(\infty)$ and $V(\infty)$. We find $a_0 = 6$ is a sufficiently large value. All required integrals are performed numerically.

From Fig 5.1 we see that for $g(a_0)$ and $V(a_0)$ to be reasonably close to their asymptotic values $g(\infty)$ and $V(\infty)$ certainly requires $a_0 > 1$. For such a value of a_0 we have that for velocities less than the speed of light (ie. $u < 1$)

$$E = \frac{1}{2}g(a_0)u^2 + V(a_0) < 2 + V(1) < V(0) \quad (5.15)$$

so that the turning point is positive ie. $a_1 > 0$. This kinematical argument demonstrates that $a > 0$.

In Fig 5.2 we plot the collective coordinate solution (5.13) and the position (as given by the upper sign in (5.6)) for the corresponding exact solution (5.3), for a velocity $u = 0.3$.

It can be seen that the collective coordinate approximation is in excellent agreement with the exact solution in this case. In Fig 5.3 we plot the collective coordinate approximation to the phase shift (5.14) and the exact phase shift (5.4), for a range of velocities $0.1 \leq u \leq 0.8$.

Again it can be seen that the collective coordinate approximation is in excellent agreement with the exact result, even for very large velocities. Once again we find that the approximation does indeed work remarkably well.

In the next section we quantize the collective coordinate approximation to study quantum kink scattering. Although, as mentioned in the introduction, such a procedure has been used to study quantum soliton scattering in other systems, the sine-Gordon theory is the only one of these systems in which other methods of studying quantum scattering are available with which to compare.

5.5 QUANTUM KINK SCATTERING

Rather than using the Lagrangian (5.8) we first make the simplification of replacing the metric $g(a)$ by its asymptotic value $g(\infty) = 4$. This is a reasonable approximation since $g(a)$ is close to its asymptotic value for all but very small a (see Fig 5.1a) where it decreases to $g(0) \approx 2$. We therefore consider the very simple Hamiltonian

$$\mathcal{H} = 2\dot{a}^2 + V(a). \quad (5.16)$$

The wave function $\Psi(a, t)$ satisfies the Schrödinger equation

$$i\frac{\partial\Psi}{\partial t} = -\frac{1}{8}\frac{\partial^2\Psi}{\partial a^2} + V\Psi \quad (5.17)$$

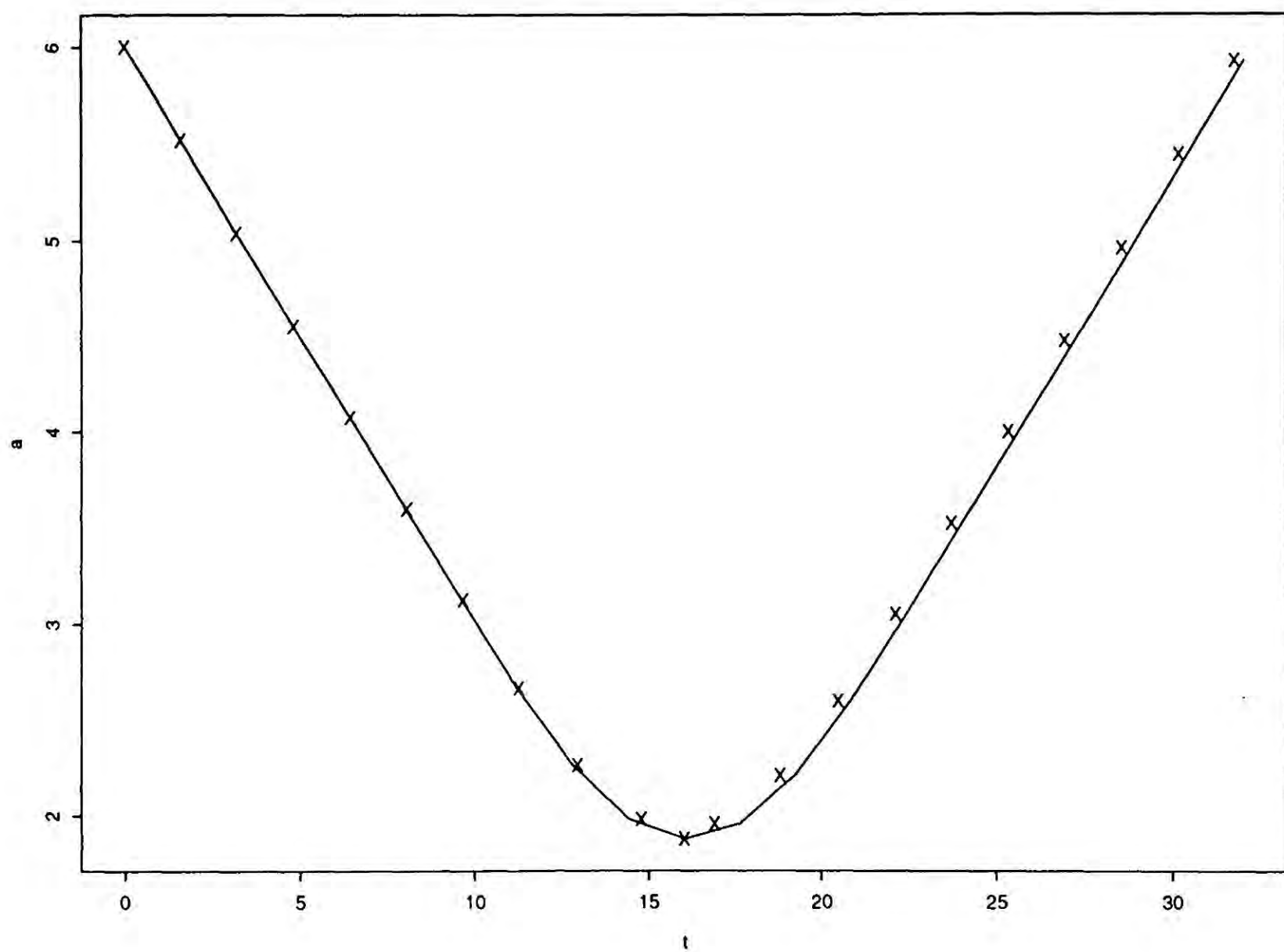


Fig 5.2 Plot of kink position against time for the exact solution (continuous curve) and approximation (crosses) for velocity $u = 0.3$.

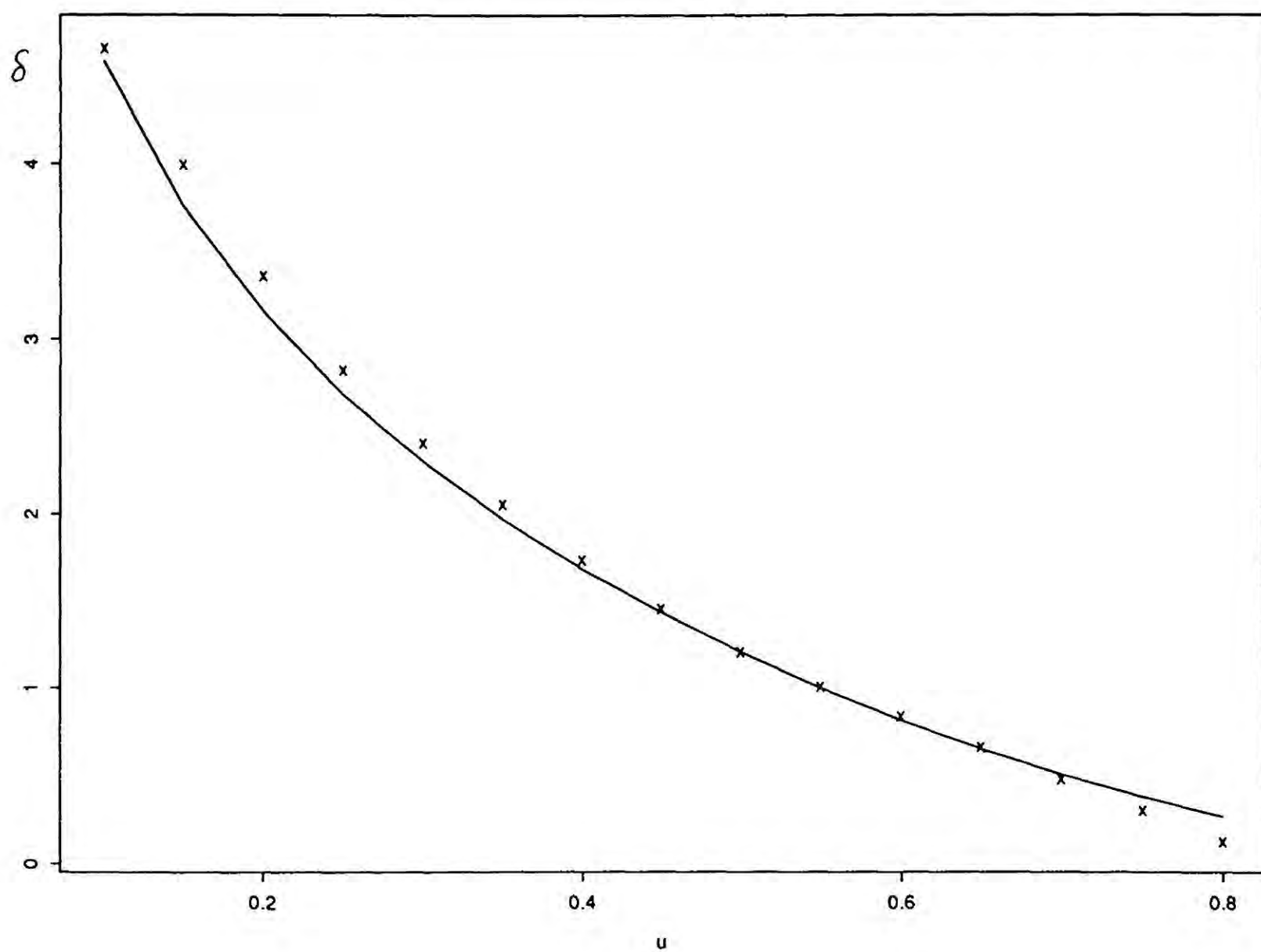


Fig 5.3 Plot of classical phase shift δ against velocity u for the approximation (crosses) and exact solution (continuous curve).

since the mass of the system is equal to 4. (We use natural units $\hbar = c = 1$.)

We require total reflection for an incident wave function so that we impose the boundary condition $\Psi(0, t) = 0$, corresponding to the choice $\mathcal{M} = \mathbf{R}^+$. As an alternative we could choose $\mathcal{M} = \mathbf{R}$ and have the wave function non-zero in the region $a \leq 0$ where $V(a) \rightarrow \infty$ as $a \rightarrow -\infty$.

By considering stationary state wavefunctions of energy E we can restrict our attention to wavefunctions $\psi(a)$ satisfying the time-independent Schrödinger equation

$$\frac{\partial^2 \psi}{\partial a^2} + 8(E - V)\psi = 0 \quad (5.18)$$

where for kink scattering with velocity u we have $E = 4 + 2u^2$.

The wavefunction has the asymptotic behaviour

$$\psi(a) \sim \sin(p(a)a + \delta) \quad \text{as} \quad a \rightarrow \infty \quad (5.19)$$

where $p(a)$ is the momentum

$$p(a) = \sqrt{8(E - V(a))} \quad (5.20)$$

and (5.19) together with the boundary condition $\psi(0) = 0$ defines the phase shift δ in the wavefunction uniquely.

The WKB approximation to the wave function then gives^[62] the phase shift to be

$$\delta = \int_{a_1}^{\infty} (p(a) - p(\infty)) da - a_1 p(\infty) \quad (5.21)$$

where a_1 is the classical turning point $V(a_1) = 4 + 2u^2$. Using equation (5.20) this becomes

$$\delta = \int_{a_1}^{\infty} (\sqrt{8(4 + 2u^2 - V(a))} - 4u) da - 4a_1 u \quad (5.22)$$

Before we go on to examine this phase shift let us first make a few remarks regarding the mass and coupling constant parameters of the sine-Gordon theory. (For more details see ref [63]).

The sine-Gordon Lagrangian density (5.1) that we have been using so far is written in terms of rescaled fields, which are used to remove the dependence upon the constants of the theory as described below.

The full sine-Gordon Lagrangian density is given by

$$\mathcal{L} = \frac{1}{8} \partial_\mu \phi \partial^\mu \phi + \frac{m_0^2}{4\beta^2} (\cos \beta \phi - 1) \quad (5.23)$$

where β is the coupling constant and m_0 is a mass-like parameter. If we define the rescaled variables $\bar{\phi} = \beta \phi$ and $\bar{x}_\mu = m_0 x_\mu$ then (5.23) becomes

$$\mathcal{L} = \frac{m_0^2}{\beta^2} \left\{ \frac{1}{8} \bar{\partial}_\mu \bar{\phi} \bar{\partial}^\mu \bar{\phi} + \frac{1}{4} (\cos \bar{\phi} - 1) \right\} \quad (5.24)$$

so that the β and m_0 only appear as factors in front of the Lagrangian density. Classically the rescaling is therefore only a trivial redefinition of the energy and length units. However, quantum mechanically it is not \mathcal{L} but $\mathcal{L}\hbar^{-1}$ that is the important quantity. In the quantum case $\beta\hbar$ is an additional dimensionless parameter of the theory. We can continue to use natural units ($\hbar = 1$) by absorbing \hbar into a redefinition of β , so that the classical limit (small \hbar) corresponds to the weak coupling limit (small β) of the theory.

If we repeat the analysis of this section using the Lagrangian density (5.23) we find the only effect on the phase shift (5.22) is the multiplication by a factor β^{-2} .

In Fig 5.4 we plot δ (continuous curve) for a range of velocities $0.1 \leq u \leq 0.7$. (We set $\beta = 1$).

The sine-Gordon model is an integrable quantum field theory and this allows the explicit construction^[65] of the exact S-matrix (which is related to the phase shift). Although we could compare our collective coordinate approximation with this exact result (which has a very complicated form) we would then be testing not only the validity of the collective coordinate approximation but also the semi-classical quantization involved in the WKB approximation. Also, we would expect our results to be valid only in the weak coupling limit since the whole procedure involved in the collective coordinate approximation is based upon neglecting the radiation components of the theory. In the quantum sine-Gordon theory this corresponds to considering only the baryonic degrees of freedom and neglecting the effects of meson waves. At large coupling, effects such as the renormalization of the bare mass-like parameter m_0 , may become significant. In addition

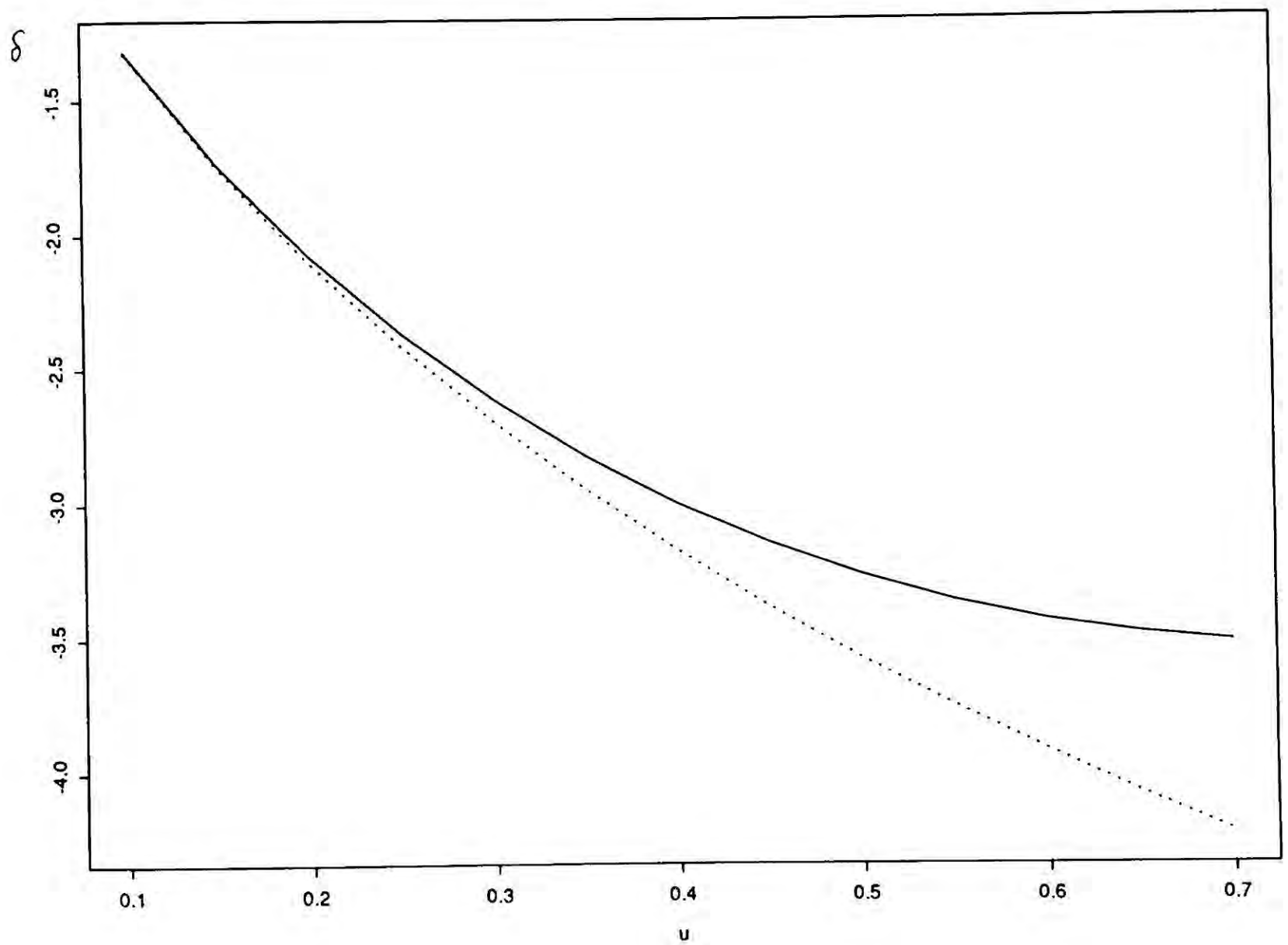


Fig 5.4 Plot of quantum phase shift δ against velocity u for the approximation (continuous curve) and semi-classical result of ref [64] (dashed curve).

to the construction of the exact S-matrix, the integrability of the sine-Gordon model allows other results to be obtained. In particular Jackiw and Woo [64] have performed a semi-classical quantization of the theory based upon the knowledge of the exact solutions. They obtained the following expression for the phase shift, which is in agreement with the exact result of [65] in the weak coupling limit ($\beta \rightarrow 0$)

$$\delta = \frac{4}{\beta^2} \int_0^u \frac{\log \zeta}{1 - \zeta^2} d\zeta \quad (5.25)$$

We plot this expression in Fig 5.4 (dashed curve) for comparison with the collective coordinate approximation. We see that even in the quantum regime the approximation is again very good up to relatively high velocities. As the velocity increases the accuracy of the approximation deteriorates. In ref [64] the authors stress that their result (5.25) is essentially relativistic, so we would expect that the non-relativistic collective coordinate approximation would be less reliable for large velocities.

Note that we could probably improve the approximation slightly for higher velocities by retaining the metric $g(a)$ and replacing the one-dimensional laplacian in the Schrödinger equation (5.18) by the covariant laplacian on \mathcal{M} . This is because at higher energies (velocities) the structure of the metric at small a is increasingly important.

5.6 CONCLUSION

We have seen how the validity of the collective coordinate approximation for studying classical and quantum soliton scattering may be tested by application to the scattering of sine-Gordon kinks. Once again, as with the limited examples in which tests of the approximation have already been made, we find that the approximation works remarkably well at the classical level. Moreover, we have made the first tests of the approximation in the quantum regime and again find that it compares well with known results. It is hoped that this study provides additional justification for both the method and the results obtained when applied to the study of classical and quantum soliton scattering in other systems.

CHAPTER VI.

Yang-Mills-Higgs Solitons

6.1 INTRODUCTION

There are many examples of integrable systems in (1+1)-dimensions which possess soliton solutions. The solitons of these systems have a simple collision behaviour and are stable under small perturbations. In (2+1)-dimensions there are few integrable systems, the Kadomtsev-Petviashvili and Davey-Stewartson equations being the most well known. However, the methods used in (1+1)-dimensions to construct soliton solutions, such as the inverse scattering transform, when applied to these higher dimensional systems generate plane wave solitons which are one-dimensional in character. It is only through special limiting procedures that truly two dimensional solitons may be constructed.

In recent years much progress has been made in unifying integrable systems, with many well known integrable equations in (1+1)-dimensions shown to fit into a general framework^[19] as reductions of the self-dual Yang-Mills equations. Integrable systems in (2+1)-dimensions may also be obtained through reduction of the self-duality equations, and provide higher dimensional generalizations of well known integrable systems. In such systems two dimensional solitons occur in a simple way, rather than under special limiting procedures, and therefore appear to be the more natural generalization of solitons to higher dimensions. It is interesting to study such solitons and to see if the characteristic properties of one-dimensional solitons, such as stability to small perturbations, extends to the solitons of such planar systems.

6.2 THE YANG-MILLS-HIGGS-BOGOMOLNY EQUATION

Consider an $SU(2)$ gauge theory in (2+1)-dimensional spacetime. The gauge potential A_μ is a 1-form on \mathbb{R}^{2+1} taking values in the lie algebra $\mathfrak{su}(2)$. Here $x^\mu = (t, x, y)$ and the metric is $\eta^{\mu\nu} = \text{diag}(-1, 1, 1)$.

The gauge field is $F_{\mu\nu} = \partial_\mu A_\nu - \partial_\nu A_\mu + [A_\mu, A_\nu]$, and the Higgs field Φ is an $\mathfrak{su}(2)$ valued scalar field.

Consider the following equation

$$D_\mu \Phi = \frac{1}{2} \epsilon_{\mu\alpha\beta} F^{\alpha\beta} \quad (6.1)$$

where D_μ is the covariant derivative and $\epsilon_{\mu\alpha\beta}$ is the totally antisymmetric tensor (with $\epsilon^{012} = +1$). This is the Yang-Mills-Higgs-Bogomolny equation, which is hyperbolic and describes the time evolution of a Yang-Mills-Higgs system in (2+1) dimensions. It is an integrable equation which results as a reduction of the self-dual Yang-Mills equations in (2+2)-dimensions under the reduction by a timelike killing vector. A similar reduction from (4+0)-dimensions (but this time by a spacelike vector) gives the Bogomolny equation for static monopoles in three space dimensions, which has a similar form. (6.1) may therefore be considered as a hyperbolic version of the Bogomolny equation for magnetic monopoles. It is the study of the soliton solutions to the (6.1) equation which forms the basis of this chapter. Notice that the equation is Lorentz invariant *ie* it has an $SO(2,1)$ symmetry, and that the length of the Higgs field *ie* $-\text{Tr}(\Phi^2)$ is a gauge invariant quantity which will be useful in describing the system.

As far as boundary conditions are concerned we shall require that both Φ and A_μ decay to zero at spatial infinity, and moreover that Φ decays sufficiently fast so that the integral of the Higgs density (*ie* $-\int \text{Tr}(\Phi^2) dx dy$) is finite. Finally, note that we can consider (6.1) for any gauge group and it will still be an integrable equation. The choice here of an $SU(2)$ gauge group is for simplicity. An $SL(2, \mathbb{C})$ gauge group, for example, could also be considered, but here we choose a real form in order to continue the monopole analogy.

6.3 TWISTOR CONSTRUCTION OF SOLITONS

The well known twistor correspondence for self-dual Yang-Mills fields in 4-dimensional spacetime is that they correspond to certain holomorphic vector bundles over the standard complex 3-dimensional twistor space. Now since (6.1) is a reduction of the self-duality equations there is a reduced version of the standard twistor correspondence to 3-dimensional spacetime, namely that gauge fields satisfying (6.1) correspond to certain holomorphic vector bundles over a mini-twistor space^[66,30,67] \mathbb{P} , which is a 2-dimensional complex manifold isomorphic to the holomorphic tangent bundle to the Riemann sphere *ie* $\mathbb{P} \cong T\mathbb{C}P^1$. Here this correspondence will be briefly described and then used explicitly in order to obtain the soliton solutions to (6.1).

The space \mathbb{P} is a fibre bundle over $\mathbb{C}\mathbb{P}^1$ with each fibre being a copy of \mathbb{C} . Let ζ be the standard coordinates on the base space $\mathbb{C}\mathbb{P}^1$. Cover this base space with the two coordinate patches $U = (\zeta : |\zeta| \leq 1)$ and $\hat{U} = (\zeta : |\zeta| \geq 1)$. The fibre coordinates γ over U and $\hat{\gamma}$ over \hat{U} are patched by $\hat{\gamma} = \zeta^{-2}\gamma$. A reality structure is introduced by defining an anti-holomorphic involution on the base space $\sigma(\zeta) = \bar{\zeta}^{-1}$, which may then be extended to \mathbb{P} by defining $\sigma: (\zeta, \gamma) \rightarrow (\bar{\zeta}^{-1}, -\bar{\gamma})$. The real sections (ie. those preserved by the involution) are then given by

$$\gamma = \bar{z}\zeta^2 - 2it\zeta - z \quad (6.2)$$

where $z = x + iy \in \mathbb{C}$, $t \in \mathbb{R}$

Solutions of (6.1) correspond to rank two holomorphic vector bundles E over \mathbb{P} satisfying the condition that E is trivial when restricted to real sections. E is also required to have a reality structure, as described below, in order to ensure that the gauge fields are $\mathfrak{su}(2)$ valued.

Let F be the 2×2 patching matrix which patches $E|_U$ to $E|_{\hat{U}}$. Then the required reality structure is that F must satisfy

$$\begin{aligned} F^\dagger &= F \\ \det F &= 1 \end{aligned} \quad (6.3)$$

where $F^\dagger(\zeta, \gamma) = F(\bar{\zeta}^{-1}, -\bar{\zeta}^{-2}\bar{\gamma})^*$, and $*$ denotes complex conjugate transpose.

For the purpose of constructing the n -soliton solution the patching matrix may be taken to have the form of the Atiyah-Ward ansätze^[68]. Namely

$$F(\zeta, \gamma) = \begin{pmatrix} \zeta^n & \Gamma(\zeta, \gamma) \\ 0 & \zeta^{-n} \end{pmatrix}. \quad (6.4)$$

where Γ is an element of the cohomology group $H^1(\mathbb{P}, \mathcal{O}(-2n))$.

This patching matrix does not satisfy the reality condition (6.3), but for some Γ it may be equivalent to one which does. Namely, there may exist a matrix K which is holomorphic on \hat{U} , such that $\tilde{F} = KF$ satisfies (6.3). Multiplication by K simply amounts to a change of coordinates in the bundle and leaves the gauge fields unaffected.

The gauge invariant quantity $-\text{Tr}(\Phi^2)$ which we are using to describe the system has a simple expression if F has the form (6.4), with $n = 1$. Namely,

$$-\text{Tr}(\Phi^2) = -\frac{1}{2}\square \log \Delta \quad (6.5)$$

where \square is the (2+1)-dimensional wave operator, and Δ is a solution of the wave equation, $\square\Delta = 0$, given by

$$\Delta = \frac{1}{2\pi i} \oint \frac{\Gamma(\zeta, \gamma)}{\zeta} d\zeta \quad (6.6)$$

where the contour of intergration is $|\zeta| = 1$.

To construct the one-soliton solution take Γ to be given by⁽³⁰⁾

$$\Gamma = \frac{f + f^{\dagger-1}}{(\zeta - \alpha)(\zeta^{-1} - \bar{\alpha})} \quad (6.7)$$

where $f = \lambda\gamma$ and α, λ are complex constants, with $|\alpha| < 1$, which determine the velocity and width of the soliton respectively.

This choice of Γ generates $\text{su}(2)$ valued gauge fields since $\tilde{F} = KF$ satisfies (6.3) with K given by

$$K = \begin{pmatrix} \zeta^{-1}(\zeta - \alpha)(\zeta^{-1} - \bar{\alpha}) & -f^{\dagger-1} \\ f^{\dagger} & 0 \end{pmatrix} \quad (6.8)$$

With this choice of Γ using (6.5) and (6.6) gives the Higgs density to be

$$-\text{Tr}(\Phi^2) = \frac{2(1 - |\alpha|^2)^2 |\lambda|^2}{(1 + |\lambda|^2 |\bar{z}\alpha^2 - 2it\alpha - z|^2)^2} \quad (6.9)$$

The static soliton corresponds to $\alpha = 0$, in which case the Higgs density is peaked at the origin with maximum value $2|\lambda|^2$. For the static one-soliton solution the integral of the Higgs density is

$$\mathcal{H} = - \int \text{Tr}(\Phi^2) d^2 z = 2\pi \quad (6.10)$$

The width μ of this soliton is defined by the formula

$$\pi = - \int_{|z| \leq \mu} \text{Tr}(\Phi^2) d^2 z \quad (6.11)$$

so that $\mu = |\lambda|^{-1}$.

Write $\alpha = -me^{-i\theta}$, then the soliton moves at an angle θ in the (x, y) plane with a velocity $v = \frac{2m}{1+m^2} < 1$.

Using a chiral field formulation (see next section) it may be shown that the static solutions of (6.1) correspond to the static solutions of the SU(2) chiral model. However, it has been shown^[69] that the only static finite energy solutions of the SU(2) chiral model are the embeddings of the static lumps of the $\mathbb{C}\mathbb{P}^1$ σ -model. This result may be used to show that the only static solutions of (6.1), for which the integral of the Higgs density is finite, are the embeddings of the $\mathbb{C}\mathbb{P}^1$ static lumps. An explicit choice for the embedding map is given by

$$\begin{aligned} A_t = A_y &= [\mathbf{P}, \partial_y \mathbf{P}] \\ A_x &= -\Phi = [\mathbf{P}, \partial_x \mathbf{P}] \end{aligned} \tag{6.12}$$

where \mathbf{P} is the one-dimensional hermitian projector of the $\mathbb{C}\mathbb{P}^1$ model. Using the W formulation the static lump solutions are given by

$$\mathbf{P} = \frac{1}{(1 + |W|^2)} \begin{pmatrix} 1 & W \\ \bar{W} & |W|^2 \end{pmatrix} \tag{6.13}$$

where W is a holomorphic (or anti-holomorphic) function of $z = x + iy$.

For W a holomorphic function of z then

$$-\text{Tr}(\Phi^2) = \frac{2|\partial W|^2}{(1 + |W|^2)^2} \tag{6.14}$$

where ∂ denotes differentiation with respect to z .

For these static solutions (6.14) is precisely the conserved energy density of the $\mathbb{C}\mathbb{P}^1$ model. Therefore, for the embedding of the $\mathbb{C}\mathbb{P}^1$ static solutions $-\text{Tr}(\Phi^2)$ corresponds to the energy density of the $\mathbb{C}\mathbb{P}^1$ model.

6.4 SIGMA MODEL FORMULATIONS

In order to study various aspects of (6.1) it is convenient to use several formulations. In this section we shall introduce two σ -model formulations which shall be useful later.

J-formulation

It has been shown^[70] that for solutions of (6.1) there exists a gauge in which the fields have the following form

$$\begin{aligned} A_t &= A_y = \frac{1}{2}J^{-1}(\partial_t J + \partial_y J) \\ A_x &= -\Phi = \frac{1}{2}J^{-1}\partial_x J \end{aligned} \tag{6.15}$$

where $J \in \text{SU}(2)$.

Then (6.1) becomes the following equation for J

$$(\eta^{\mu\nu} + V_\alpha \epsilon^{\alpha\mu\nu})\partial_\mu(J^{-1}\partial_\nu J) = 0 \tag{6.16}$$

where V^α is the spacelike vector $V^\alpha = (0, 1, 0)$.

This is a chiral equation with torsion term^[71] and has the same conserved positive definite energy functional as the chiral field equations. This energy functional is given by

$$\mathcal{E} = \frac{1}{2} \int \delta^{\mu\nu} \text{Tr}(\partial_\mu J \partial_\nu J^{-1}) dx dy. \tag{6.17}$$

In terms of the twistor formalism the gauge choice (6.15) corresponds to a particular framing of the bundles over \mathbb{P}^1 which determine the solutions of (6.1).

(6.1) has an $\text{SO}(2,1)$ spacetime symmetry, which is broken when the J-formulation is used ie (6.16) has only an $\text{SO}(1,1)$ symmetry. This occurs due to the fact that the vector V^α must pick out a particular direction in spacetime. Taking V^α to be spacelike means that the symmetry which remains is an $\text{SO}(1,1)$ symmetry. Since in the J-formulation the equations have no radial symmetry, a numerical study of stability is more difficult. However the J-formulation has been useful in investigating soliton interactions^[71], where it has been shown that such interactions are trivial.

Q-formulation

For solutions of (6.1) it is always possible to choose a gauge in which the fields have the following form

$$\begin{aligned}
 \Phi &= \frac{i}{2}(H^{-1}.\partial_t H + \partial_t H^*.H^{*-1}) \\
 A_t &= \frac{1}{2}(H^{-1}.\partial_t H - \partial_t H^*.H^{*-1}) \\
 A_x &= (H^{-1}.\partial_z H - \partial_z H^*.H^{*-1}) \\
 A_y &= -i(H^{-1}.\partial_{\bar{z}} H + \partial_z H^*.H^{*-1})
 \end{aligned} \tag{6.18}$$

where $H \in SL(2, \mathbb{C})$.

This gauge choice appears naturally in the twistor formalism if we again consider framed bundles over \mathbb{P} . The two gauge choices (6.15) and (6.18) arise from the choice of lines along which the bundles over \mathbb{P} are framed.

Define the matrix Q by

$$Q = HH^* \tag{6.19}$$

then Q is hermitian and has unit determinant.

With the above definitions (6.1) becomes the following equation for Q

$$(\eta^{\mu\nu} + i\tilde{V}_\alpha \epsilon^{\alpha\mu\nu})\partial_\mu(Q^{-1}.\partial_\nu Q) = 0 \tag{6.20}$$

where \tilde{V}^α is the timelike vector $\tilde{V}^\alpha = (1, 0, 0)$.

Again the $SO(2,1)$ symmetry of (6.1) is broken. In the Q -formulation the vector \tilde{V}^α in (6.20) is a timelike vector so that the symmetry which remains is an $SO(2)$ symmetry. This symmetry may then be used when studying the stability of the static one-soliton solution.

The Higgs density may be expressed in terms of the matrix Q as

$$-\text{Tr}(\Phi^2) = \frac{1}{2}\text{Tr}(Q^{-1}.\partial_t Q)^2. \tag{6.21}$$

Note that (6.21) implies that in order to obtain a non-zero Higgs density, Q must be time dependent. For the static one-soliton solution the time dependence of Q must occur in a special way such that $-\text{Tr}(\Phi^2)$ is time independent.

Both the J and Q-formulations remove the gauge degrees of freedom and so are much more convenient for numerical simulations. Also we shall see that when studying the stability of the one-soliton solution it is important that an exact solution to the discretized problem can be found. This can be achieved with little effort using the Q-formulation.

6.5 SOLITON STABILITY

In this section we investigate numerically the stability of the one-soliton solution under radially symmetric perturbations. As shown earlier the static soliton solutions to (6.1) are simply the embeddings of the static lump solutions of the $\mathbb{C}\mathbb{P}^1$ σ -model, and so it is useful to compare the stability of solitons in this model with that of lumps in the $\mathbb{C}\mathbb{P}^1$ model. Lumps of the $\mathbb{C}\mathbb{P}^1$ model, in (2+1)-dimensions, possess a topological stability, as described earlier, that is due to the topological nature of the target manifold. Only field configurations with finite energy are considered, which requires that the field must take the same value at all points of spatial infinity. The upshot of this is that the space may be compactified from \mathbb{R}^2 to S^2 , so at any fixed time the field configuration may be considered as a map from S^2 into $\mathbb{C}\mathbb{P}^1$. The homotopy group relation

$$\pi_2(S^2) = \mathbb{Z} \quad (6.22)$$

then implies that to each field configuration there may be associated an integer, known as the topological charge, which is conserved and represents the winding number of the field as a map from space to the target manifold. An n-lump configuration is defined to be a field configuration with topological charge n. This means that the one-lump solution cannot decay to the vacuum, since the vacuum has zero topological charge. This topological stability implies that the lumps of the $\mathbb{C}\mathbb{P}^1$ model have no negative modes. However, it was found^[43] that the lumps do possess zero modes, which are modes of instability in which the width of the lumps becomes either infinite or zero.

Now for the model considered in this chapter there is no such topological stability. This is because the fields of equation (6.1) take values in the gauge group $SU(2)$, which has group manifold S^3 .

The corresponding equation to (6.22) in this case is that

$$\pi_2(S^3) = 0. \quad (6.23)$$

There is no winding number for such a map, and hence no topological charge. This means

that the solitons of this model may possibly possess both negative modes (ie they may decay to the vacuum), and also zero modes in a way similar to those found for the $\mathbb{C}\mathbb{P}^1$ lumps. It is important that when the equations of motion are discretized then an exact one-soliton solution exists for this discrete system, otherwise the process of discretization will induce perturbations upon the soliton, over which we have little or no control. This problem was overcome in the study of the stability of $\mathbb{C}\mathbb{P}^1$ lumps by use of a topological approach^[43], based upon the discretization of the Bogomolny equations, which give the static lumps of the $\mathbb{C}\mathbb{P}^1$ model. Since we have no topological properties for the model studied here, this method cannot be used and so a new method must be found.

The method of discretization used here is to replace derivatives by symmetric finite differences, and to perform the time evolution of the system numerically by use of a fourth-order Runge-Kutta method. If we were to simply apply this scheme to (6.1) then the discretized one-soliton solution would not satisfy the discrete version of (6.1). This is where the Q -formulation of the previous section is useful. Parameterize Q in the following way

$$Q = \frac{1}{\varphi} \begin{pmatrix} 1 & \bar{\rho} \\ \rho & \varphi^2 + |\rho|^2 \end{pmatrix}. \quad (6.24)$$

where $\rho \in \mathbb{C}$, $\varphi \in \mathbb{R}$.

Then in terms of these variables

$$-\text{Tr}(\Phi^2) = \frac{1}{4\varphi^2} ((\partial_t \varphi)^2 + |\partial_t \rho|^2) \quad (6.25)$$

and the static one-soliton solution located at the origin is given by

$$\begin{aligned} \varphi &= \varphi_{st} = 1 + \lambda^2 r^2 \\ \rho &= \rho_{st} = -2it\lambda \end{aligned} \quad (6.26)$$

where $r^2 = x^2 + y^2$.

Then (6.20) may be written as equations for ρ and φ . These equations are then discretized according to the above scheme. The advantage of this method is that since the static one-soliton solution given by (6.26) is only quadratic in the spacetime variables, then symmetric finite difference approximations are exact for these functions, and so an exact solution to the discrete problem is easily obtained by simply taking the discrete version of (6.26).

Imposing radial symmetry on the equations of motion for ρ and φ we find that they are given by

$$\begin{aligned} -\varphi\Box\varphi + (\partial_t\varphi)^2 - (\partial_r\varphi)^2 - |\partial_t\rho|^2 + |\partial_r\rho|^2 &= 0 \\ -\varphi\Box\rho + 2(\partial_t\varphi\cdot\partial_t\rho - \partial_r\varphi\cdot\partial_r\rho) &= 0 \end{aligned} \quad (6.27)$$

where

$$\Box = \partial_t^2 - r^{-1}\partial_r(r\partial_r)$$

is now the radially symmetric wave operator in (2+1)-dimensions.

Radially symmetric perturbations of the static one-soliton solution (6.26) were then investigated using the above described numerical procedure. The simulations were performed using an AMDAHL 5860, with the MTS operating system at Durham, and also a SUN SPARC workstation. The grid used consists of 300 points in the radial direction with a unit lattice spacing. The soliton was taken to be of width $\mu = 30$ and the time step taken was 0.2.

The first type of perturbation considered is that in which the Higgs density at time $t = 0$ is that of the static one-soliton. From (6.25) it can be seen that this is achieved by perturbing ρ at $t = 0$ but in such a way so that its first time derivative is initially unaffected. Explicitly take the fields at $t = 0$ to be given by

$$\begin{aligned} \varphi &= \varphi_{st} \\ \rho &= \rho_{st} + \frac{\eta_1}{(1 + \lambda^2 r^2)^2} \end{aligned} \quad (6.28)$$

where the perturbing term tends to zero as $r \rightarrow \infty$, in order to ensure that \mathcal{H} , the integral of the Higgs density, remains finite. η_1 is a complex parameter that determines the initial rate of change of the Higgs density. The results of such a perturbation are qualitatively the same for all values of η_1 . Fig 6.1 shows the Higgs density at varying times throughout the evolution for the value $\eta_1 = 0.1\lambda$.

The first point to note is that there are no negative modes excited by such a perturbation. This suggests that there may be no negative modes present for this one-soliton solution, although numerical simulations can not rule out this possibility. The Higgs density remains that of a one-soliton solution, although initially there are also additional waves of radiation that flow from the centre of the soliton as it oscillates. We can therefore use the width of the soliton as a sensible parameter. In order to calculate the width μ

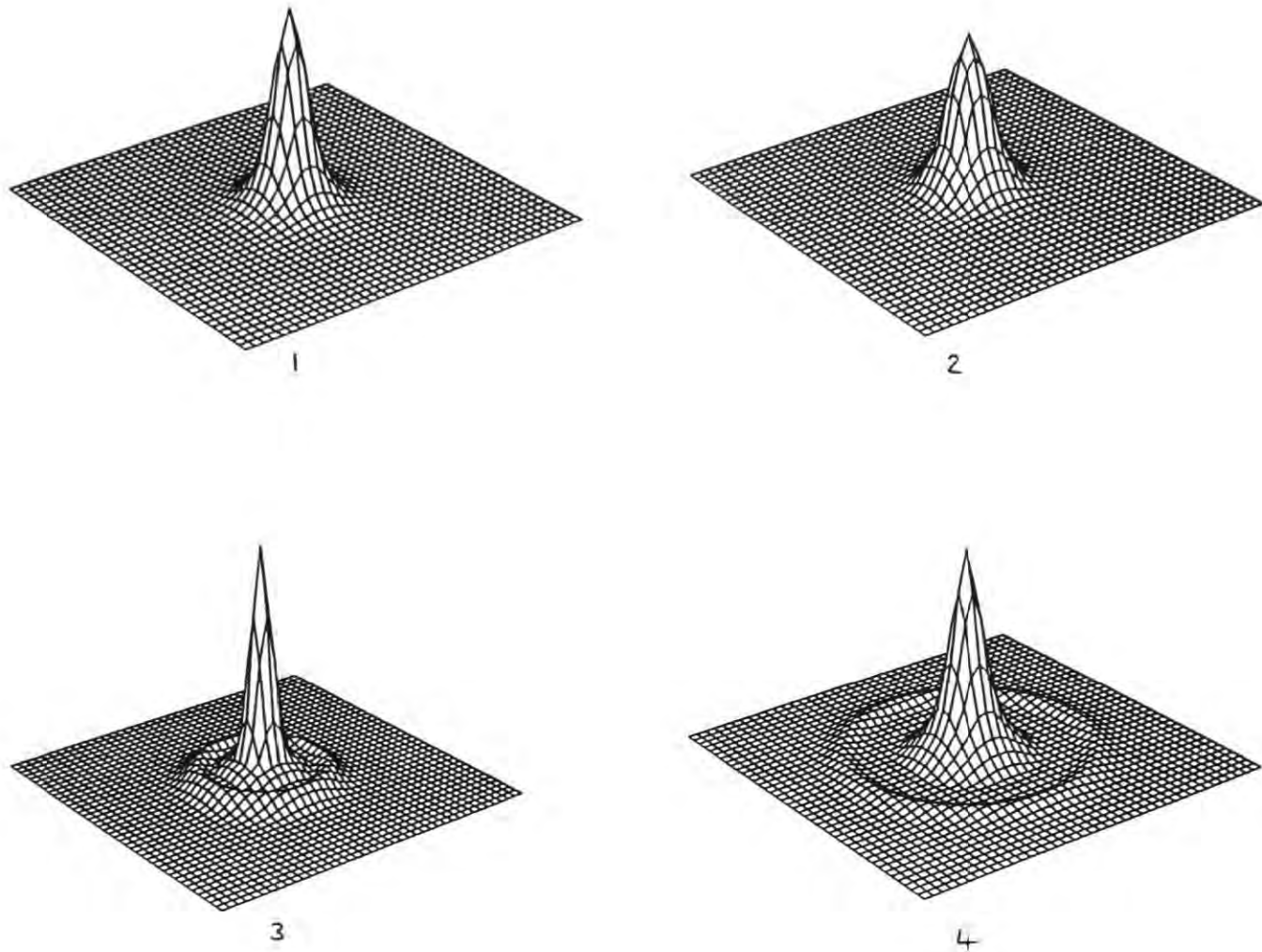


Fig 6.1 The Higgs density $-\text{Tr}(\Phi^2)$ at increasing times for a soliton of initial width $\mu = 30$ and perturbation parameter $\eta_1 = \frac{1}{10\mu}$

of the soliton in numerical simulations one may try to use the discrete version of (6.11). With unit radial lattice spacing this gives an approximation $\tilde{\mu}$ to the width defined by

$$2\pi \sum_{n=0}^{\tilde{\mu}-1} \left(n + \frac{1}{2}\right) T_n < \pi < 2\pi \sum_{n=0}^{\tilde{\mu}} \left(n + \frac{1}{2}\right) T_n \quad (6.29)$$

where T_n denotes $-\text{Tr}(\Phi^2)$ evaluated at radial lattice site n . $\tilde{\mu}$ is therefore integer valued. However, there is an alternative method which may be used to calculate the width numerically and which leads to an approximation $\hat{\mu}$ which is real valued. From (6.9) note that for the static soliton solution

$$-\text{Tr}(\Phi^2)|_{r=0} = 2|\lambda|^2 = 2\mu^{-2} \quad (6.30)$$

which motivates the definition

$$\hat{\mu} = \sqrt{\frac{2}{T_0}} \quad (6.31)$$

In the numerical simulations described here both $\tilde{\mu}$ and $\hat{\mu}$ were calculated. It was found that $\hat{\mu}$ appears to be the most useful measure of the width of the soliton, and in particular includes all the information obtained from calculating $\tilde{\mu}$ since the following relation was valid throughout the simulations

$$\tilde{\mu} = \text{Int}(\hat{\mu}) \quad (6.32)$$

where Int denotes the integer part.

Fig 6.2a shows the plot of the width $\hat{\mu}$ as a function of time throughout the evolution.

It can be seen that this width oscillates around its initial value with the amplitude of the oscillations decaying exponentially. The initial amplitude of oscillations is related to $|\eta_1|$ but in all cases this oscillation decays in the same manner until the soliton returns to its initial unperturbed state. This oscillation is accompanied by a ring of radiation that spreads from the centre of the soliton towards the boundary, moving with the speed of light. Fixed boundary conditions are used in our simulations and so when this ring of radiation reaches the boundary it is reflected back. In order to ensure that this reflected radiation does not affect the soliton we choose the size of the grid to be large enough so that the radiation does not have time to travel to the boundary and back to the soliton

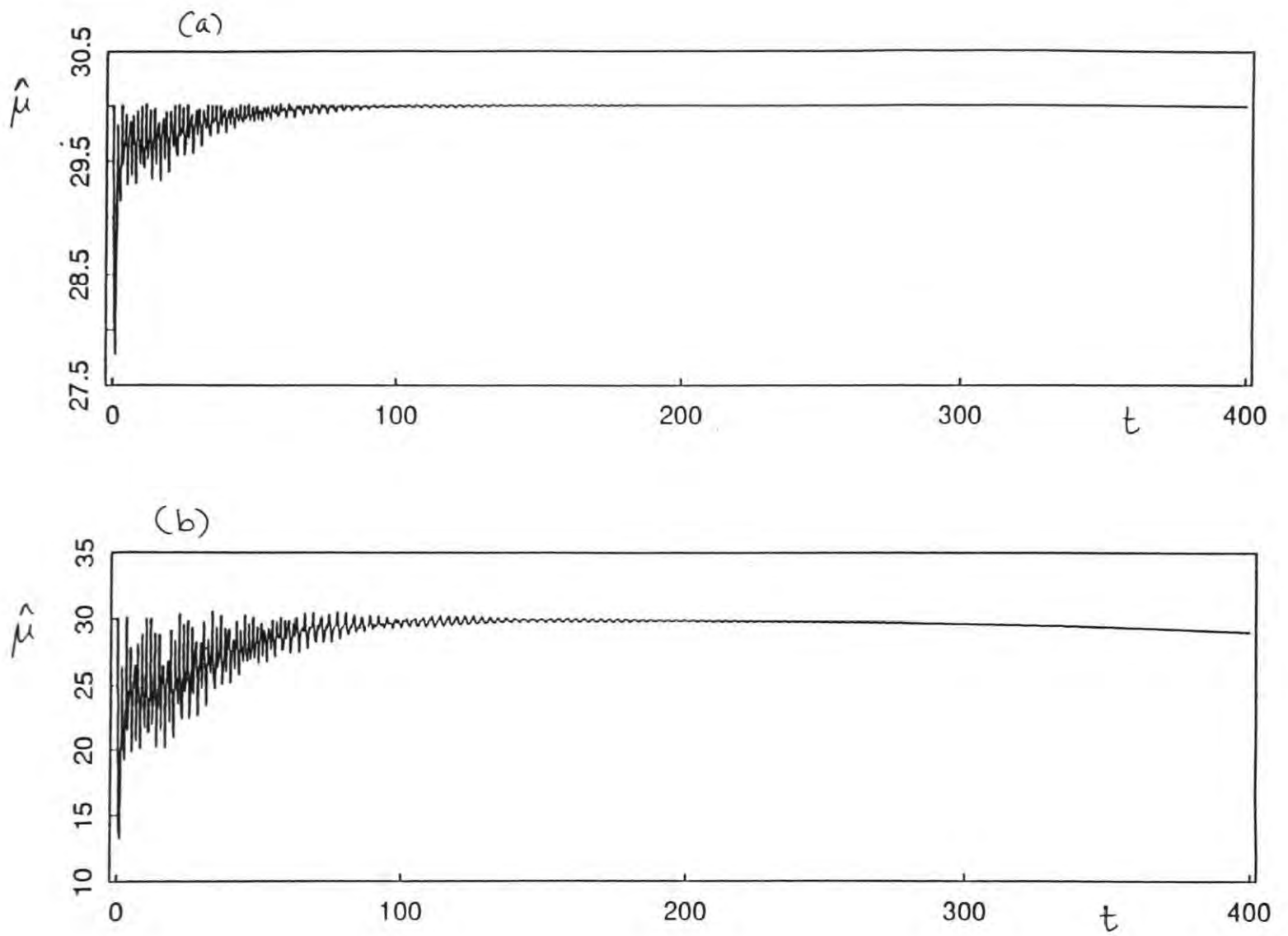


Fig6.2 Plot of the width $\hat{\mu}$ as a function of time for (a) the simulation shown in Fig 6.1. (b) the modified equation with parameters $\epsilon_1 = \dots = \epsilon_4 = 10^{-2}$.

during the time span of any particular simulation. This requires the use of a large grid, which is costly in terms of computing time, but is possible due to the fact that imposing radial symmetry effectively reduces the number of space dimensions to one.

Not only are negative modes not excited by this perturbation but there are also no zero modes excited, so it appears that the soliton is stable to this form of perturbation. This is in contrast to the $\mathbb{C}\mathbb{P}^1$ lumps where a perturbation involving initial time derivatives always results in zero modes being excited, which are clearly evident in numerical simulations.

A second form of perturbation we may consider is the interaction of a soliton with a radial wave of radiation. Explicitly this is achieved with the fields taking the form

$$\begin{aligned}
 \varphi|_{t=0} &= \varphi_{st}|_{t=0} \\
 \rho|_{t=0} &= \rho_{st}|_{t=0} \\
 \partial_t \varphi|_{t=0} &= 2\lambda^2 r^2 \eta_2 \exp(-\eta_3^2 \lambda^2 r^2) \\
 \partial_t \rho|_{t=0} &= \partial_t \rho_{st}|_{t=0}
 \end{aligned} \tag{6.33}$$

where η_2 and η_3 are two real parameters which determine the size of the ring of radiation as described below.

The fields of (6.33) give the additional radiation contribution to $-\text{Tr}(\Phi^2)$ of

$$-\text{Tr}(\Phi^2)_{rad} = \left(\frac{\lambda^2 r^2 \eta_2 \exp(-\eta_3^2 \lambda^2 r^2)}{(1 + \lambda^2 r^2)} \right)^2 \tag{6.34}$$

which is a ring structure with the peak at $r = (|\eta_3|/\lambda)^{-1}$ at which it takes the value $\eta_2^2(1 + \eta_3^2)^{-1}$.

Simulations for varying values of the parameters η_1 and η_2 have been performed and all resemble qualitatively the evolution of the first type of perturbation considered. A ring of radiation moves towards the boundary at the speed of light leaving the soliton behind. The interaction of the radiation with the soliton is merely to set the width of the soliton in oscillation, with an amplitude which again follows an exponential decay. The initial change in the width of the soliton is related to the parameters of the radiation ring through the relation

$$\partial_t \lambda|_{t=0} = \eta_2 \lambda$$

Other perturbations of the soliton have been performed, such as the inclusion of random noise, but all produce similar results to those above. When the width of the

soliton oscillates it is always accompanied by a ring of radiation which interacts with the soliton as described above.

Although numerical simulations cannot prove soliton stability the fact that no unstable modes can be found with many varied perturbations is compelling evidence for the stability of the solitons under radially symmetric perturbations.

6.6 MODIFIED EQUATIONS

We have seen how the one-soliton solution to equation (6.27) is stable against small perturbations of the soliton. In this section we consider modifying (6.27) and ask how the stability of the solitons is affected by such modifications. There is no obvious choice for modifying (6.27), although restrictions are imposed if we require the static one-soliton (6.26) to still be a solution of the modified equations. Note that

$$\begin{aligned}\partial_t \varphi_{st} &= 0 \\ \partial_r \rho_{st} &= 0\end{aligned}\tag{6.35}$$

so that terms involving $\partial_t \varphi$, and $\partial_r \rho$, may be added to (6.27), and (6.26) will still be a solution.

The modified equations we consider are

$$\begin{aligned}-\varphi \square \varphi + (\partial_t \varphi)^2 - (\partial_r \varphi)^2 - |\partial_t \rho|^2 + |\partial_r \rho|^2 &= \epsilon_1 \partial_t \varphi \cdot \partial_r \varphi \\ -\varphi \square \rho + 2(\partial_t \varphi \cdot \partial_t \rho - \partial_r \varphi \cdot \partial_r \rho) &= \epsilon_2 (\partial_t \varphi)^2 + \epsilon_3 (\partial_r \rho)^2 + \epsilon_4 \partial_t \varphi \cdot \partial_r \rho\end{aligned}\tag{6.36}$$

where $\epsilon_1, \dots, \epsilon_4$ are real constants. The unmodified equation (6.27) corresponds to $\epsilon_1 = \dots = \epsilon_4 = 0$

Again results are similar for all sets of values for the ϵ 's, providing at least one is non-zero. The Higgs density resembles that of a one-soliton, and allows us to use the width of the soliton as a parameter to describe the time evolution of the configuration. Fig 6.2b shows a plot of the soliton width $\hat{\mu}$ against time for a simulation with the parameter values $\epsilon_1 = \epsilon_2 = \epsilon_3 = \epsilon_4 = 10^{-2}$. The perturbation parameters are the same as those used to produce Fig 6.2a. Initially the width oscillates around its initial value, and the evolution is similar to that of the unmodified equation. However, once the oscillations die down the width of the soliton no longer tends to the constant value that it was initially. It begins to decay exponentially, which suggests that the instability present is a negative mode. This

is in contrast to the zero mode instabilities present in \mathbb{CP}^1 lumps,^[43] in which the width of the lump decays in a linear fashion. The rate of this decay is related to the size of the ϵ 's and the decay can be replaced by a growth depending upon their sign. The important point is not the details of this instability but the fact that there appear to be instability present for all non-zero values of the ϵ 's.

This demonstrates how the equation of motion (6.1) is very special in having stable soliton solutions. The stability appears to be derived from the property that the equation is integrable, as described in the following section, and any small modification results in the loss of this integrability property.

6.7 INTEGRABILITY

Equation (6.1) is integrable in the sense that it may be written as the compatibility condition for an overdetermined linear system, and hence possesses an infinite number of conservation laws. This is most easily seen in terms of the J-formulation described earlier. (6.16) is the compatibility condition for the following linear system

$$\begin{aligned}(\lambda\partial_x - D_u)\Psi &= 0 \\(\lambda\partial_v - D_x)\Psi &= 0\end{aligned}\tag{6.37}$$

where D_μ is the covariant derivative

$$D_\mu = \partial_\mu + J^{-1}\partial_\mu J\tag{6.38}$$

and $u = \frac{t+y}{2}$, $v = \frac{t-y}{2}$ are light-cone coordinates. λ is a constant known as the spectral parameter.

The linear system (6.37) is a Lax pair formulation for (6.16) and allows the construction of an infinite number of conservation laws, as described below.

Expand Ψ in terms of the spectral parameter as

$$\Psi = \sum_{n=0}^{\infty} \lambda^n \Psi_n\tag{6.39}$$

Substituting this expansion into (6.37) and equating powers of λ gives

$$\begin{aligned}\Psi_0 &= J^{-1} \\ \partial_x \Psi_{n-1} &= D_u \Psi_n \quad n = 1, 2, \dots \\ \partial_v \Psi_{n-1} &= D_x \Psi_n\end{aligned}\tag{6.40}$$

Then (6.40) give the infinite set of continuity equations

$$\partial_v(D_u\Psi_n) = \partial_x(D_x\Psi_n) \quad n = 1, 2, \dots \quad (6.41)$$

It seems likely that the stability of the solitons in this model, as with integrable models in lower dimensions, is due to the infinite number of conservation laws. There is at present no proof of this conjecture, although the reasoning is something along the following lines. If the initial configuration consists of n solitons then in the large time limit the infinite number of conservation laws so constrain the system that the only configuration allowed is again n solitons.

Any slight perturbation of the equations of motion results in the loss of this infinite number of conserved charges, and hence to the property of stability. The soliton stability in this model is therefore derived from the precise details of the equation of motion rather than from its general form. All this may be compared with the planar Skyrmions of chapter III. These Skyrmions are stable in the same sense as the solitons of (6.1), ie. they have neither negative or zero modes. However, it is important to note that the way in which the stability is achieved in the two cases is very different. The planar Skyrme model does not have an infinite number of conserved charges and is certainly not integrable. The Skyrmions have a fixed width, which is dependent upon arbitrary parameters in the model, and any slight perturbation of these parameters (and hence of the equations of motion) results in a modification of this width but still the Skyrmions remain stable. It is the general form of the equations of motion, rather than the precise details, from which the Skyrmion stability is derived. Thus there appears to be two completely different ways in which stable solitons arise in $(2+1)$ -dimensions.

6.8 REMARKS ON SOLITON SCATTERING

Explicit multi-soliton solutions of this model have been found^[71] which correspond to solitons that interact in a trivial manner. On scattering the solitons suffer no change in velocity and no phase shift. As described earlier, the static solitons of this model are the embeddings of the \mathbb{CP}^1 static lumps, so it would be interesting to see the relationship between the trivial scattering multi-soliton solutions and the lumps of the \mathbb{CP}^1 model in $(2+1)$ -dimensions. The lumps of this latter model have a non-trivial scattering^[41,42] in which solitons scatter at right angles to their initial direction of motion for head-on collisions.

It has been described here the effect upon stability of modifying the integrable equations, and in particular it has been shown that stability is lost. The question now arises as to what effect a modification of the equations will have upon soliton scattering. The above issues will be studied in the following chapter, using the J -formulation of the model.

6.9 CONCLUSION

It has been demonstrated how the soliton stability property of integrable models in (1+1)-dimensions appears to extend to an integrable model in (2+1)-dimensions. Modifications of the model lead to the loss of this integrability property and hence appear to destroy soliton stability. If, however, the modifications are in some sense small, then the time scale required for the instability of the soliton to manifest itself is large. This allows the possibility of studying models which are 'almost integrable'. Such models may have relevance to the physically interesting non-integrable theories in which soliton-like structures exist which have many of the properties of solitons in integrable models.

CHAPTER VII.

Soliton Scattering in an Integrable Chiral model

7.1 INTRODUCTION

In integrable models the scattering of solitons is usually trivial, with a phase shift being the only (if any) affect upon solitons which collide. Such a trivial elastic collision behaviour is one of the properties of solitons in integrable systems that allows the analytic construction of exact multi-soliton solutions. In integrable planar systems the possibilities for soliton dynamics are much greater than in (1+1)-dimensions, where solitons are confined to motion in a line. The inelastic scattering of solitons in non-integrable systems, such as the planar Skyrme model of chapter *III*, is far from simple, and although it usually involves a radiation component this can be extremely small. Whether this type of non-trivial soliton scattering can occur in integrable models is an interesting question, which lies at the heart of connecting solitons of integrable and non-integrable systems.

There are some limited examples of integrable systems where soliton dynamics can be non-trivial. In (1+1)-dimensions there are exact solutions, known as Boomerons,^[72] which represent solitons which have time dependent velocities. In (2+1)-dimensions there is the recent discovery of Dromions,^[73] which are solitons which decay exponentially in all space directions, for which collisions need not even conserve Dromion numbers. In this chapter we study an integrable Chiral model, for which solitons that scatter trivially have already been found, and through the connection with the $O(3)$ σ -model demonstrate that soliton scattering can be highly non-trivial in integrable models.

7.2 THE INTEGRABLE CHIRAL MODEL

Consider the following modified $SU(2)$ chiral model due to Ward^[71]

$$(\eta^{\mu\nu} + V_\alpha \epsilon^{\alpha\mu\nu}) \partial_\mu (J^{-1} \partial_\nu J) = 0 \quad (7.1)$$

Here J is a map from \mathbf{R}^{2+1} to $SU(2)$. The coordinates on \mathbf{R}^{2+1} are $x^\mu = (t, x, y)$ with the Minkowski metric $\eta^{\mu\nu} = \text{diag}(-1, 1, 1)$. V^α is the spacelike vector $V^\alpha = (0, 1, 0)$ and $\epsilon^{\alpha\mu\nu}$ is the totally antisymmetric tensor.

In section 6.4 we briefly described this equation and gave a conserved energy functional. The model (7.1) is integrable in the sense that it may be written as the compatibility condition for an overdetermined linear system, and hence possesses an infinite number of conservation laws.

Multisoliton solutions to (7.1) may be constructed using the 'Riemann problem with zeros' ; for full details see [71,74].

To construct an n-soliton solution requires n distinct, and non-real, complex constants $\{\mu_k : k = 1, \dots, n\}$ which determine the soliton velocities. For each k a meromorphic function f_k of the linear combination

$$\omega_k = x + \frac{\mu_k}{2}(t + y) + \frac{\mu_k^{-1}}{2}(t - y) \quad (7.2)$$

is required and determines the shape of the soliton.

The solution obtained by this method is

$$(J^{-1})_{ab} = \frac{1}{\sqrt{\alpha}}(\delta_{ab} + \sum_{k,l=1}^n \frac{1}{\mu_k} (\Gamma^{-1})^{kl} \bar{m}_a^l m_b^k), \quad (7.3)$$

where

$$\Gamma^{kl} = \sum_{a=1}^2 (\bar{\mu}_k - \mu_l)^{-1} \bar{m}_a^k m_a^l$$

$$\alpha = \prod_{k=1}^n \frac{\bar{\mu}_k}{\mu_k}$$

and the two-component object $m_a^k = (1, f_k)$.

In this chapter we are concerned with finite energy soliton solutions and so f_k may be taken to be a rational function of ω_k . The scattering of these solitons is trivial^[71] with each soliton suffering no change in velocity and no phase shift upon scattering. Infinite energy extended wave solutions may be constructed by taking f_k to be an exponential function of ω_k . Such extended wave solutions suffer a phase shift upon scattering^[75] although again there is no change in velocity.

In the following section we describe the connection of this model with the O(3) σ -model and compare the solitons of the two models.

7.3 CONNECTION WITH THE O(3) σ -MODEL

The static solutions of (7.1) are the same as those for the unmodified chiral model

$$\partial_\mu(J^{-1}\partial^\mu J) = 0 \quad (7.4)$$

(ie. (7.1) with $V^\alpha = (0, 0, 0)$) since the term proportional to V^α is identically zero for static J .

The unmodified SU(2) chiral model is equivalent to the O(4) σ -model through the relation

$$J = \mathbf{1}\phi_0 + i\boldsymbol{\sigma} \cdot \boldsymbol{\phi} \quad (7.5)$$

where $\mathbf{1}$ is the 2 by 2 identity matrix, $\boldsymbol{\sigma}$ are the usual Pauli matrices, and $(\phi_0, \boldsymbol{\phi}) = (\phi_0, \phi_1, \phi_2, \phi_3)$ is a four component vector of real fields that are constrained to lie on S^3 , ie.

$$\phi_0^2 + \boldsymbol{\phi} \cdot \boldsymbol{\phi} = 1 \quad (7.6)$$

The only static finite energy solutions of the O(4) σ -model correspond to the embeddings of the solutions of the O(3) σ -model^[76]. Therefore the only static solutions of (7.1) are the O(3) embeddings that we shall now describe.

Consider the embedding given by $\phi_0 = 0$, so that the the field $\boldsymbol{\phi}$ is now a solution of the O(3) model. The static soliton solutions are most easily written in terms of the \mathbb{CP}^1 W formulation ie.

$$W = \frac{\phi_1 + i\phi_2}{1 - \phi_3} \quad (7.7)$$

The static solitons are simply the lumps (anti-lumps) of the O(3) model given by W a holomorphic (anti-holomorphic) function of $z = x + iy$.

Let us compare this construction of the static solitons with that of section 2. Recall that for each soliton there is a complex number μ_k which determines the velocity of the soliton. In order to obtain static solitons requires $\mu_k = i$ for every k , in which case $\omega_k = z$. However, the set $\{\mu_k : k = 1, \dots, n\}$ are required to be distinct so that we must have $n = 1$.

The solution (7.3) then gives (using the O(4) notation (7.5))

$$\phi_0 = 0 \quad f_1(z) = \frac{\phi_1 + i\phi_2}{1 - \phi_3} \quad (7.8)$$

and by comparison with (7.7) we see that the solution (7.3) gives the O(3) embedding $\phi_0 = 0$ with $W = f_1$.

In the O(4) model the O(3) embedding is totally geodesic. However, this is not the case for the model (7.1) and it can be shown that if we have an embedding (7.7) then the condition on W so that the solution remains in the O(3) subspace is

$$V_\alpha \epsilon^{\alpha\mu\nu} \partial_\mu W \partial_\nu \bar{W} = 0 \quad (7.9)$$

If we now take $W(\omega_1)$ then the condition (7.9) gives that $i\mu_1 \in \mathbf{R}$. Recall that μ_1 determines the velocity of the soliton and the restriction of μ_1 to be purely imaginary means that the x -component of the velocity is zero. Such a soliton corresponds to the O(3) embedding of a Lorentz boosted lump (which can be performed since the O(3) model is Lorentz invariant ie. has an SO(2,1) symmetry). The model (7.1) is not Lorentz invariant and indeed is not even radially symmetric (ie. there is no SO(2) symmetry) due to the fact that the vector V^α picks out a particular direction in space. There is, however, an SO(1,1) symmetry corresponding to Lorentz invariance in the y -direction which explains why only solitons moving in the y -direction correspond to O(3) embeddings of Lorentz boosted lumps. Further remarks regarding the lack of an SO(2,1) symmetry for (7.1) will be made later.

At the level of the one-soliton solution it therefore appears, at least for solitons whose motion is restricted to the y -direction, that the model (7.1) is no different from the O(3) model. This is because for the one-soliton solution (static or Lorentz boosted in the y -direction) the term in (7.3) proportional to V^α is zero so that the model behaves like the O(4) model, for which the O(3) embedding is totally geodesic. However, for more general time dependent configurations the term proportional to V^α is non-zero and will affect the evolution of the field, which will in general not lie in an O(3) subspace of O(4). An example of this more general time dependence is given by the perturbation of a one-soliton solution. In the O(3) model a lump has zero modes and is unstable^[43] whereas, as seen in the previous chapter, in the integrable model (7.1) the soliton has no such zero modes and is stable.

Before examining the two-soliton solution let us first briefly mention the topological aspects of the $O(3)$ and $O(4)$ σ -models. Recall that in compactified space the field of the $O(3)$ model, at fixed time, is a map $\phi : S^2 \rightarrow S^2$, and due to the homotopy relation

$$\pi_2(S^2) = \mathbb{Z} \quad (7.10)$$

such maps are classified by an integer winding number N which is therefore a conserved topological charge. An expression for this charge is given by

$$N = \frac{1}{8\pi} \int \epsilon_{ij} \phi \cdot (\partial_i \phi \wedge \partial_j \phi) d^2 x \quad (7.11)$$

where $i = 1, 2$ with $x^i = (x, y)$.

Now for the $O(4)$ model (here we are only interested in the topological aspects of the theory so the argument is the same for both equation (7.1) and the $O(4)$ model) the field is a map $(\phi_0, \phi) : S^2 \rightarrow S^3$ and the corresponding relation to (7.10) is

$$\pi_2(S^3) = 0 \quad (7.12)$$

so that there is no winding number. However, when studying soliton solutions that correspond to some initial embedding of $O(3)$ space into $O(4)$ there is a topological quantity, as described below, that may still prove useful.

Consider an $O(4)$ configuration which at some time corresponds to an $O(3)$ embedding, which we choose to be $\phi_0 = 0$ for definiteness. At this time the field is restricted to an S^2 equator of the possible S^3 target space. Suppose that the field never maps to the anti-podal points $\{\mathcal{N}, \mathcal{S}\} = \{\phi_0 = 1, \phi_0 = -1\}$ for all time, so that the target space is $S_0^3 = S^3 - \{\mathcal{N}, \mathcal{S}\}$. Now $S_0^3 \cong S^2 \times \mathbb{R}$ so that we now have the homotopy relation

$$\pi_2(S_0^3) = \pi_2(S^2 \times \mathbb{R}) = \pi_2(S^2) \oplus \pi_2(\mathbb{R}) = \mathbb{Z} \quad (7.13)$$

and again have a topological winding number for this map.

An expression for this winding number is easy to give, since it is simply the winding number of the map after projection onto the chosen S^2 equator (in this case given by $\phi_0 = 0$) ie

$$\hat{N} = \frac{1}{8\pi} \int \epsilon_{ij} \hat{\phi} \cdot (\partial_i \hat{\phi} \wedge \partial_j \hat{\phi}) d^2 x \quad (7.14)$$

where $\hat{\phi} = \frac{\phi}{|\phi|}$.

If the field does map to the anti-podal points $\{\mathcal{N}, \mathcal{S}\}$ at some time then the winding number is ill defined at this time and if considered as a function of time \widehat{N} will be integer valued but may suffer discontinuous jumps as the field moves through the anti-podal points. The continuity of \widehat{N} will therefore be a useful indication of the extent to which the evolution of the field remains close to the $O(3)$ embedding.

Let us now consider the two-soliton solution given by (7.3) with $n = 2$. In order to simplify the analysis we shall consider the situation in which there are two identical solitons which lie on the y -axis, equidistant from the origin, and which move towards each other with equal speed. Explicitly this is achieved by choosing the following

$$\begin{aligned}\mu_1 &= i\alpha \\ \mu_2 &= i\epsilon\alpha^{-1} \\ f_k &= \frac{\lambda\omega_k}{v}\end{aligned}\tag{7.15}$$

where λ is an arbitrary constant which determines the scale of the solitons and $\epsilon = \pm 1$. α is a real constant with $\alpha > 1$ which determines the speed v of the solitons through the relation

$$v = \frac{\alpha^2 - 1}{\alpha^2 + 1}\tag{7.16}$$

Before comparing the solution J given by (7.3) and (7.15) with the $O(3)$ embedding it is convenient to perform the transformation

$$J \rightarrow \sigma_1 J \sigma_2\tag{7.17}$$

This transformation does not affect the equation of motion (7.1) due to the chiral symmetry

$$J \rightarrow g J h\tag{7.18}$$

where g and h are constant $SU(2)$ matrices.

Let us study the solitons in the asymptotic limit $|t| \rightarrow \infty$, in which the two solitons are infinitely separated. Formally this can be achieved by taking the limit $|f_{k'}| \rightarrow \infty$ while f_k remains finite (here $1' = 2$, $2' = 1$). Let S_k denote the soliton located at $\omega_k = 0$.

In this limit (using the notation of (7.5) and (7.7)) we find that for soliton S_k the field is asymptotically given by

$$\phi_0 = 0 \quad W = f_k \quad (7.19)$$

so that the configuration represents an embedding of two $O(3)$ lumps, which scatter trivially. For S_1 we have that the topological charge $N = 1$, whereas for soliton S_2 we have $N = \epsilon$.

If we now study the solution at time $t = 0$ (when the two solitons are both located at the origin) we find that it is given by

$$(\phi_0, \phi) = (0, 0, 0, 1) \quad (7.20)$$

which is obviously not an embedding of two $O(3)$ lumps.

The configuration (7.20) has zero potential energy, so that at the time when the solitons collide the energy is totally kinetic, and is in the form of a peak located at the origin. This is in contrast to the scattering of lumps in the $O(3)$ model^{[42][41][77]} in which the kinetic energy is small throughout the scattering process and in which scattering is highly non-trivial, with lumps scattering at right angles to the initial direction of motion for a head-on collision.

In summary we find that the two-soliton solution given by (7.3) corresponds asymptotically to the embedding of two $O(3)$ lumps, although the subsequent evolution as the solitons approach each other is completely different from that of the $O(3)$ model.

Through the connection made with the $O(3)$ model there is an alternative method in which we may construct a configuration that corresponds asymptotically to that of the two-soliton solution. This configuration is the one used in the study of scattering in the $O(3)$ model and consists of choosing an initial condition (at time $t = 0$) which consists of a product ansatz for the field W . Explicitly take

$$\phi_0 = 0, \quad W = \frac{\lambda}{2\gamma(b - vt)}(x + i\gamma(y - b + vt))(x + i\gamma(y + b - vt)) \quad (7.21)$$

where $\gamma = (1 - v^2)^{-\frac{1}{2}}$ is the usual Lorentz factor.

In the asymptotic limit $b \rightarrow \infty$ this represents two identical solitons located at $y = \pm b$, which are locally Lorentz boosted so that they move along the y -axis towards each other with velocity v . Both solitons have topological charge $N = 1$, so that the total charge of the configuration is 2.

The question which now arises is what will be the evolution of the solitons given by the initial conditions (7.21), and will the scattering again be trivial due to the integrable nature of the model. In order to answer this question we turn to a numerical evolution of the field equations as described in the following section.

7.4 SOLITON - SOLITON SCATTERING

In order to evolve equation (7.1) numerically the $O(4)$ parametrization (7.5) is used. The equation is evolved on a 201×201 grid using a steplength $\delta x = \delta y = 0.02$, with space derivatives approximated by symmetric finite differences and a nine point formula used to evaluate the Laplacian. The time evolution is performed using a fourth-order Runge-Kutta method with a time step $\delta t = 0.01$. The boundary conditions are of an absorbing type, with a 20-point wide mesh surrounding the boundary of the grid in which the time derivatives of all fields are damped. The damping factor increases linearly from the start of the mesh, at which there is no damping, to the edge of the mesh, at which there is total damping, so that the fields remain fixed. Such boundary conditions appear to be the most useful for dealing with waves of radiation which reach the boundary. In the case of fixed boundary conditions such waves are simply reflected whereas the boundary conditions used here result in the wave being almost totally absorbed as it reaches the boundary. Such boundary conditions obviously lead to a small violation of energy conservation but are believed to be the most effective method to simulate an infinite plane.

The relation (7.6) should be true throughout the simulation and so a useful quantity in estimating the errors associated with the numerical procedure is

$$\text{Err} = \phi_0^2 + \phi \cdot \phi \quad (7.22)$$

Throughout the simulations described here it is found that $|\text{Err} - 1| < 10^{-7}$. An effective method for enforcing the constraint (7.6) is to rescale the fields every few iterations by dividing each field by the quantity $\sqrt{\text{Err}}$.

The numerical method just described was implemented on a SUN SPARC workstation. Total energy was conserved throughout the simulations to within an accuracy of 1% .

The first simulation performed was an attempt to reproduce the known analytical results for two-soliton scattering given by (7.3) with (7.15). The initial conditions for the simulation were taken from this exact solution and Fig 7.1. shows a plot of the total energy density at various times for a velocity $v = 0.6$ and scale $\lambda = 2$.

It can be seen that the solitons approach along the y-axis, form a peak as they collide and emerge unaltered from the interaction. The numerical simulation indeed reproduces the known result of trivial scattering. The projected topological charge \hat{N} is not continuous throughout the simulation, but jumps from $\hat{N} = 2$ initially to $\hat{N} = 0$ as the solitons merge, and finally jumps back to $\hat{N} = 2$ as the solitons separate.

Next we use the initial conditions (7.21) with a velocity $v = 0.6$, scale $\lambda = 2$ and position $b = 1$. Fig 7.2 shows a plot of the total energy density at various times for this simulation.

Again the solitons approach along the y-axis, however unlike in the previous case, where a peak was formed during the collision process, a ring structure is formed. From this ring emerge two solitons whose motion is at right angles to the initial direction of motion. This highly non-trivial 90° scattering is virtually identical to that of the O(3) model ^[77], suggesting that the modifying term in (7.1) has little affect for this process. The projected topological charge $\hat{N} = 2$ for the whole of this simulation. Furthermore, the projected charge density \hat{q} is

$$\hat{N} = \int \hat{q} dx dy \quad (7.23)$$

has an almost identical distribution (upto a scale) to that of the energy density. This is exactly the situation in the scattering of O(3) lumps and further demonstrates the similarity of the two models with regard to this scattering process.

The kinetic energy remains small throughout the scattering process and hence the formation of a ring rather than a peak at collision (compare Fig 7.1.). The right angle scattering between solitons of the O(3) model has an explanation ^[42] in terms of the geometry of the parameter space of static solutions (known as moduli space). Such an explanation of right angle scattering was first given for the case of monopoles ^[46] and relies on the assumption that the configuration at any time is well approximated by a

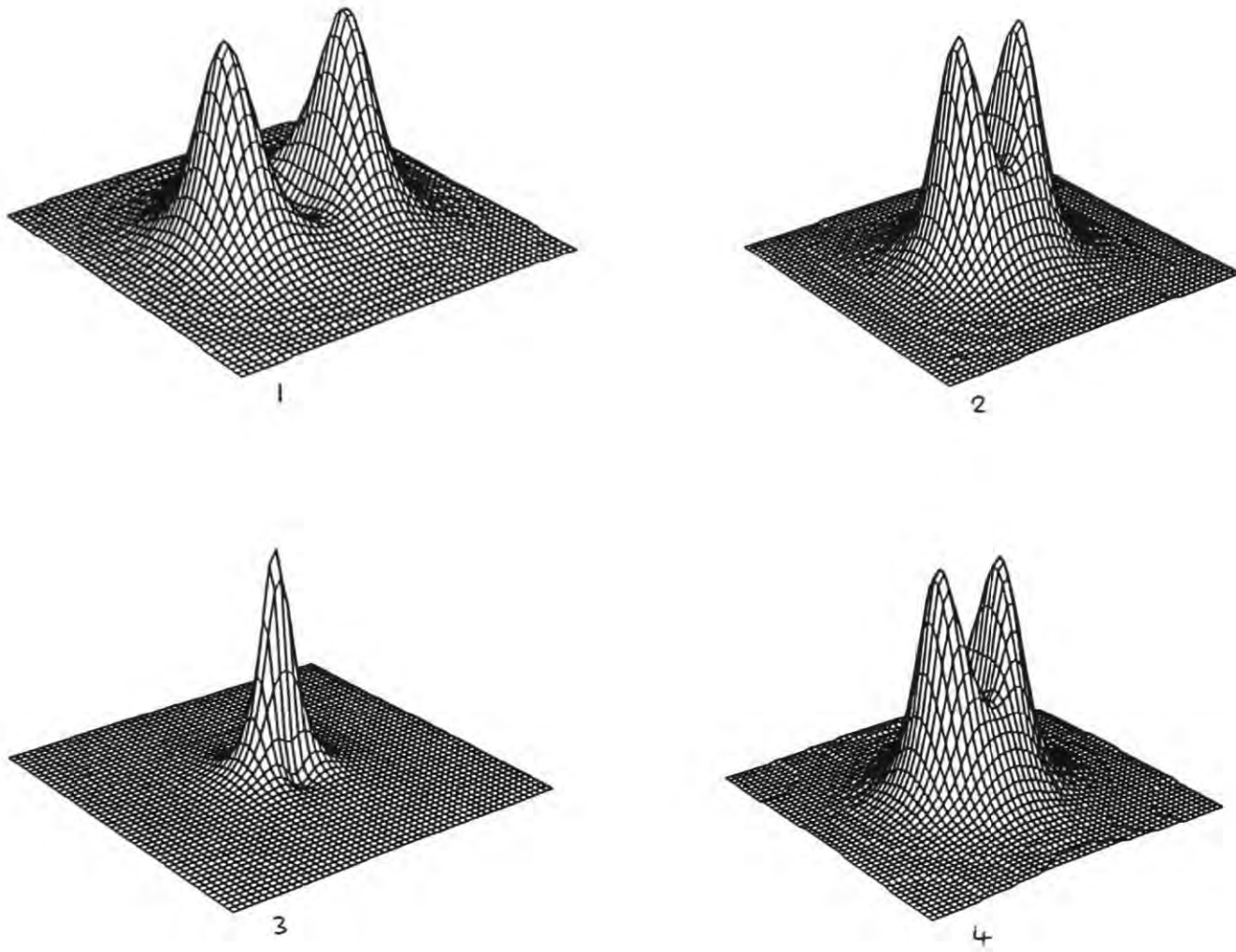


Fig 7.1 Energy density at increasing times, where the initial conditions are taken from the exact solution.

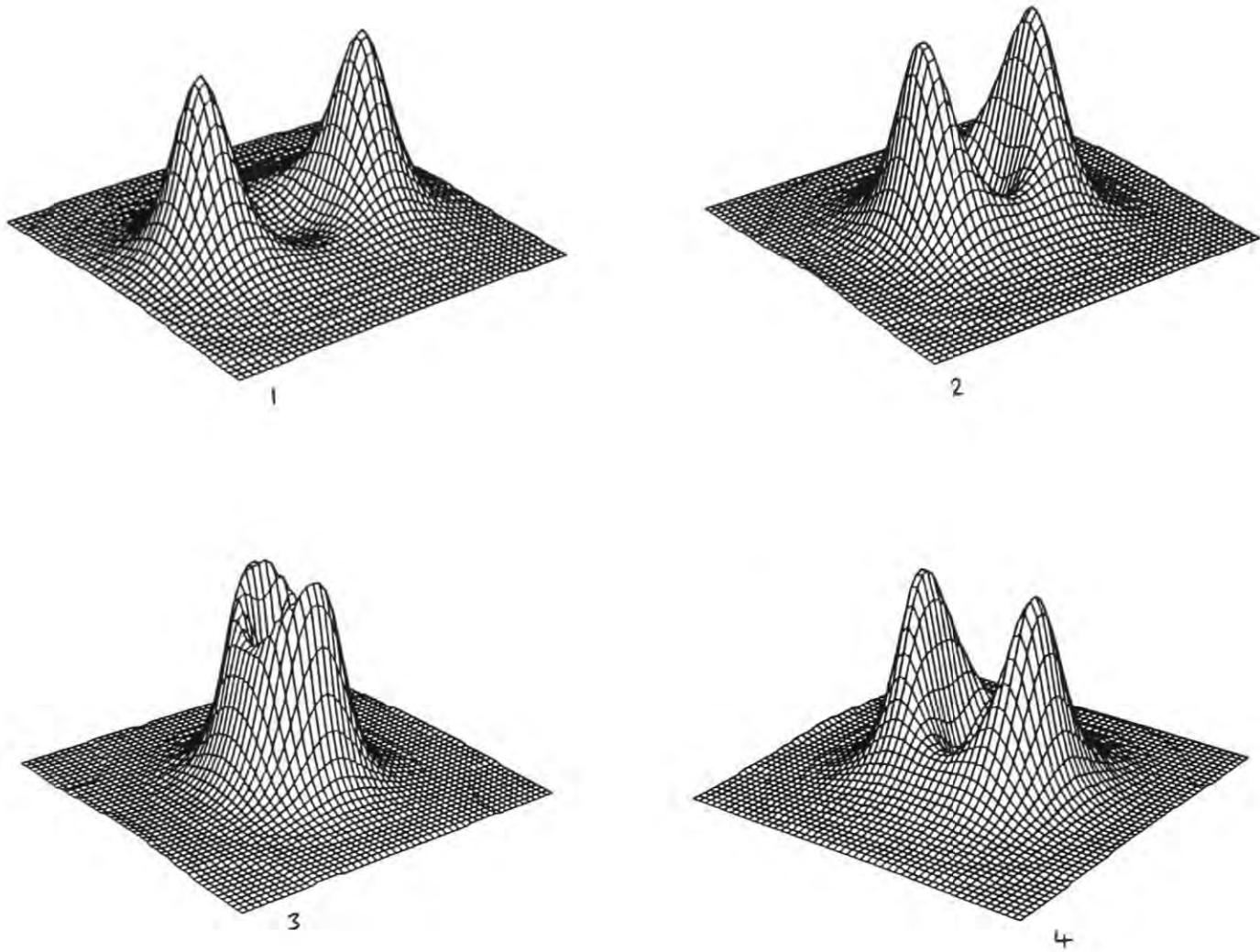


Fig 7.2 Energy density at increasing times, with the initial condition of embedding two Lorentz boosted $O(3)$ lumps.

static solution of the model. Ring structures occur in the soliton scattering of many planar systems ^[77,59] including the planar Skyrme model of chapter III, and are an approximation to the charge 2 soliton.

As mentioned earlier the model (7.1) is not rotationally invariant due to the presence of the vector V^α which picks out a particular direction in space. In the simulations discussed so far we have considered initial conditions which correspond to solitons moving in the y -direction only. However, due to the lack of rotational symmetry, we may find different results if we consider more general motions. If, for example, we wish to study the $O(3)$ embedding of two Lorentz boosted lumps moving along the x -axis, rather than the y -axis, then we immediately encounter a problem. The model is not Lorentz invariant in the x -direction and so a Lorentz boost cannot be performed to give the initial conditions. A solution to this problem is given by making use of the Yang-Mills-Higgs formulation of the previous chapter, which does have an $SO(2,1)$ symmetry. Recall that the solution J of (7.1) together with its derivatives with respect to the spacetime coordinates give the gauge potential and Higgs field of the equivalent system (in a particular gauge). The $SO(2)$ symmetry of the Yang-Mills-Higgs system means that given any solution J we can in principle convert it to gauge fields perform a coordinate rotation (together with a gauge transformation) and then recover the corresponding J' which will describe the same solution as J but with a rotated coordinate system. We therefore see that any simulations which we perform restricting the initial motion to the y -direction can be reproduced in any direction but require far more complicated initial conditions. To obtain these initial conditions will therefore be more than simply a coordinate rotation when viewed for the model (7.3).

Having found that embedding a charge 2 soliton configuration produces an evolution very similar to that of the $O(3)$ model one may now wonder how more general $O(3)$ configurations will evolve in this model. In the following section we investigate the evolution of a charge zero soliton - anti-soliton embedding.

7.5 SOLITON - ANTI-SOLITON SCATTERING

In the $O(3)$ model there is an attractive force between lumps of opposite topological charge. If the lump and anti-lump are initially well separated then they attract and eventually annihilate ^[77] into a wave of pure radiation. To investigate the soliton - anti-

soliton interaction in the integrable model we begin with an initial condition

$$W = \frac{\lambda(z - b)(\bar{z} + \bar{b})}{2b} \quad (7.24)$$

where $b \in \mathbb{C}$, $\lambda \in \mathbb{R}$. This represents a soliton (with charge $N = 1$) located at $z = b$ together with an anti-soliton (with charge $N = -1$) at $z = -b$. The scale of the soliton and anti-soliton are taken to be equal and are determined by λ . As with all the simulations described here the results are independent of this choice of scale.

Fig 7.3a shows a plot of the total energy density at various times for a simulation with parameters $b = i$ and $\lambda = 2$.

The evolution is initially similar to that of the $O(3)$ model, with the soliton and anti-soliton moving along the y -axis towards each other at an accelerating rate until they merge at the origin and form a peak. Note that a peak is formed rather than a ring since the energy is mainly kinetic when a soliton and anti-soliton merge. However, rather than the peak dissipating in a wave of radiation it now reforms into a two structures which then scatter at 90° to the original direction of motion. The topological charge N , is zero throughout the simulation and so at first sight it appears that the peak has reformed into a soliton - anti-soliton pair. However, if we examine the topological charge density (see Fig 5.3b) we find that this is not the case. Initially the soliton and anti-soliton are clearly visible as distinct structures, having respectively $+1$ and -1 units of topological charge concentrated in a single lump. As they approach the topological charge of the soliton becomes localised in to two separate peaks, each with a $\frac{1}{2}$ unit of charge. The charge of the anti-soliton also separates in a similar manner, and during the interaction there is a change of partners. Each of the structures which emerge from the scattering process has no overall topological charge, but is composed of two $\frac{1}{2}$ units of charge with opposite sign. These structures are not embeddings of lumps or anti-lumps, and are certainly very different from the initial incoming soliton - anti-soliton pair. This process clearly merits further study, and it would be interesting to determine the nature of the outgoing structures in the large time limit. The formation of two localised structures from soliton - anti-soliton scattering is a surprising result that is surely linked to the integrable nature of the model.

One reason that the incoming and outgoing structures of soliton - anti-soliton scattering appear so different may perhaps be related to the asymmetry between the x and

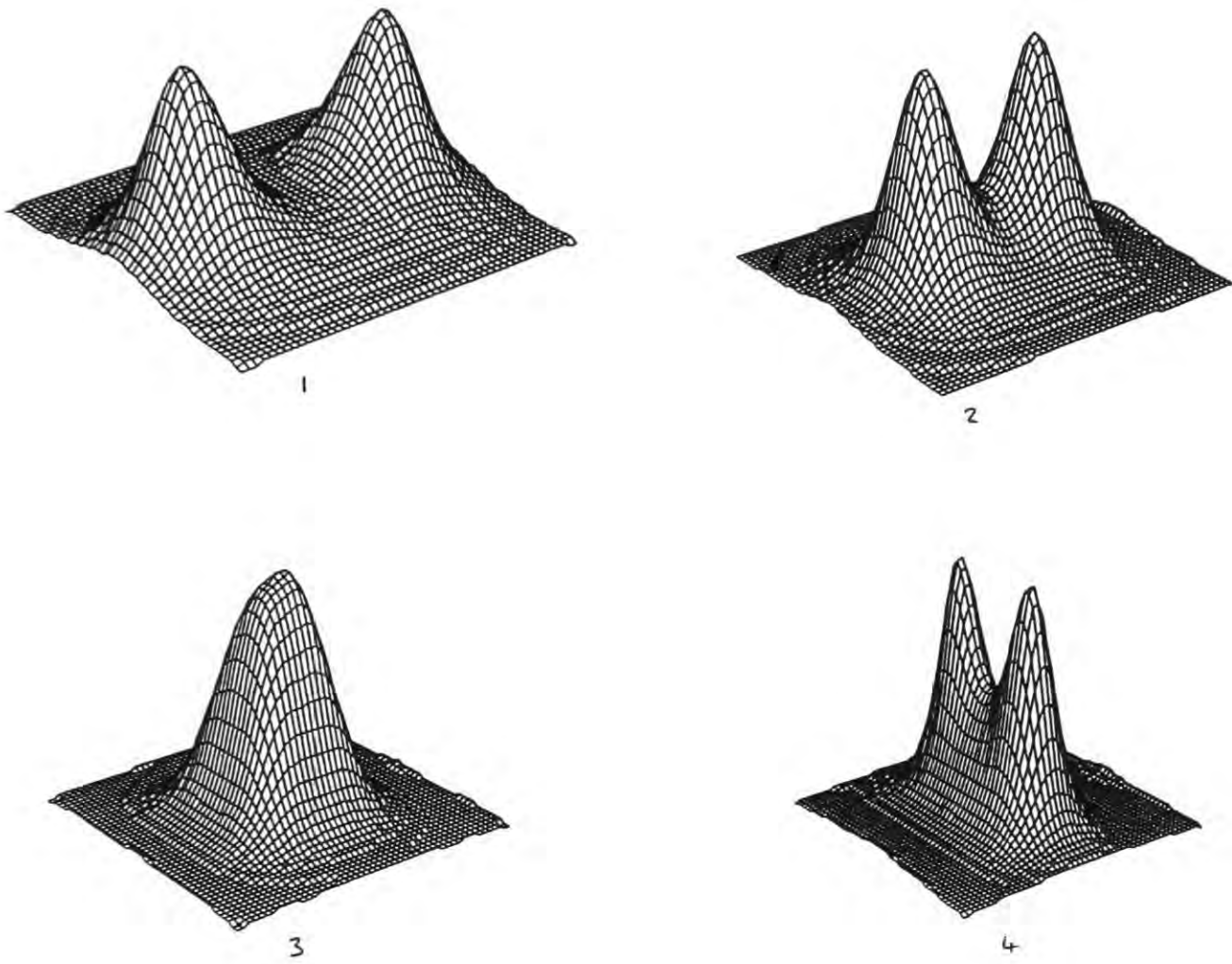


Fig 7.3a Energy density at increasing times for soliton - anti-soliton scattering.

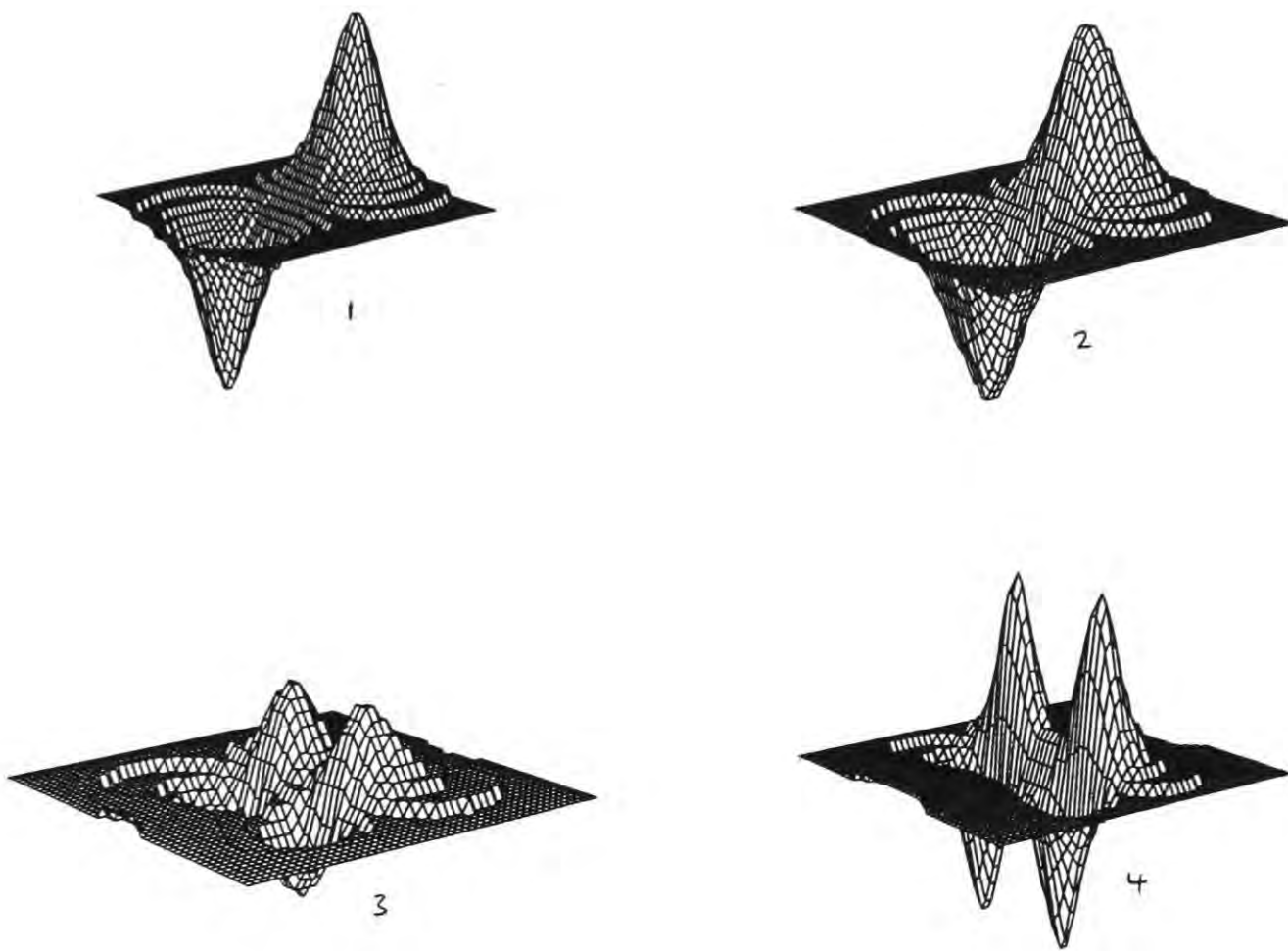


Fig 7.3b Topological charge density at increasing times for soliton - anti-soliton scattering.

y coordinates in the equation of motion (7.1) as already discussed. To study the $x \leftrightarrow y$ asymmetry effects we can take the initial condition (7.24) with $b = 1$ so that the soliton and anti-soliton are now located on the x -axis rather than the y -axis. The results of such a simulation are that the soliton and anti-soliton now repel. They remain on the x -axis throughout the simulation but with an increasing separation. The soliton and anti-soliton therefore appear to attract in the y -direction but repel in the x -direction. For a soliton and an anti-soliton located at arbitrary positions in the (x, y) plane the combined effect of these two forces is to produce curved trajectories with non-zero impact parameter. Fig 7.4 shows the total energy density for a simulation with parameter value $b = 0.1 + i$.

The initial condition (7.24) is not the most general configuration to describe a soliton - anti-soliton pair of equal size. Consider the charge one static $O(3)$ soliton solution

$$W^{-1} = \frac{\lambda}{(z - b)} \quad (7.25)$$

The position of the soliton is b , and λ is a complex constant whose modulus determines the size scale of the soliton. The phase of λ can be set to zero without loss of generality due to the $O(3)$ model having a global $U(1)$ symmetry

$$\phi_1 + i\phi_2 \rightarrow e^{i\theta}(\phi_1 + i\phi_2) \quad (7.26)$$

where θ is a real constant.

Now consider a soliton - anti-soliton pair. Again the global $U(1)$ symmetry allows us to choose the phase of the soliton (or the anti-soliton) to be zero, but the relative phase between the soliton and the anti-soliton cannot be neglected. Explicitly take

$$W^{-1} = \frac{\lambda}{(z - b)} - \frac{\lambda e^{i\chi}}{(\bar{z} + \bar{b})} \quad (7.27)$$

where $0 \leq \chi \leq \pi$ is the relative phase. Again the scale of the soliton and anti-soliton are set equal and are determined by λ , which may be taken to be real. In the $O(3)$ model there is a dipole-like interaction^{[78] [79]} between soliton and anti-soliton which will depend on this relative phase, and will therefore affect the scattering process. Scattering of a soliton - anti-soliton pair with a relative phase, together with other more general soliton - anti-soliton configurations, produce many interesting results and exotic soliton trajectories^[80] in several models, including the $O(3)$ model, the planar Skyrme model of chapter III and the integrable model (7.1).

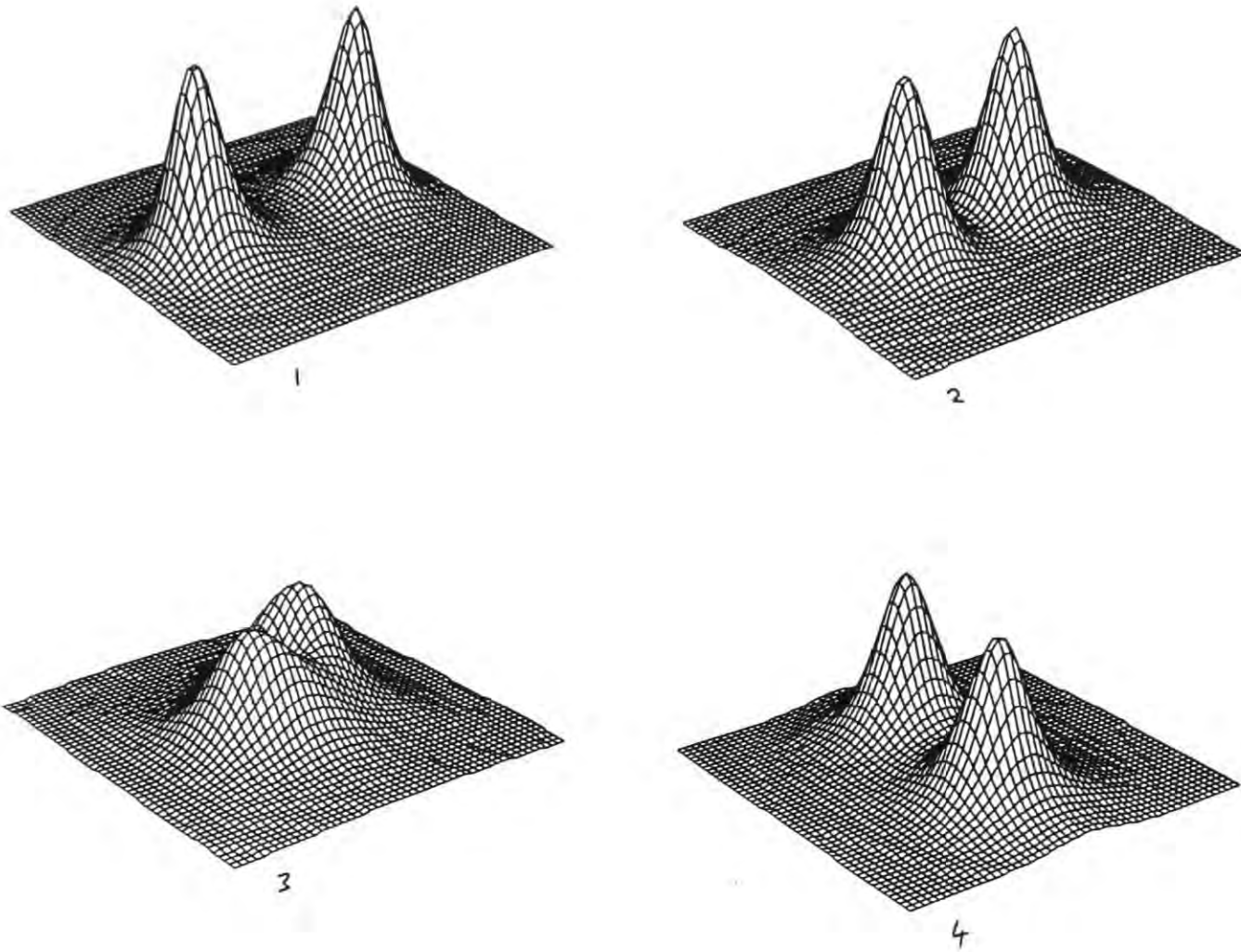


Fig 7.4 Energy density at increasing times for soliton - anti-soliton scattering with non-zero impact parameter.

7.6 AN INTERPOLATING CHIRAL MODEL

Consider the one-parameter Chiral equation

$$(\eta^{\mu\nu} + \kappa V_\alpha \epsilon^{\alpha\mu\nu}) \partial_\mu (J^{-1} \partial_\nu J) = 0 \quad (7.28)$$

where κ is a real and positive constant. If $\kappa = 0$ then (7.28) is the pure SU(2) Chiral equation, whereas if $\kappa = 1$ then (7.28) is the integrable Chiral model (7.1). By allowing κ to take any value in the interval $[0, 1]$ we can interpolate between these two cases. The static solutions of (7.28) are the same for all values of κ , and it is interesting to study how the scattering of solitons is affected by varying κ . The conserved energy density of the pure SU(2) Chiral model is also conserved for this model, independent of the value of κ .

In the last chapter we saw how modifying the integrable equation, so that the integrability property is lost, results in the solitons becoming unstable. We therefore expect that the solitons of (7.28) will be unstable for $\kappa \neq 1$, although soliton scattering may still be studied before the instabilities develop.

As described earlier, the embedding of two O(3) lumps in the integrable model (7.1) produced a result very similar to that for the pure SU(2) chiral model, for which the embedding is totally geodesic. We therefore expect that this scattering process will be very similar for all intermediate values of κ , and this is indeed the case.

If we begin with the initial conditions that arise from the exact solution of the integrable equation ($\kappa = 1$), then we find the following result. If the deviation of κ from 1 is less than approximately 10 % (the precise value depends upon the particular soliton parameters), then the results are very similar to the integrable equation, with trivial soliton scattering, although the solitons do tend to shrink slightly as the deviation of κ from 1 increases. For values $\kappa < 0.9$ then the solitons collapse completely upon collision (recall there is no topological stability), and a wave of radiation is formed. Fig 7.5 shows the energy density at increasing times for such a simulation with $\kappa = 0.5$.

A similar result is obtained for the scattering of embedded O(3) lump - anti-lump scattering. The only slight difference is that the wave of radiation appears to be more peaked at right angles to the original direction of motion, than in the above scattering.

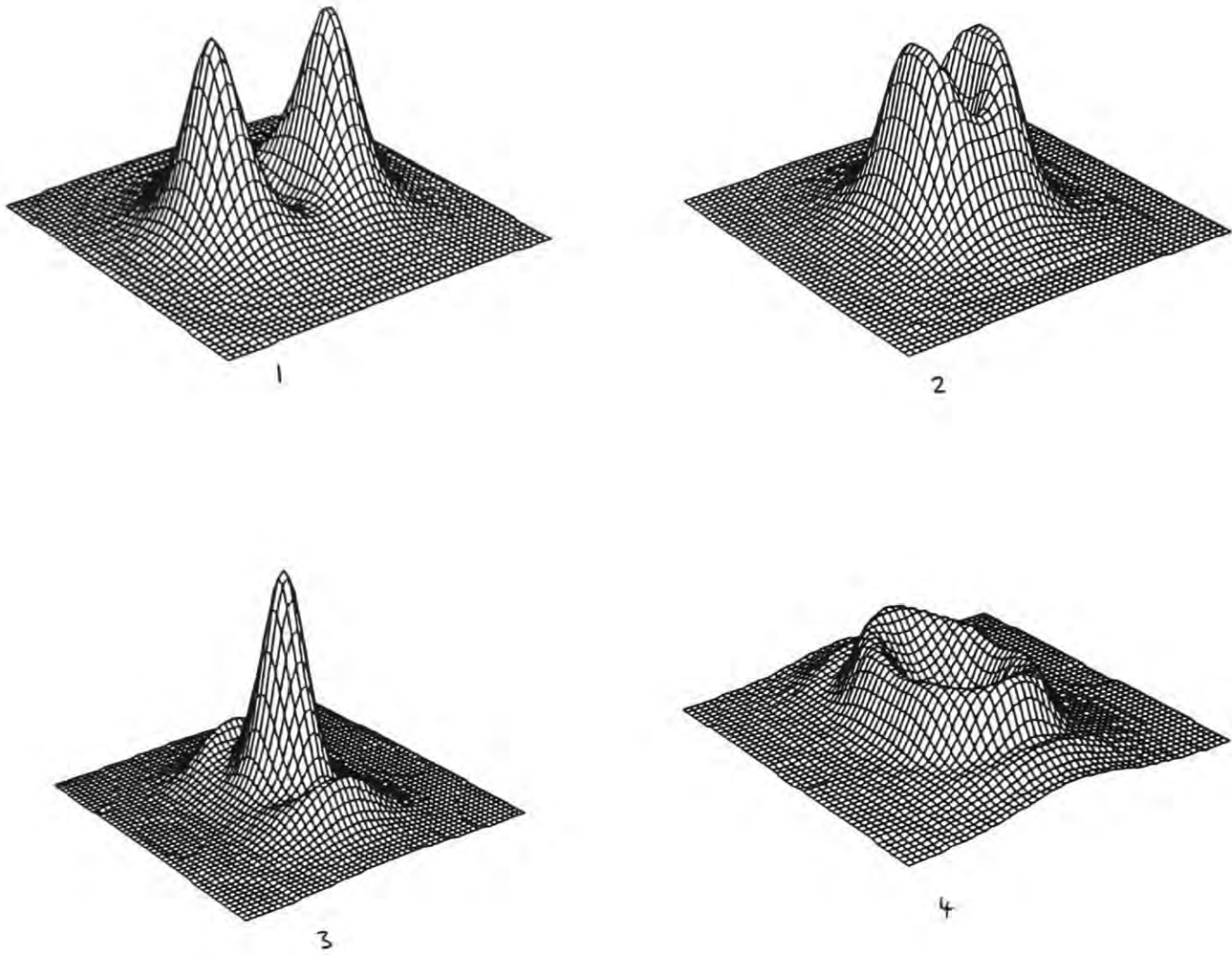


Fig 7.5 Energy density at increasing times for soliton - soliton scattering in the interpolating model with $\kappa = 0.5$.

7.7 REMARKS ON OTHER METHODS

The integrable nature of (7.1) means that there are a variety of methods for constructing exact solutions. Together with the 'Riemann problem with zeros', discussed briefly in section 2, both twistor techniques^[67] and a full inverse scattering formalism^[81] have been applied to the model. Perhaps one of these methods could be used to construct explicitly the soliton solutions described here. In the inverse scattering formalism it would be interesting just to calculate the spectral decomposition of the initial conditions.

The numerical procedure described here is a relatively simple evolution scheme but requires large amounts of computing time. The scheme makes no use of the integrability property of the equation and maybe a better procedure can be found through a numerical implementation of one of the above methods. In the numerical studies of integrable systems in (1+1)-dimensions pseudo-spectral methods^[82] and schemes based upon an integrable discretization^[83] of the equations vastly reduce the computing time required. Perhaps similar methods may be employed in (2+1)-dimensions.

7.8 CONCLUSION

The infinite number of conservation laws associated with a given integrable equation place severe constraints upon possible soliton dynamics. The ability to construct exact analytic multi-soliton solutions, with trivial scattering properties, derives from such integrability properties. In this chapter it has been shown that soliton scattering can be highly non-trivial in an integrable planar chiral model. In this planar model there are, in addition to the process of trivial soliton scattering, other possibilities which resemble the scattering of solitons in several non-integrable planar models. This is of importance to higher dimensional soliton theory and suggests an area in which new phenomena may occur that are not present in (1+1)-dimensions. Such results also have relevance in connecting integrable and non-integrable equations possessing soliton solutions.

CHAPTER VIII.

Outlook

The planar Skyrme model of chapter III is a modification of the $\mathbb{C}\mathbb{P}^1$ σ -model which is successful in stabilizing the lump solutions. It is interesting to attempt to find other modifications of the $\mathbb{C}\mathbb{P}^1$ model, or indeed any σ -model, in which the lumps can be stabilized. A particularly promising modification is the coupling of the $\mathbb{C}\mathbb{P}^1$ model to a background magnetic field, as described briefly below.

The $\mathbb{C}\mathbb{P}^1$ model is given by the Lagrangian

$$\mathcal{L} = \frac{\partial_\mu W \partial^\mu \bar{W}}{(1 + |W|^2)^2} \quad (8.1)$$

and has a global $U(1)$ symmetry under transformations of the phase of W ie

$$W \rightarrow e^{i\alpha} W \quad (8.2)$$

where α is a real constant.

By Noethers theorem this symmetry leads to a conserved Noether current

$$j_\mu = \frac{i(W \partial_\mu \bar{W} - \bar{W} \partial_\mu W)}{(1 + |W|^2)^2} \quad (8.3)$$

Let A_μ be the electromagnetic $U(1)$ potential, with field strength $F_{\mu\nu} = \partial_\mu A_\nu - \partial_\nu A_\mu$, and couple this to the $\mathbb{C}\mathbb{P}^1$ field by replacing (8.1) with

$$\mathcal{L} = \frac{\partial_\mu W \partial^\mu \bar{W}}{(1 + |W|^2)^2} + j_\mu A^\mu \quad (8.4)$$

The potential A_μ is taken to be a non-dynamical field, so that it has a given, time independent, form. This corresponds to the $\mathbb{C}\mathbb{P}^1$ model in the presence of a background electromagnetic field.

As a particular example choose

$$\begin{aligned} A_0 &= 0 \\ A_i &= -\frac{b}{2}\epsilon_{ij}x_j \end{aligned} \quad (8.5)$$

where $i = 1, 2$, ϵ_{ij} is the totally antisymmetric tensor on two indices with $\epsilon_{12} = 1$, and b is a positive constant. The electric and magnetic fields are given by

$$\begin{aligned} \mathcal{E}_i &= F_{i0} = 0 \\ \mathcal{B} &= \frac{1}{2}\epsilon_{ij}F_{ij} = b \end{aligned} \quad (8.6)$$

With this choice the model (8.4) therefore represents $\mathbb{C}\mathbb{P}^1$ lumps in the presence of a constant uniform background magnetic field.

It is easily verified that this model has the radially symmetric charge N lump solution

$$W = \exp(it\sqrt{Nb})(\lambda z)^N \quad (8.7)$$

where the scale, λ , is arbitrary, and N is a positive integer which must satisfy $N \geq 2$ for finite energy.

This lump rotates in internal space with an angular velocity determined by the product of the topological charge and the magnetic field. A collective coordinate investigation of radially symmetric lumps suggests that this rotation may be sufficient to stabilize the lumps, and certainly a study of stability using a numerical evolution of the full field equations is required. In the limit $b \rightarrow 0$ we recover the $\mathbb{C}\mathbb{P}^1$ model, so that there are no forces between static lumps. In the limit of small b the force between rotating lumps will therefore be weak, so that a collective coordinate approach can be used to study lump interactions and scattering.

The success of the collective coordinate approach to the planar Skyrme model, together with the rich structure found, suggests that considerable further investigation of the collective coordinate model will be worthwhile. In particular it would be interesting to study the Riemannian structure of the coordinates C and D , and to determine the global features of the potential $V(C, D)$.

Computer simulation of systems invariably requires the continuous coordinates of space and time to be approximated by a finite number of discrete points in the form of a lattice. Simple finite difference approximations for spatial derivatives will usually provide an adequate numerical scheme, although in planar (and higher dimensional) systems this requires large amounts of computing time. The efficiency of more sophisticated methods such as the pseudo-spectral^[82] technique, where numerical Fourier transforms are used in the approximation of spatial derivatives, needs to be investigated for models of the type described in this thesis. Linked to this issue is the question of discretization of integrable planar models, to obtain integrable planar lattice models. Simple discretizations will in general destroy the integrability of the model, and it is certainly a highly non-trivial problem.^[84] Integrable discretizations of systems, such as the KdV equation, have been obtained by making use of the Hirota bilinear formalism. It would be interesting to see if a bilinear formalism for the integrable Chiral model could be found, which may then suggest a discretization procedure.

The work described in chapter *VII* is, to my knowledge, the first example of inelastic soliton scattering in an integrable model. This provides a major link between soliton dynamics in integrable and non-integrable systems. Furthermore, there is the possibility that these interacting soliton solutions may be constructed explicitly (since the model is after all integrable), which would be the first example of an exact closed form solution describing inelastic soliton scattering in either an integrable or non-integrable model. To give a flavour of what may be involved in constructing these solutions explicitly let us once again return to the 'Riemann problem with zeros', with the notation as in chapter *VII*. There we described the solution in which the set of soliton velocities $\{\mu_k : k = 1, \dots, n\}$ were complex constants. However, this is not the most general solution since the soliton velocities are required to satisfy a set of differential equations, of which a particular solution is that they are constants. The most general solution to this differential equation is given by the implicit formula for μ

$$h(\mu, \omega) = 0 \quad (8.8)$$

where h is any differentiable function and

$$\omega = x + \frac{\mu}{2}(t + y) + \frac{\mu^{-1}}{2}(t - y). \quad (8.9)$$

The trivial scattering n -soliton solution corresponds to the choice

$$h = (\mu - \mu_1)(\mu - \mu_2)\dots(\mu - \mu_n) \quad (8.10)$$

for the set of constants $\{\mu_k : k = 1, \dots, n\}$.

As an example, if we choose $h = \omega$ then the resulting solution^[81] is an implode-decay wave. To construct an interacting soliton solution we require a function h such that its solution μ has the asymptotic behaviour $\mu \rightarrow \mu_1$ as $t \rightarrow -\infty$ and $\mu \rightarrow \mu_2$ as $t \rightarrow +\infty$, where μ_1 and μ_2 are complex constants with $\mu_1 \neq \mu_2$. A major difficulty in choosing the function h is to ensure that all functions are single-valued and that the resulting solution has finite energy.

REFERENCES

1. P. M. Sutcliffe, *Nonlinearity* **4** (1991) 1109.
2. P. M. Sutcliffe, *Phys. Lett.* **283B** (1992) 85.
3. P. M. Sutcliffe, *Durham preprint DTP-92-21*. To appear in *Phys. Lett. B*.
4. P. M. Sutcliffe, *Durham preprint DTP-92-31*.
5. P. M. Sutcliffe, *Durham preprint DTP-91-27*. To appear in *Phys. Rev. D*.
6. P. M. Sutcliffe, *J. Math. Phys.* **33** (1992) 2269.
7. D. J. Korteweg and G. de Vries, *Philos. Mag. Ser. 5* **39** (1895) 422.
8. N. J. Zabusky and M. D. Kruskal, *Phys. Rev. Lett.* **15** (1965) 240.
9. C. S. Gardner, J. M. Green, M. D. Kruskal and R. M. Muira, *Phys. Rev. Lett.* **19** (1967) 1095.
10. R. M. Muira, C. S. Gardner and M. D. Kruskal, *J. Math. Phys.* **9** (1968) 1204.
11. P. D. Lax, *Comm. Pure. Appl. Math.* **21** (1968) 467.
12. I. M. Gelfand and B. M. Levitan, *Am. Math. Soc. Transl. Ser. 2.* **1** (1955) 259.
13. L. P. Eisenhart, *A Treatise on the differential geometry of curves and surfaces*. (Ginn and Co, Boston 1909).
14. *Soliton theory: a Survey of results*. Ed. A. P. Fordy (Manchester University Press 1990).
15. G. L. Lamb, *Phys. Letts.* **A25** (1967) 181.
16. R. Hirota, *Phys. Rev. Lett.* **27** (1971) 1192.
17. S. Novikov, S. V. Manakov, L. P. Pitaevskii and V. E. Zakharov, *Theory of Solitons*. (Consultants Bureau, New York, 1984).
18. A. Davey and K. Stewartson, *Proc. Roy. Soc. Lond.* **A338** (1974) 101.
19. R. S. Ward, *Phil. Trans. R. Soc.* **A315** (1985) 451.
20. L. J. Mason and G. A. J. Sparling, *Phys. Lett.* **A137** (1989) 29.
21. L. J. Mason. *Oxford preprint; Twistor Newsletter* 30.
22. I. A. B. Strachan, *PhD thesis, University of Durham (1991), unpublished*.

23. M. J. Ablowitz and P. A. Clarkson. *Solitons, Nonlinear Evolution Equations and Inverse Scattering* (Cambridge University Press, 1991).
24. N. S. Manton, *Nucl. Phys.* **135B** (1978) 319.
25. C. Rebbi, *Phys. Rev.* **D17** (1978) 483.
26. H. J. de Vega, *Comm. Math. Phys.* **116** (1988) 659.
27. A. A. Belavin and V. E. Zakharov, *Phys. Lett.* **73B** (1978) 53.
28. R. S. Ward and R. O. Wells, *Twistor Geometry and Field Theory*. (Cambridge University Press 1990).
29. R. S. Ward, *Phys. Lett.* **A61** (1977) 81.
30. R. S. Ward, *J. Math. Phys.* **30** (1989) 2246.
31. W. J. Zakrzewski, *Low Dimensional Sigma Models*. (Adam Hilger, Bristol, 1989).
32. T. H. R. Skyrme, *Proc. R. Soc.* **A262** (1961) 237.
33. T. H. R. Skyrme, *Nucl. Phys.* **31** (1962) 556.
34. E. Witten, *Nucl. Phys.* **B160** (1979) 57.
35. C. Nash and S. Sen, *Topology and Geometry for Physicists*. (Academic Press, London, 1983).
36. G. S. Adkins, C. R. Nappi and E. Witten, *Nucl. Phys.* **228B** (1983) 552.
37. E. Braaten, L. Carson and S. Townsend,
University of Minnesota preprint TP1-MINN-89/20T.
38. M. F. Atiyah and N. S. Manton, *Phys. Lett.* **222B** (1989) 438.
39. A. A. Belavin and A. M. Polyakov, *JETP Lett.* **22** (1975) 245.
40. G. Woo, *J. Math. Phys.* **18** (1977) 1264
41. R. S. Ward, *Phys. Lett.* **158B** (1985) 424.
42. R. A. Leese, *Nucl. Phys.* **344B** (1990) 33.
43. R. A. Leese, M. Peyrard and W. J. Zakrzewski, *Nonlinearity* **3** (1990) 387.
44. R. A. Leese, M. Peyrard and W. J. Zakrzewski, *Nonlinearity* **3** (1990) 773.
45. N. S. Manton, *Phys. Rev. Lett.* **60B** (1988) 1916.

46. M. F. Atiyah and N. J. Hitchin, *The Geometry and Dynamics of Magnetic Monopoles* (Princeton University Press, Princeton, 1988).
47. P. J. Ruback, *Nucl. Phys.* **296B** (1988) 669.
48. M. Peyrard, B. Piette and W. J. Zakrzewski, *Nonlinearity* **5** (1992) 563.
49. K. J. Eskola and K. Kajantie, *Z. Phys. C.* **44** (1989) 347.
50. J. K. Perring and T. H. R. Skyrme, *Nucl. Phys.* **31** (1962) 550.
51. E. Witten, *Phys. Rev. Lett.* **38** (1977) 121.
52. G. S. Adkins and C. R. Nappi, *Nucl. Phys.* **233B** (1984) 109.
53. J. J. M. Verbaarschot, *Phys. Lett.* **195B** (1987) 235.
54. A. D. Jackson and M. Rho, *Phys. Rev. Lett.* **51** (1983) 751.
55. H. Weigel, B. Schwesinger and G. Holzwarth, *Phys. Lett.* **168B** (1986) 321.
56. G. W. Gibbons and N. S. Manton, *Nucl. Phys.* **274B** (1986) 183.
57. T. M. Samols, *Comm. Math. Phys.* **145** (1992) 149.
58. I. A. B. Strachan, *J. Math. Phys.* **33** (1992) 102.
59. E. P. S. Shellard and P. J. Ruback, *Phys. Lett.* **209B** (1988) 262.
60. W. J. Zakrzewski, *Nonlinearity* **4** (1991) 429.
61. R. Hirota, *J. Phys. Soc. Japan* **33** (1972) 1459.
62. M. V. Berry and K. E. Mount, *Rep. Prog. Phys.* **35** (1972) 315.
63. S. Coleman, *Aspects of Symmetry* (Cambridge University Press, 1985).
64. R. Jackiw and G. Woo, *Phys. Rev.* **12D** (1975) 1643.
65. A. B. Zamolodchikov and Al. B. Zamolodchikov, *Ann. Phys.(NY)* **120** (1979) 253.
66. N. J. Hitchin, *Comm. Math. Phys.* **83** (1982) 579
67. R. S. Ward, *Comm. Math. Phys.* **128** (1990) 319.
68. M. F. Atiyah and R. S. Ward, *Comm. Math. Phys.* **55** (1977) 117.
69. K. Uhlenbeck, *J. Diff. Geom.* **30** (1989) 1.
70. 30
71. R. S. Ward, *J. Math. Phys.* **29** (1988) 386.

72. F. Calogero and A. Degasperis, in *Solitons* Eds. R. K. Bullough and P. J. Caudrey. (Springer, Berlin, 1980).
73. M. Boiti, J. J. P. Leon, L. Martina and F. Pempinelli, *Phys. Lett.* **132** (1988) 432.
74. P. Forgács, Z. Horvath and L. Palla, *Phys. Rev. Lett.* **46** (1981) 392.
75. R. A. Leese, *J. Math. Phys.* **30** (1989) 2072.
76. M. J. Borchers and W. D. Garber, *Comm. Math. Phys.* **72** (1980) 77.
77. W. J. Zakrzewski, *Nonlinearity* **4** (1991) 429.
78. D. Forster, *Nucl. Phys.* **130B** (1977) 38.
79. A. P. Bukhvostov and L. N. Lipatov, *Nucl. Phys.* **B180** (1981) 116.
80. B. Piette, P. M. Sutcliffe and W. J. Zakrzewski - *Durham preprint DTP-91-69.*
To appear in Int. J. Mod. Phys. C.
81. J. Villarroel, *Stud. Appl. Math.* **83** (1990) 221.
82. B. Fornberg and G. B. Whitham, *Phil. Trans. Roy. Soc.* **289** (1978) 373.
83. T. R. Taha and M. J. Ablowitz, *J. Comp. Phys.* **55** (1984) 203.
84. R. S. Ward, *Phys. Lett.* **165A** (1992) 325.

